THE UNIVERSITY of ADELAIDE

The Role and Function of Cation Chloride Cotransporters in Plants

Daniel Mckay

School of Agriculture, Food and Wine

Faculty of Sciences

University of Adelaide

April 2021

Table of Contents

Abstract

Ion transport across cellular membranes is essential for the viability of all organisms. This includes both ion transport into and out of cells, as well as across the membranes of intracellular organelles. One such organelle is the Trans-Golgi Network (TGN/EE), which is vital for the sorting and delivery of proteins in cells. Ion transport is typically mediated by membrane-spanning ion pumps, channels and transporters. Together with a proton pump, ion transporters maintain the low luminal pH of the TGN/EE. The regulation of this pH is an important aspect for TGN/EE function and therefore endomembrane trafficking. In this thesis, a new regulator of TGN/EE pH is identified and characterised, the cation chloride cotransporter (AtCCC1), which is the first pH regulatory component in the TGN/EE that does not transport protons itself. AtCCC1 is ubiquitously expressed and the transporter localises to the TGN/EE. Arabidopsis *Atccc1* knockouts have a higher TGN/EE luminal pH and the mutants show defects in osmoregulatory capacity of the TGN/EE, which might indicate alterations in ion efflux. These defects in ion and pH regulation were found to impact TGN/EE function with *Atccc1* exhibiting reduced rates of both endo- and exocytosis. This is accompanied by a severe and extensive mutant phenotype with reduced cell elongation, stunted growth, and altered root and shoot morphology. Interestingly, a reduction in the osmotic stress induced internalisation of protein was observed in *Atccc1* in addition to a reduction in plasmolysis. The potential connection between TGN/EE pH and osmotic stress was assayed by measuring TGN/EE pH in response to salt and osmotic stress. Stress treatments resulted in an increased pH, revealing that the TGN/EE pH is dynamic in wildtype plants. In contrast, TGN/EE pH did not change in *Atccc1*. In conclusion, these results demonstrate that AtCCC1 contributes to regulation of ion fluxes and pH in the TGN/EE, which is important for endomembrane trafficking and for response to stresses.

Thesis Declaration

I certify that this work contains no material which has been accepted for the award of any other degree or diploma in my name, in any university or other tertiary institution and, to the best of my knowledge and belief, contains no material previously published or written by another person, except where due reference has been made in the text. In addition, I certify that no part of this work will, in the future, be used in a submission in my name, for any other degree or diploma in any university or other tertiary institution without the prior approval of the University of Adelaide and where applicable, any partner institution responsible for the joint-award of this degree.

I give permission for the digital version of my thesis to be made available on the web, via the University's digital research repository, the Library Search and also through web search engines, unless permission has been granted by the University to restrict access for a period of time.

I acknowledge the support I have received for my research through the provision of an Australian Government Research Training Program Scholarship.

Daniel McKay 01/04/2021

Acknowledgements

I would like to begin here by thanking my incredible supervisory team. To my principle supervisor, Stefanie Wege, thank you for the time, effort and support you have given me. Over the course of this project, you have regularly challenged me and I have a learned a lot from you. To my co-supervisor, Matthew Gilliham, I thank you for your support and guidance. Between meetings and informal check-ups in the office, your insight and input has been incredibly valuable to me and the project. I also thank my independent advisor, Matthew Tucker. I truly value and appreciate the feedback you have given.

I also wish to express my gratitude to many of the people in the Gilliham lab. Their comments, thoughts and feedback have inspired experiments and helped shape the way we interpreted results. I would specifically like to thank Philip Brewer and Steve Tyerman. Both have regularly provided insightful feedback, suggested experiments and discussed results. I also have to thank the research and lab managers who make so much of this possible and have never hesitated to help. Ali Mafakheri, Wendy Sullivan and Rebecca Vandeleur have regularly assisted me and for that, I thank you

I also wish to thank those from outside the lab who supported or assisted in this project. Firstly, I would like to thank Heather McFarlane. Heather suggested experiments and discussed results with me. Her insight helped drive the experiments looking at endomembrane trafficking. This project entailed a great deal of microscopy which was undertaken at Adelaide Microscopy. I would like to thank Gwenda Mayo and Jane Sibbons from Adelaide Microscopy for the support they gave. I would also like to thank Rachel Burton, Kylie Neumann and Sandy Khor. The polysaccharide analysis was run in the Burton lab with the assistance of Kylie and Sandy who also engaged in discussion regarding the cell wall aspects of this project. I also thank Jayden Ingles who aided the project at multiple points with mathematical equations and IT insights.

Finally, I thank the University of Adelaide for giving me this opportunity and providing me with a scholarship. I thank the School of Agriculture, Food and Wine for support. I would also like to thank the ARC COE in Plant Energy Biology, through which I received a scholarship, attended workshops and got to experience annual forums.

Chapter 1

Introduction

1.0 Introduction

Ion transport in plants underpins essential processes such as growth, reproduction, cellular signalling, response to environmental stimuli and nutrition (Tang et al., 2020). Transporters at both the plasma membrane (PM) and tonoplast are particularly important for nutrient uptake and re-distribution, osmoregulation and tolerance to salt and toxic elements. Ion transporters are, however, present in all membranes, including membranes of smaller intracellular organelles, yet, the roles of these endomembrane ion transporters are much less understood. This is despite the observation that plants with defects in endomembrane ion transporters exhibit severe phenotypes, pointing to crucial and currently unknown roles of ion transport in smaller organelles (Sze and Chanroj, 2018).

The Arabidopsis (*Arabidopsis thaliana*) Cation Chloride Cotransporter (AtCCC1) is a Cl^- and K^+/Na^+ symporter that has been suggested to localise to endomembranes, as extrapolated from data obtained using a heterologous expression system. *Atccc1* knockouts have severely stunted growth, reduced fertility, increased shoot branching and necrosis of stems (Fig. 1) (Colmenero-Flores et al., 2007; Henderson et al., 2015). The grapevine (*Vitis vinifera*) homolog of *AtCCC1*, *VviCCC1*, when expressed in *Atccc1* plants, rescued the knockout phenotype, suggesting a conserved role of the two proteins (Henderson et al., 2015). The rice (*Oryza sativa*) homolog of AtCCC1, OsCCC1.1, is also important for plant growth. Similar to *Atccc1*, *Osccc1.1* knockouts are dwarfed with low seed yield (Chen et al., 2016; Henderson et al., 2018). *OsCCC1.1* is expressed in all cells of both shoots and roots (Kong et al., 2011; Chen et al., 2016). Similarly, *VviCCC1* is expressed in flowers, tendrils, berries, leaves, petioles, and roots of grapevines, which constitutes all tissues tested (Henderson et al., 2015). *AtCCC1* expression, however, was suggested to be restricted to specific cell and tissue types; expression was assayed using a short 700bp putative promoter, which suggested that AtCCC1 expression is specific to the root tip, vasculature, stamen, hydathodes and pollen (Colmenero-Flores et al., 2007). RNAseq results in Arabidopsis, however, indicate expression of *AtCCC1* in all root cells (Lan et al., 2013; Zhang et al., 2019). It is therefore likely that *AtCCC1* expression would be detected in more cell types with a longer promoter and a more sensitive approach. A broad expression of *AtCCC1*, in combination with the severe phenotypic defects of the knockouts, would suggest a core and fundamental cellular role for the protein in plant growth and

development. Characterising the role of AtCCC1 will therefore contribute to our understanding of intracellular ion transporters and their importance in plant development.

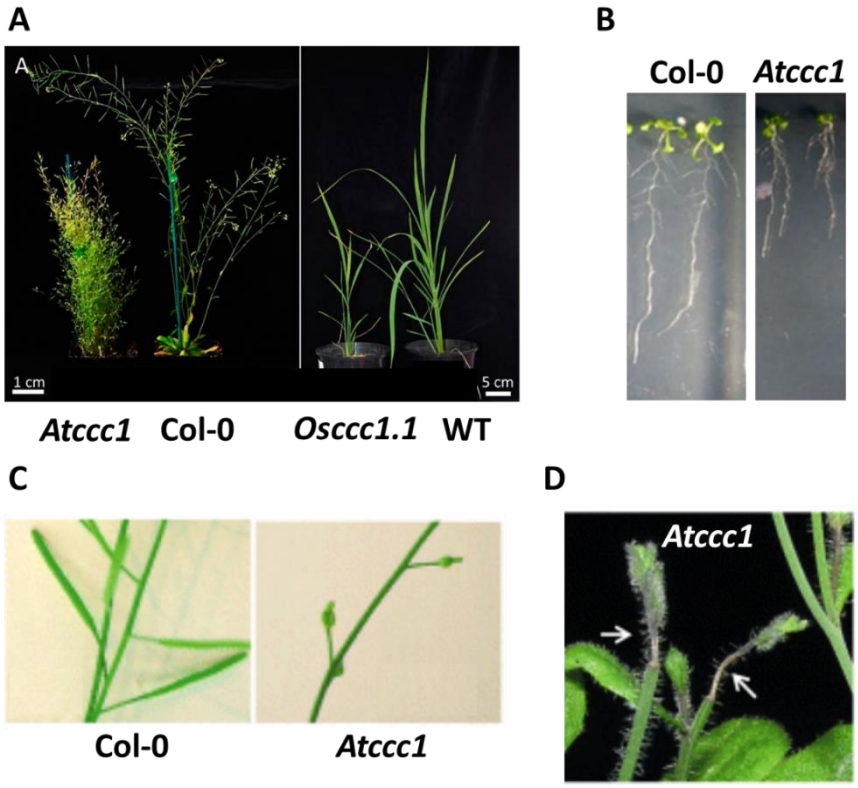

Figure 1. *Atccc1* and *Osccc1.1* knockouts have severe growth and development defects. A) *Atccc1* and *Osccc1.1* plants are dwarfed. *Atccc1* plants exhibit increased shoot branching, B) have shorter roots, C) small siliques with reduced fertility and D) exhibit frequent stem necrosis. Images (modified) from A) Henderson et al. (2018), B) Henderson et al. (2015) and C-D) Colmenero-Flores et al. (2007).

1.1 The Endomembrane System

The endomembrane system is the name given to a group of specialised organelles that, together, mediate the synthesis and delivery of specific proteins and molecules to their target destination. The endomembrane system is labelled as having a forward (anterograde) and backward (retrograde) direction due to the typical flow of cargo through the system (Fig. 2). Synthesis of proteins to be delivered by the endomembrane system occurs in the Endoplasmic Reticulum (ER). From the ER, proteins are transported to the Golgi (Brandizzi, 2018). The Golgi consists of several tubular cisternae. The Golgi is arranged so that the youngest of the cisterna is closest to the ER while the oldest is the furthest from the ER. The side closest to the ER is therefore known as the *cis*-Golgi and the side furthest from the ER is the *trans*-Golgi. The Golgi is the

site of synthesis for molecules such as polysaccharides, which are important for protein glycosylation and cell wall formation (Sinclair et al., 2018). The Golgi derived molecules join the ER derived proteins as cargo of the endomembrane system. The various cargos progress through the Golgi and eventually reach the *trans*-Golgi. The cisternae of the *trans*-Golgi mature and dissociate from the Golgi and become the Trans-Golgi Network/Early Endosome (TGN/EE) (Viotti et al., 2010). The plant TGN/EE is referred to as such because it performs the roles of two separate animal compartments, the TGN and EE (Dettmer et al., 2006). In animals, the TGN is responsible for the delivery of newly synthesised cargo. Meanwhile, the EE is responsible for receiving and sorting cargo endocytosed from the PM. Plant TGN/EE perform both roles and act as a hub for cargo trafficking in plant cells. Cargo from the TGN/EE is typically delivered to the PM or vacuole. At these destinations, soluble cargo is released into the apoplast or vacuole while membrane integral cargo is incorporated into the PM or tonoplast.

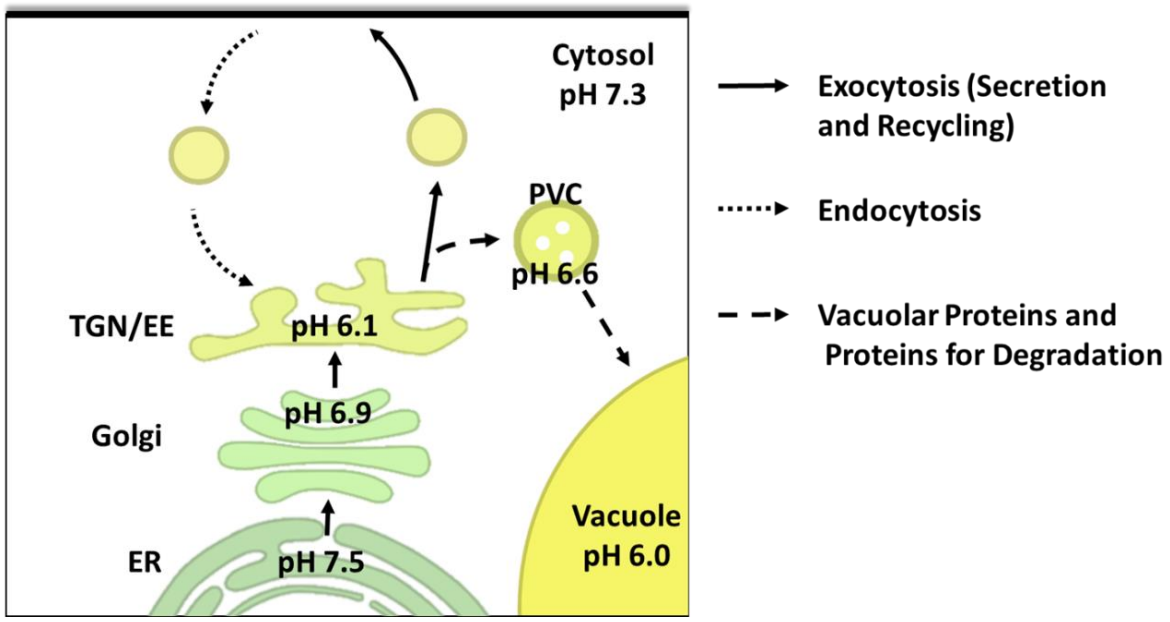

Figure 2. The pH of the endomembrane system typically follows a gradient from endoplasmic reticulum (ER) to vacuole. The pH of each organelle of the endomembrane system as measured in tobacco leaves (Martinière et al., 2013). Arrows indicate the forwards flow of protein cargo through the endomembrane system. Cargo proteins are synthesised in to the ER before transport through the Golgi to the TGN/EE. At the TGN/EE, proteins are either secreted to the PM or to the vacuole through pre-vacuolar compartments (PVC). PM proteins are endocytosed back to the TGN/EE where they are either recycled back to the PM or delivered to the vacuole for degradation.

1.2 TGN and EE

The Plant TGN/EE performs two roles as a site of sorting for both secretory and endocytic trafficking. Secretory trafficking describes the above process where newly synthesised cargo are delivered to the PM or vacuole. In the TGN/EE, this cargo is packed into membrane bound vesicles for delivery. In addition to vesicles, vacuole destined cargo may be packed into Pre-Vacuolar Compartments (PVCs). PVCs are synthesised and cargo is packed into PVCs at the TGN/EE (Cui et al., 2016). The sorting of soluble proteins to the vacuole is mediated by VACUOLAR SORTING RECEPTORS (VSRs). Soluble proteins are, by default, destined for the apoplast. Binding of cargo by VSRs diverts the cargo to the vacuole. VSRs are thought to bind to cargo in the ER or *cis*-Golgi (Robinson and Neuhaus, 2016). The VSRs remain bound to the cargo as it travels through the Golgi and are thought to dissociate from the cargo in the TGN/EE or PVC. After dissociation, the VSR is recycled back to the ER/*cis*-Golgi by the retromer complex (Heucken and Ivanov, 2018). The dissociation of the VSR from its cargo is thought to be mediated by pH (Robinson and Neuhaus, 2016). The pH of the endomembrane system gradually decreases in the forward direction (Fig. 2)(Martinière et al., 2013; Shen et al., 2013). The pH of a solution can impact the strength of protein-protein binding (Kirsch et al., 1994; Robinson and Neuhaus, 2016). The first plant VSR identified, BP-80 from *Pisum sativum* L., has the strongest binding of ligands *in vitro* at pH 6 (Kirsch et al., 1994). Binding is reduced to 50% of maximum at pH 5 and 7.5. This may result in VSR-cargo binding occurring in the ER/*cis*-Golgi where the pH is close to 7, but in the TGN/EE where the pH is around 5.5, VSR-Cargo binding strength may be much lower resulting in dissociation (Robinson and Neuhaus, 2016). Consistent with this, the binding of Arabidopsis VSR2;1 with the cargo, aleurain, is pH sensitive. Decreases in pH as small as 0.25 result in reduced VSR2;1-aleurain binding (Reguera et al., 2015). Cargo bound by VSRs include both hydrolytic proteins and seed storage proteins (Robinson and Neuhaus, 2016; Ashnest and Gendall, 2018). These two groups of proteins have two different destinations. Hydrolytic proteins are delivered to the lytic vacuole while seed storage proteins are delivered to the specialised protein storage vacuole in seeds. While VSRs mediate the sorting of soluble proteins entering the secretory pathway, it is not yet known how membrane integral proteins are sorted for delivery to the PM or tonoplast.

In animal cells, the EE is an important site for endocytic trafficking (Scott et al., 2014). At the PM, vesicles are formed that carry PM integral proteins to the EE. In plants, endocytic cargo is delivered to the TGN/EE (Dettmer et al., 2006). At the TGN/EE, the endocytosed PM proteins are either recycled or delivered to the vacuole. Recycled proteins are delivered from the TGN/EE to the PM to resume function. PM proteins delivered to the vacuole are degraded there (Schwihla and Korbei, 2020). Sorting of PM proteins in the endocytic pathway is mediated by the Endosomal Sorting Complex Required for Transport (ESCRT) complex. The ESCRT complex binds cargo in the TGN/EE and packs the protein into PVCs for delivery to the vacuole. Binding of proteins by the ESCRT complex was thought to be mediated by ubiquitination, however, it was recently demonstrated that ESCRT can bind the PM associated abscisic acid (ABA) receptor, PYRABACTIN RESISTANCE1-LIKE 4 (PYL4) without a ubiquitin tag (García-León et al., 2019). In contrast, ubiquitination of the brassinosteroid receptor, BRASSINOSTEROID INSENSITIVE 1 (BRI1), and the boron transporter, REQUIRES HIGH BORON 1 (BOR1), is required for degradation. A ubiquitination-defective BRI1, with no sites for ubiquitination displays no trafficking of the BRI1 construct to the vacuole (Martins et al., 2015). Likewise, removal of a ubiquitination site in BOR1, resulted in constitutive recycling of BOR1 from the TGN/EE to the PM and a lack of protein being sent to the vacuole for degradation (Kasai et al., 2011). The relationship between recycling and degradation routes for endocytic cargo is important for regulating protein abundance at the PM. VACUOLAR PROTEIN SORTING 23A (VPS23A) is an ESCRT complex subunit that interacts with PYL4. *vps23A* knockouts exhibit reduced PYL4 degradation and are ABA sensitive (Yu et al., 2016). Likewise, expression of mutant *BRI1* with no ubiquitin sites results in brassinosteroid sensitivity (Martins et al., 2015).

1.3 Luminal Regulation of the Endomembrane System

Each organelle of the endomembrane system has a distinct pH. While the pH of the cytosol, vacuole and apoplast of plants has been assayed multiple times in the past decades, without dyes specific to endomembrane organelles, the pH of endomembrane organelles could not be measured (Taiz, 1992; Bibikova et al., 1998; Scott and Allen, 1999). In 2013, two groups published the first results measuring the pH of the smaller endomembrane system organelles (Martinière et al., 2013; Shen et al., 2013). Both groups used the genetically encoded pH sensor pHluorin. The sensor was directed to specific compartments by fusion with known markers of

the respective compartments. Martinière et al. (2013) transiently expressed the constructs in tobacco epidermal leaf cells. They obtained pH values for the ER (pH = 7.5), *trans*-Golgi (pH = 6.9), TGN/EE (pH = 6.1), PVC (pH = 6.6) and late PVC (pH = 7.1) (Fig. 2). Shen et al. (2013) transiently expressed sensors in Arabidopsis leaf protoplasts. pH values were measured for the ER (pH = 7.2), *cis*-Golgi (pH = 6.7), TGN/EE (pH = 6.9), PVC (pH = 6.1) and vacuole (pH = 7.0). More recently, the pH sensor pHusion was utilised for endomembrane pH measurement (Luo et al., 2015). pHusion features a tandem EGFP-mRFP for pH detection (Gjetting et al., 2012). pHusion was tagged to rat (*Rattus norvegicus*) ST and Arabidopsis SYP61, and stably expressed in Arabidopsis to measure the pH of *trans*-Golgi (pH = 6.3) and TGN/EE (pH = 5.6) in Arabidopsis roots (Luo et al., 2015). The pH values measured with pHusion were lower than previously measured with pHlurion. This may reflect the different tissue assayed, leaf or root, and preparation methods.

A limited number of transporters involved in the pH regulation of the Arabidopsis TGN/EE lumen have been identified (Sze and Chanroj, 2018). The lumen is acidified by a proton pump, the V-H^+-ATPase (Luo et al., 2015). V-H^+-ATPase is a complex localised at both the TGN/EE and tonoplast. Specific subunits define the localisation of the V-H^+-ATPase with subunit a1 resulting in TGN/EE localisation (Dettmer et al., 2006). The cation proton antiporters, SODIUM HYDROGEN EXCHANGER 5 (NHX5) and NHX6, exchange luminal protons for cytosolic K^+ resulting in an alkaline shift in the TGN/EE pH (Bassil et al., 2011; Reguera et al., 2015). Two putative anion proton antiporters, CHLORINE CHANNEL D (CLCd) and CLCf, also localise to the TGN/EE (Marmagne et al., 2007; von der Fecht-Bartenbach et al., 2007). The transport of Cl^- is likely essential to this network to provide the counter ion to the positively charged H^+, however, work in mice has shown that the antiporter function of lysosomal CLCs is important for their function as well (Novarino et al., 2010). Combining the pump and transporters, the current model of the TGN/EE pH regulating network contains influx and efflux pathways for H^+, while for K^+ and Cl^-, only the influx pathways are known (Fig. 3). No mechanism for efflux of K^+ and Cl^- has been identified in the TGN/EE, which would be essential to regulate ion accumulation and complete the dynamic transport circuit

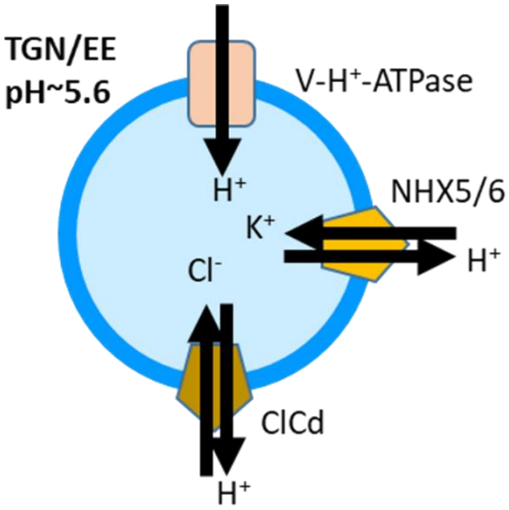

Figure 3. The TGN/EE luminal pH is regulated by proton and ion transporters. Currently identified members of the TGN/EE pH regulatory network include the TGN/EE localised proton pump, V-H^+-ATPase; the K^+/H^+ antiporters, NHX5 and 6; and the Cl^-/H^+ antiporter, CLCd. Not yet identified is a mechanism for ion efflux to prevent accumulation of Cl^- and K^+ imported by the antiporters. The displayed pH of 5.6 is as measured in Arabidopsis epidermal root cells (Luo, 2015).

The pH of the TGN/EE is important for its function. Plants with disrupted TGN/EE pH regulation show severe generalised phenotypes. *de-etiolated 3 (det3)* is a mutant with a weak mutation in subunit C of the V-H^+-ATPase. These plants have a higher TGN/EE pH and exhibit severe growth and developmental defects (Schumacher et al., 1999; Luo et al., 2015). *nhx5/nhx6* double mutants have a lower TGN/EE pH, which similarly leads to severe growth impairments (Bassil et al., 2011; Reguera et al., 2015). In addition to both *det3* and *nhx5/nhx6* plants being much smaller than wildtype, both plants have defects in the endocytic trafficking pathway, particularly, recycling (Dettmer et al., 2006; Bassil et al., 2011; Luo et al., 2015; Dragwidge et al., 2019). The stunted growth and reduced protein recycling in these pH regulatory mutants highlights the importance of TGN/EE pH in endomembrane trafficking and therefore plant development. Interestingly, it is speculated that pH is important for VSR binding, but both mutants have defects in the endocytic pathway, a pathway in which VSRs are not thought to be involved. In mammalian cells, it was found the pH of the TGN lumen is important for the recruitment of proteins involved in the formation of vesicles (Hurtado-Lorenzo et al., 2006; Marshansky, 2007). If this is the case in plant TGN/EE as well, then

TGN/EE regulatory mutants may have defective vesicle formation resulting in reduced trafficking.

1.4 The Cargo of the Endomembrane System

The cargo of the endomembrane system might be a key part of defining the observed phenotypes of trafficking defective mutants. Characterised cargo of endomembrane trafficking include proteins involved in hormone signalling, cell wall regulation, pathogen detection, nutrient uptake and water transport. Proteins important for the signal transduction of a few different hormones have been identified. Abscisic acid (ABA) is a hormone important for response to abiotic stress. The abundance of PYL4 at the PM is dependent on TGN/EE mediated recycling (Belda-Palazon et al., 2016). Brassinosteroids are growth hormones. In the absence of brassinosteroid detection, plants are severely dwarfed (Clouse et al., 1996). Defective trafficking of the brassinosteroid receptor, BRI1, and altered brassinosteroid response have been observed in several endomembrane trafficking mutants including *det3* and *nhx5/nhx6* (Luo et al., 2015; Dragwidge et al., 2019). Salicylic acid is a hormone involved in pathogen response. Defects in the ESCRT complex can result in upregulation of salicylic signalling (Katsiarimpa et al., 2013). The source of the upregulation is yet to be identified.

In addition, auxin transporters are highly dependent on a fully functioning endomembrane system. Auxin is a hormone vital for plant growth and development. Auxin impacts cell expansion, cell differentiation, cell division, lateral root formation, shoot architecture and flowering (Leyser, 2018). Due to the core role of auxin in regulating plant development, defects in auxin are highly conspicuous. PM localised auxin transporters are important for both cellular response to auxin and for mediating normal distribution of the hormone at the tissue level (Grones and Friml, 2015). AUXIN RESISTANT 1 (AUX1) imports auxin into cells while PM localised PIN-FORMED (PIN) proteins efflux auxin from cells. Endomembrane trafficking is important for the delivery and regulation of AUX1 and PINs such as PIN1 and PIN2 (Feraru and Friml, 2008). Defects in PIN1 and PIN2 abundance at the PM, such as in *nhx5/nhx6*, result in changes to auxin distribution (Dragwidge et al., 2018).

In addition to proteins, the endomembrane system is also important for synthesis and delivery of cell wall components. Polysaccharides such as pectins and xyloglucans are synthesised in the Golgi before trafficking through the TGN/EE and secretion into the apoplast (Driouich et al., 2012). Knockouts of the TGN/EE proteins *echidna* (*ech)* or *ypt/rab gtpase interacting protein 4a* (*yip4a)* and *yip4b* results in reduced secretion of pectins and xyloglucan as well as a drastic reduction in cell elongation (Gendre et al., 2013; McFarlane et al., 2013). Cell wall structural proteins such as arabinogalactan are thought to be delivered to the apoplast through the endomembrane system (Sinclair et al., 2018). Some cell wall components such as cellulose are synthesised at the PM by cellulose synthase complexes (Endler and Persson, 2011). The trafficking of cellulose synthases is reduced in *det3* plants, as is total cell wall cellulose, indicating a role of the TGN/EE in the delivery or regulation of these proteins (Luo et al., 2015). The cell wall is the first line of defence for plants against pathogens. Changes in cell wall composition results in changes to pathogen resistance, with *det3* plants having an increased resistance to pathogens (Rogers et al., 2005; Molina et al., 2021). In addition to cell wall changes, endomembrane trafficking mutants may also have altered pathogen resistance due to the role of trafficking in the delivery and maintenance of the pathogen receptor FLAGELLIN SENSITIVE 2 (FLS2) (Gu et al., 2017). *clcd* plants lack a TGN/EE H^+/Cl^- antiporter and have increased resistance to *Pseudomonas syringae* pv. tomato DC30000 (*pst.* DC3000) and increased pathogen triggered immunity responses (Guo et al., 2014).

At the PM there are numerous channels and transporters involved in nutrient acquisition, regulation of toxic elements, regulation of water permeability and osmoregulation. Both deficiency and over accumulation of many micronutrients such as iron, zinc and boron, have negative impacts on plants (Schat, 1999). Therefore, tight regulation of micronutrient transporters is important to maintain safe concentrations.

The boron transporter, BOR1, is a PM localised transporter reliant on ESCRT mediated degradation to regulate abundance and therefore boron accumulation (Kasai et al., 2011). The iron transporter, IRT1, accumulates in the TGN/EE of root hairs (Barberon et al., 2011). The primary site of activity for IRT1, however, is the PM. IRT1 cycles between the TGN/EE and PM and this was proposed as a mechanism that allows for much tighter regulation of IRT1 activity and therefore, tight regulation over iron accumulation (Barberon et al., 2011).

Phosphorous is a plant macronutrient that is obtained through root uptake via transporters such as PHT1. Under phosphate sufficient conditions, PHT1 undergoes ESCRT mediated degradation (Cardona-López et al., 2015). Aquaporins regulate membrane water permeability and in response to osmotic stress, several PM aquaporins such as PLASMA MEMBRANE INTRINSIC PROTEIN 2;1 (PIP2;1) and PIP2;7 are internalised (Boursiac et al., 2008; Hachez et al., 2014). Internalisation of PIPs reduces the water permeability of the PM and therefore can reduce the loss of water and volume when cells are challenged with osmotic stress. Six hours after treatment with salt, PIP2;1 is found in vacuolar lumens (Ueda et al., 2016). PIP2;1 undergoes constitutive cycling between the TGN/EE and PM , but in response to salt or osmotic shock, it is likely that there is a reduction in the recycling of PIPs such as PIP2;1 and an increased trafficking towards the vacuole to mediate degradation of the proteins (Li et al., 2011b). Other PM proteins are likely to require conditional regulation of abundance, such as transporters involved in salt tolerance. However, much less is known about the role of the endomembrane system in salt and osmotic stress tolerance.

1.5 The Role of the Endomembrane System in Salt and Osmotic Tolerance

Salt stress in plants can result in reduced water uptake, nutrient depletion, reduced growth and even plant death (Isayenkov and Maathuis, 2019). Salt stress is a combinatorial stress made up of two factors, ionic toxicity and osmotic stress. Ionic toxicity is primarily caused by over accumulation of Na^+, which competes with crucial K^+, and results in K^+ depletion (Assaha et al., 2017). Osmotic stress is caused by high concentrations of Na^+ and Cl^- in the soil, causing an increased soil osmolality. Root cells rely on an osmotic potential to mediate water uptake and turgor driven cell growth. The high osmotic potential is created in root cells by maintaining a higher osmolality in root cells compared to the surrounding soil. This osmotic potential is reduced as the osmolality of the surrounding soil increase and therefore results in constraints in cell growth and water uptake. To mitigate osmotic stress, plants will increase the uptake of soil osmolytes and induce the synthesis of organic osmolytes such as proline and glycine betaine (Shabala and Lew, 2002; Sharma et al., 2019).

There is increasing evidence that the endomembrane system may be important for salt and osmotic stress responses. Knockouts of ARA6, a Rab GTPase involved in TGN/EE to PM trafficking, are salt sensitive (Ebine et al., 2011). VPS4 is required for the disassembly and

recycling of the ESCRT complex. VPS4 knockdowns are salt sensitive and seedlings exhibit a drastically increased Na^+/K^+ ratio (Ho et al., 2010). Two members of the TGN/EE pH regulatory network also exhibit salt sensitivity, with *det3* and *nhx5/nhx6* plants both being salt sensitive (Krebs et al., 2010; Bassil et al., 2011). Interestingly, overexpression of Arabidopsis NHX5 in soybean (*Glycine max*) or paper mulberry (*Broussonetia papyrifera* L. Vent) resulted in salt tolerant plants (Li et al., 2011a; Wu et al., 2016). In both cases, concentrations of proline were higher in NHX5 overexpressing plants than wildtype. In the paper mulberry plants, overexpression of Arabidopsis NHX5 also resulted in improved drought tolerance and an increase of Na^+ and K^+ in leaves. These results indicate that the endomembrane system may also have a role in salt tolerance of plants.

1.6 Cation Chloride Cotransporter

AtCCC1 is a Cl^- and K^+/Na^+ symporter that stoichiometrically links the transport of anions and cation. The sub-cellular localisation of AtCCC1 was assayed by transiently expressing an AtCCC1-GFP fusion in tobacco (*Nicotiana tabacum*) leaf cells (Henderson et al., 2015). AtCCC1-GFP was found to partially co-localise with markers of the *cis*-Golgi (MAN1-RFP) and the TGN/EE (RFP-SYP61). AtCCC1 has also been identified in the TGN/EE through several proteomics studies (Sadowski et al., 2008; Drakakaki et al., 2012; Groen et al., 2014; Nikolovski et al., 2014; Parsons et al., 2019). It was further noted as a marker of the TGN/EE by Parsons et al. (2019) and used as part of a training dataset for their study. Contradictory to this, imaging of *AtCCC1-GFP* stably expressed in Arabidopsis pollen tubes was interpreted by authors as PM localisation in pollen tube shanks and cytoplasmic in tips (Domingos et al., 2019). Similar localisation attempts have been made with OsCCC1.1. The signal pattern of transiently expressed OsCCC1.1-GFP in onion epidermal cells was interpreted as PM localisation (Kong et al., 2011). Localisation of OsCCC1.1 in fixed rice root cells using antibodies may indicate PM localisation in addition to other membranes (Chen et al., 2016).

AtCCC1 has been identified to have a role in several plant processes including cell growth, cell wall synthesis, pathogen response and root to shoot transport. The underlying mechanism by which AtCCC1 influences these processes was not previously identified. The cell wall composition of *Atccc1* is altered and mutants show a large reduction in cellulose compared to wildtype plants, in tissue specified as either hypocotyl or leaves (Han et al., 2020). There was

an increase in the abundance of all other cell wall material assayed. This is similar to observations in *det3*. *det3* plants also have decreased cell wall cellulose and increased fucose, rhamnose and xylose (Rogers et al., 2005; Luo et al., 2015). *Atccc1* leaves are also more susceptible to infection by the bacterial pathogen, *pst.* DC3000 (Han et al., 2020). While the resistance to *pst.* DC3000 was reduced in *Atccc1*, the early pathogen triggered immunity response was increased. Compared to wildtype, *Atccc1* plants displaying increased ROS production and salicylic acid in response to the bacterial marker flg22. Interestingly, defective endocytosis of the flg22 receptor, FLS2, results in increased early pathogen triggered immunity response and decreased late response, including a decreased resistance to *pst.* DC3000 (Gu et al., 2017). This may suggest that AtCCC1 is important for endocytosis.

Due to AtCCC1 being capable of transporting Cl^- and Na^+/K^+, there has been interest in its potential role in salinity tolerance. *Atccc1* plants display alterations in root to shoot ion transport. Hydroponically grown *Atccc1* plants exhibit increased accumulation of K^+, Cl^- and Na^+ in shoots under high salt (50 mM NaCl) conditions (Henderson et al., 2015). No other ions were measured, however, and the increased ion content might therefore not be directly connected to the transport of these ions through AtCCC1 but rather, could be a general effect. Soil grown *Atccc1* plants were found to have increased shoot, and decreased root, Cl^- accumulation when grown in 50 mM Cl^- salts (Colmenero-Flores et al., 2007). Similarly, no other ions were investigated. It was suggested that AtCCC1, a Cl^- and K^+/Na^+ transporter, is involved in the uptake of ions from the xylem to reduce shoot Cl^-, Na^+ and K^+ accumulation during salt stress. This, however, does not match the expression pattern of *AtCCC1* or the putative sub-cellular localisation of AtCCC1. These results do, however, support other previously mentioned studies that suggest a possible link between the TGN/EE and salt tolerance.

Atccc1 plants share phenotypical characteristics with *det3* plants. Therefore, given the expression and putative localisation of AtCCC1, it may be possible that AtCCC1 is important for the function of the TGN/EE like the V-H^+-ATPase. The V-H^+-ATPase is part of the pH regulatory network that includes NHX5, NHX6 and CLCd. The current model of this network includes mechanisms of Cl^- and K^+ influx but is yet to identify a mechanism for efflux of these ions. AtCCC1 has the potential to fulfil the role of a K^+ and Cl^- shunt in the TGN/EE pH

regulatory network, therefore regulating luminal K^+ and Cl^- concentrations, enabling efficient activity of the other transporters and maintaining pH regulation.

1.7 Aims

AtCCC1 appears to have a crucial, previously uncharacterised role, in plant growth and development. This thesis aims to address this by further characterising the role of AtCCC1. We postulate that AtCCC1 may be involved in regulation of the TGN/EE, however, the localisation of AtCCC1 is somewhat disputed. We therefore aim to address the localisation of AtCCC1 by stably expressing a fluorescently tagged AtCCC1 and perform a quantitative co-localisation analysis. This project aims to investigate the role of AtCCC1 in the TGN/EE by measuring the pH of the TGN/EE in *Atccc1* plants and assaying the osmoregulatory capacity of the TGN/EE without AtCCC1. The role of AtCCC1 in the TGN/EE will be further supported by assaying endomembrane trafficking in *Atccc1* to detect if the protein is required for normal TGN/EE function. We also aim to investigate the source of some phenotypes in *Atccc1* and if trafficking has the potential to impact them. In particular, we will investigate the role of the TGN/EE in osmotic and salt tolerance, where there may be a previously uncharacterised link between the TGN/EE and osmotic tolerance.

1.8 References

Ashnest, J.R., and Gendall, A.R. (2018). Trafficking to the seed protein storage vacuole. Functional Plant Biology **45,** 895-910.

Assaha, D.V.M., Ueda, A., Saneoka, H., Al-Yahyai, R., and Yaish, M.W. (2017). The role of Na^+ and K^+ transporters in salt stress adaptation in glycophytes. Frontiers in Physiology **8,** 509.

Barberon, M., Zelazny, E., Robert, S., Conéjéro, G., Curie, C., Friml, J., and Vert, G. (2011). Monoubiquitin-dependent endocytosis of the iron-regulated transporter 1 (IRT1) transporter controls iron uptake in plants. Proceedings of the National Academy of Sciences **108,** E450-458.

Bassil, E., Ohto, M.A., Esumi, T., Tajima, H., Zhu, Z., Cagnac, O., Belmonte, M., Peleg, Z., Yamaguchi, T., and Blumwald, E. (2011). The Arabidopsis intracellular Na^+/H^+ antiporters NHX5 and NHX6 are endosome associated and necessary for plant growth and development. Plant Cell **23,** 224-239.

Belda-Palazon, B., Rodriguez, L., Fernandez, M.A., Castillo, M.C., Anderson, E.M., Gao, C., Gonzalez-Guzman, M., Peirats-Llobet, M., Zhao, Q., De Winne, N., Gevaert, K., De Jaeger, G., Jiang, L., León, J., Mullen, R.T., and Rodriguez, P.L. (2016). FYVE1/FREE1 interacts with the PYL4 ABA receptor and mediates its delivery to the vacuolar degradation pathway. Plant Cell **28,** 2291-2311.

Bibikova, T.N., Jacob, T., Dahse, I., and Gilroy, S. (1998). Localized changes in apoplastic and cytoplasmic pH are associated with root hair development in *Arabidopsis thaliana*. Development **125,** 2925-2934.

Boursiac, Y., Boudet, J., Postaire, O., Luu, D.T., Tournaire-Roux, C., and Maurel, C. (2008). Stimulus-induced downregulation of root water transport involves reactive oxygen species-activated cell signalling and plasma membrane intrinsic protein internalization. Plant Journal **56,** 207-218.

Brandizzi, F. (2018). Transport from the endoplasmic reticulum to the Golgi in plants: Where are we now? Seminars in Cell and Developmental Biology **80,** 94-105.

Cardona-López, X., Cuyas, L., Marín, E., Rajulu, C., Irigoyen, M.L., Gil, E., Puga, M.I., Bligny, R., Nussaume, L., Geldner, N., Paz-Ares, J., and Rubio, V. (2015). ESCRT-III-associated protein ALIX mediates high-affinity phosphate transporter trafficking to maintain phosphate homeostasis in Arabidopsis. Plant Cell **27,** 2560-2581.

Chen, Z.C., Yamaji, N., Fujii-Kashino, M., and Ma, J.F. (2016). A cation-chloride cotransporter gene is required for cell elongation and osmoregulation in rice. Plant Physiology **171,** 494-507.

Clouse, S.D., Langford, M., and McMorris, T.C. (1996). A brassinosteroid-insensitive mutant in *Arabidopsis thaliana* exhibits multiple defects in growth and development. Plant Physiology **111,** 671-678.

Colmenero-Flores, J.M., Martínez, G., Gamba, G., Vázquez, N., Iglesias, D.J., Brumós, J., and Talón, M. (2007). Identification and functional characterization of cation-chloride cotransporters in plants. Plant Journal **50,** 278-292.

Cui, Y., Shen, J., Gao, C., Zhuang, X., Wang, J., and Jiang, L. (2016). Biogenesis of plant prevacuolar multivesicular bodies. Molecular Plant **9,** 774-786.

Dettmer, J., Hong-Hermesdorf, A., Stierhof, Y.D., and Schumacher, K. (2006). Vacuolar H^+-ATPase activity is required for endocytic and secretory trafficking in Arabidopsis. Plant Cell **18,** 715-730.

Domingos, P., Dias, P.N., Tavares, B., Portes, M.T., Wudick, M.M., Konrad, K.R., Gilliham, M., Bicho, A., and Feijó, J.A. (2019). Molecular and electrophysiological characterization of anion transport in *Arabidopsis thaliana* pollen reveals regulatory roles for pH, Ca^{2+} and GABA. New Phytologist **223,** 1353-1371.

Dragwidge, J.M., Scholl, S., Schumacher, K., and Gendall, A.R. (2019). NHX-type $Na^+(K^+)/H^+$ antiporters are required for TGN/EE trafficking and endosomal ion homeostasis in *Arabidopsis thaliana*. Journal of Cell Science **132**.

Dragwidge, J.M., Ford, B.A., Ashnest, J.R., Das, P., and Gendall, A.R. (2018). Two endosomal NHX-type Na^+/H^+ antiporters are involved in auxin-mediated development in *Arabidopsis thaliana*. Plant Cell Physiology **59,** 1660-1669.

Drakakaki, G., van de Ven, W., Pan, S., Miao, Y., Wang, J., Keinath, N.F., Weatherly, B., Jiang, L., Schumacher, K., Hicks, G., and Raikhel, N. (2012). Isolation and proteomic analysis of the SYP61 compartment reveal its role in exocytic trafficking in Arabidopsis. Cell research **22,** 413-424.

Driouich, A., Follet-Gueye, M.L., Bernard, S., Kousar, S., Chevalier, L., Vicré-Gibouin, M., and Lerouxel, O. (2012). Golgi-mediated synthesis and secretion of matrix polysaccharides of the primary cell wall of higher plants. Frontiers in Plant Science **3,** 79.

Ebine, K., Fujimoto, M., Okatani, Y., Nishiyama, T., Goh, T., Ito, E., Dainobu, T., Nishitani, A., Uemura, T., Sato, M.H., Thordal-Christensen, H., Tsutsumi, N., Nakano, A., and Ueda, T. (2011). A membrane trafficking pathway regulated by the plant-specific RAB GTPase ARA6. Nature Cell Biology **13,** 853-859.

Endler, A., and Persson, S. (2011). Cellulose synthases and synthesis in Arabidopsis. Molecular Plant **4,** 199-211.

Feraru, E., and Friml, J. (2008). PIN polar targeting. Plant Physiology **147,** 1553-1559.

García-León, M., Cuyas, L., El-Moneim, D.A., Rodriguez, L., Belda-Palazón, B., Sanchez-Quant, E., Fernández, Y., Roux, B., Zamarreño Á, M., García-Mina, J.M., Nussaume, L., Rodriguez, P.L., Paz-Ares, J., Leonhardt, N., and Rubio, V. (2019). Arabidopsis ALIX regulates stomatal aperture and turnover of abscisic acid receptors. Plant Cell **31,** 2411-2429.

Gendre, D., McFarlane, H.E., Johnson, E., Mouille, G., Sjödin, A., Oh, J., Levesque-Tremblay, G., Watanabe, Y., Samuels, L., and Bhalerao, R.P. (2013). Trans-Golgi network localized ECHIDNA/Ypt interacting protein complex is required for the secretion of cell wall polysaccharides in Arabidopsis. Plant Cell **25,** 2633-2646.

Gjetting, K.S., Ytting, C.K., Schulz, A., and Fuglsang, A.T. (2012). Live imaging of intra- and extracellular pH in plants using pHusion, a novel genetically encoded biosensor. Journal of Experimental Botany **63,** 3207-3218.

Groen, A.J., Sancho-Andrés, G., Breckels, L.M., Gatto, L., Aniento, F., and Lilley, K.S. (2014). Identification of trans-golgi network proteins in *Arabidopsis thaliana* root tissue. Journal of proteome research **13,** 763-776.

Grones, P., and Friml, J. (2015). Auxin transporters and binding proteins at a glance. Journal of cell science **128,** 1-7.

Gu, Y., Zavaliev, R., and Dong, X. (2017). Membrane trafficking in plant immunity. Molecular Plant **10,** 1026-1034.

Guo, W., Zuo, Z., Cheng, X., Sun, J., Li, H., Li, L., and Qiu, J.L. (2014). The chloride channel family gene CLCd negatively regulates pathogen-associated molecular pattern (PAMP)-triggered immunity in Arabidopsis. Journal of Experimental Botany **65,** 1205-1215.

Hachez, C., Veljanovski, V., Reinhardt, H., Guillaumot, D., Vanhee, C., Chaumont, F., and Batoko, H. (2014). The Arabidopsis abiotic stress-induced TSPO-related protein reduces cell-surface expression of the aquaporin PIP2;7 through protein-protein interactions and autophagic degradation. Plant Cell **26,** 4974-4990.

Han, B., Jiang, Y., Cui, G., Mi, J., Roelfsema, M.R.G., Mouille, G., Sechet, J., Al-Babili, S., Aranda, M., and Hirt, H. (2020). CATION-CHLORIDE CO-TRANSPORTER 1 (CCC1) mediates plant resistance against *Pseudomonas syringae*. Plant Physiology **182,** 1052-1065.

Henderson, S.W., Wege, S., and Gilliham, M. (2018). Plant cation-chloride cotransporters (CCC): evolutionary origins and functional insights. International Journal of Molecular Sciences **19**

Henderson, S.W., Wege, S., Qiu, J., Blackmore, D.H., Walker, A.R., Tyerman, S.D., Walker, R.R., and Gilliham, M. (2015). Grapevine and Arabidopsis cation-chloride cotransporters localize to the Golgi and trans-Golgi network and indirectly influence long-distance ion transport and plant salt tolerance. Plant Physiology **169,** 2215-2229.

Heucken, N., and Ivanov, R. (2018). The retromer, sorting nexins and the plant endomembrane protein trafficking. Journal of Cell Science **131**.

Ho, L.-W., Yang, T.-T., Shieh, S.-S., Edwards, G.E., and Yen, H.E. (2010). Reduced expression of a vesicle trafficking-related ATPase SKD1 decreases salt tolerance in Arabidopsis. Functional Plant Biology **37,** 962-973.

Hurtado-Lorenzo, A., Skinner, M., El Annan, J., Futai, M., Sun-Wada, G.H., Bourgoin, S., Casanova, J., Wildeman, A., Bechoua, S., Ausiello, D.A., Brown, D., and Marshansky, V. (2006). V-ATPase interacts with ARNO and Arf6 in early endosomes and regulates the protein degradative pathway. Nature Cell Biology **8,** 124-136.

Isayenkov, S.V., and Maathuis, F.J.M. (2019). Plant salinity stress: many unanswered questions remain. Frontiers in Plant Science **10,** 80.

Kasai, K., Takano, J., Miwa, K., Toyoda, A., and Fujiwara, T. (2011). High boron-induced ubiquitination regulates vacuolar sorting of the BOR1 borate transporter in *Arabidopsis thaliana*. Journal of Biological Chemistry **286,** 6175-6183.

Katsiarimpa, A., Kalinowska, K., Anzenberger, F., Weis, C., Ostertag, M., Tsutsumi, C., Schwechheimer, C., Brunner, F., Hückelhoven, R., and Isono, E. (2013). The deubiquitinating enzyme AMSH1 and the ESCRT-III subunit VPS2.1 are required for autophagic degradation in Arabidopsis. Plant Cell **25,** 2236-2252.

Kirsch, T., Paris, N., Butler, J.M., Beevers, L., and Rogers, J.C. (1994). Purification and initial characterization of a potential plant vacuolar targeting receptor. Proceedings of the National Academy of Sciences **91,** 3403-3407.

Kong, X.Q., Gao, X.H., Sun, W., An, J., Zhao, Y.X., and Zhang, H. (2011). Cloning and functional characterization of a cation-chloride cotransporter gene OsCCC1. Plant Molecular Biology **75,** 567-578.

Krebs, M., Beyhl, D., Görlich, E., Al-Rasheid, K.A., Marten, I., Stierhof, Y.D., Hedrich, R., and Schumacher, K. (2010). Arabidopsis V-ATPase activity at the tonoplast is required for efficient nutrient storage but not for sodium accumulation. Proceedings of the National Academy of Sciences **107,** 3251-3256.

Lan, P., Li, W., Lin, W.D., Santi, S., and Schmidt, W. (2013). Mapping gene activity of Arabidopsis root hairs. Genome Biololgy **14,** R67.

Leyser, O. (2018). Auxin signaling. Plant Physiology **176,** 465-479.

Li, M., Li, Y., Li, H., and Wu, G. (2011a). Overexpression of AtNHX5 improves tolerance to both salt and drought stress in Broussonetia papyrifera (L.) Vent. Tree physiology **31,** 349-357.

Li, X., Wang, X., Yang, Y., Li, R., He, Q., Fang, X., Luu, D.T., Maurel, C., and Lin, J. (2011b). Single-molecule analysis of PIP2;1 dynamics and partitioning reveals multiple modes of Arabidopsis plasma membrane aquaporin regulation. Plant Cell **23,** 3780-3797.

Luo, Y., Scholl, S., Doering, A., Zhang, Y., Irani, N.G., Rubbo, S.D., Neumetzler, L., Krishnamoorthy, P., Van Houtte, I., Mylle, E., Bischoff, V., Vernhettes, S., Winne, J., Friml, J., Stierhof, Y.D., Schumacher, K., Persson, S., and Russinova, E. (2015). V-ATPase activity in the TGN/EE is required for exocytosis and recycling in Arabidopsis. Nature Plants **1,** 15094.

Marmagne, A., Vinauger-Douard, M., Monachello, D., de Longevialle, A.F., Charon, C., Allot, M., Rappaport, F., Wollman, F.A., Barbier-Brygoo, H., and Ephritikhine, G. (2007). Two members of the Arabidopsis CLC (chloride channel) family, AtCLCe and AtCLCf, are associated with thylakoid and Golgi membranes, respectively. Journal of Experimental Botany **58,** 3385-3393.

Marshansky, V. (2007). The V-ATPase a2-subunit as a putative endosomal pH-sensor. Biochemical Society Transactions **35,** 1092-1099.

Martinière, A., Bassil, E., Jublanc, E., Alcon, C., Reguera, M., Sentenac, H., Blumwald, E., and Paris, N. (2013). In vivo intracellular pH measurements in tobacco and Arabidopsis reveal an unexpected pH gradient in the endomembrane system. Plant Cell **25,** 4028-4043.

Martins, S., Dohmann, E.M., Cayrel, A., Johnson, A., Fischer, W., Pojer, F., Satiat-Jeunemaître, B., Jaillais, Y., Chory, J., Geldner, N., and Vert, G. (2015). Internalization and vacuolar targeting of the brassinosteroid hormone receptor BRI1 are regulated by ubiquitination. Nature Communications **6,** 6151.

McFarlane, H.E., Watanabe, Y., Gendre, D., Carruthers, K., Levesque-Tremblay, G., Haughn, G.W., Bhalerao, R.P., and Samuels, L. (2013). Cell wall polysaccharides are mislocalized to the vacuole in *echidna* mutants. Plant Cell Physiology **54,** 1867-1880.

Molina, A., Miedes, E., Bacete, L., Rodríguez, T., Mélida, H., Denancé, N., Sánchez-Vallet, A., Rivière, M.P., López, G., Freydier, A., Barlet, X., Pattathil, S., Hahn, M., and Goffner, D. (2021). Arabidopsis cell wall composition determines disease resistance specificity and fitness. Proceedings of the National Academy of Sciences **118**.

Nikolovski, N., Shliaha, P.V., Gatto, L., Dupree, P., and Lilley, K.S. (2014). Label-free protein quantification for plant Golgi protein localization and abundance. Plant Physiology **166,** 1033-1043.

Novarino, G., Weinert, S., Rickheit, G., and Jentsch, T.J. (2010). Endosomal chloride-proton exchange rather than chloride conductance is crucial for renal endocytosis. Science **328,** 1398-1401.

Parsons, H.T., Stevens, T.J., McFarlane, H.E., Vidal-Melgosa, S., Griss, J., Lawrence, N., Butler, R., Sousa, M.M.L., Salemi, M., Willats, W.G.T., Petzold, C.J., Heazlewood, J.L., and Lilley, K.S. (2019). Separating Golgi proteins from cis to trans reveals underlying properties of cisternal localization. Plant Cell **31,** 2010-2034.

Reguera, M., Bassil, E., Tajima, H., Wimmer, M., Chanoca, A., Otegui, M.S., Paris, N., and Blumwald, E. (2015). pH regulation by NHX-type antiporters is required for receptor-mediated protein trafficking to the vacuole in Arabidopsis. Plant Cell **27,** 1200-1217.

Robinson, D.G., and Neuhaus, J.M. (2016). Receptor-mediated sorting of soluble vacuolar proteins: myths, facts, and a new model. Journal of Experimental Botany **67,** 4435-4449.

Rogers, L.A., Dubos, C., Surman, C., Willment, J., Cullis, I.F., Mansfield, S.D., and Campbell, M.M. (2005). Comparison of lignin deposition in three ectopic lignification mutants. New Phytologist **168,** 123-140.

Sadowski, P.G., Groen, A.J., Dupree, P., and Lilley, K.S. (2008). Sub-cellular localization of membrane proteins. Proteomics **8,** 3991-4011.

Schat, H. (1999). Plant responses to inadequate and toxic micronutrient availability: general and nutrient-specific mechanisms. In Plant Nutrition — Molecular Biology and Genetics, G. Gissel-Nielsen and A. Jensen, eds (Dordrecht: Springer Netherlands), pp. 311-326.

Schumacher, K., Vafeados, D., McCarthy, M., Sze, H., Wilkins, T., and Chory, J. (1999). The Arabidopsis *det3* mutant reveals a central role for the vacuolar H^+-ATPase in plant growth and development. Genes & Development **13,** 3259-3270.

Schwihla, M., and Korbei, B. (2020). The beginning of the end: initial steps in the degradation of plasma membrane proteins. Frontiers in Plant Science **11,** 680.

Scott, A.C., and Allen, N.S. (1999). Changes in cytosolic pH within Arabidopsis root columella cells play a key role in the early signaling pathway for root gravitropism. Plant Physiology **121,** 1291-1298.

Scott, C.C., Vacca, F., and Gruenberg, J. (2014). Endosome maturation, transport and functions. Seminars in Cell and Developmental Biology **31,** 2-10.

Shabala, S.N., and Lew, R.R. (2002). Turgor regulation in osmotically stressed Arabidopsis epidermal root cells. Direct support for the role of inorganic ion uptake as revealed by concurrent flux and cell turgor measurements. Plant Physiology **129,** 290-299.

Sharma, A., Shahzad, B., Kumar, V., Kohli, S.K., Sidhu, G.P.S., Bali, A.S., Handa, N., Kapoor, D., Bhardwaj, R., and Zheng, B. (2019). Phytohormones regulate accumulation of osmolytes under abiotic stress. Biomolecules **9**

Shen, J., Zeng, Y., Zhuang, X., Sun, L., Yao, X., Pimpl, P., and Jiang, L. (2013). Organelle pH in the Arabidopsis endomembrane system. Molecular Plant **6,** 1419-1437.

Sinclair, R., Rosquete, M.R., and Drakakaki, G. (2018). Post-Golgi trafficking and transport of cell wall components. Frontiers in Plant Science **9,** 1784.

Sze, H., and Chanroj, S. (2018). Plant endomembrane dynamics: studies of K^+/H^+ antiporters provide insights on the effects of pH and ion homeostasis. Plant Physiology **177,** 875-895.

Taiz, L. (1992). The Plant vacuole. Journal of Experimental Botany **172,** 113-122.

Tang, R.J., Luan, M., Wang, C., Lhamo, D., Yang, Y., Zhao, F.G., Lan, W.Z., Fu, A.G., and Luan, S. (2020). Plant membrane transport research in the post-genomic era. Plant Communications **1,** 100013.

Ueda, M., Tsutsumi, N., and Fujimoto, M. (2016). Salt stress induces internalization of plasma membrane aquaporin into the vacuole in *Arabidopsis thaliana*. Biochemical and biophysical research communications **474,** 742-746.

Viotti, C., Bubeck, J., Stierhof, Y.D., Krebs, M., Langhans, M., van den Berg, W., van Dongen, W., Richter, S., Geldner, N., Takano, J., Jürgens, G., de Vries, S.C., Robinson, D.G., and Schumacher, K. (2010). Endocytic and secretory traffic in Arabidopsis merge in the trans-Golgi network/early endosome, an independent and highly dynamic organelle. Plant Cell **22,** 1344-1357.

von der Fecht-Bartenbach, J., Bogner, M., Krebs, M., Stierhof, Y.D., Schumacher, K., and Ludewig, U. (2007). Function of the anion transporter AtCLC-d in the trans-Golgi network. Plant Journal **50,** 466-474.

Wu, X.X., Li, J., Wu, X.D., Liu, Q., Wang, Z.K., Liu, S.S., Li, S.N., Ma, Y.L., Sun, J., Zhao, L., Li, H.Y., Li, D.M., Li, W.B., and Su, A.Y. (2016). Ectopic expression of *Arabidopsis thaliana* $Na^+(K^+)/H^+$ antiporter gene, AtNHX5, enhances soybean salt tolerance. Genetics and Molecular Research **15**

Yu, F., Lou, L., Tian, M., Li, Q., Ding, Y., Cao, X., Wu, Y., Belda-Palazon, B., Rodriguez, P.L., Yang, S., and Xie, Q. (2016). ESCRT-I component VPS23A affects ABA signaling by recognizing ABA receptors for endosomal degradation. Molecular Plant **9,** 1570-1582.

Zhang, T.Q., Xu, Z.G., Shang, G.D., and Wang, J.W. (2019). A single-cell RNA sequencing profiles the developmental landscape of Arabidopsis root. Molecular Plant **12,** 648-660.

Chapter 2

Plant Trans-Golgi Network/Early Endosome pH Regulation Requires Cation Chloride Cotransporter 1 (CCC1)

Statement of Authorship

Title of Paper	Plant Trans-Golgi Network/Early Endosome pH regulation requires Cation Chloride Cotransporter (CCC1)
Publication Status	☐ Published ☐ Accepted for Publication ☐ Submitted for Publication ☑ Unpublished and Unsubmitted work written in manuscript style
Publication Details	

Principal Author

Name of Principal Author (Candidate)	Daniel W. McKay		
Contribution to the Paper	DWM performed most experiments in the manuscript including phenotyping, co-localisation, pH measurements and trafficking assays. DWM contributed to experimental design, data analysis and writing the manuscript.		
Overall percentage (%)	75%		
Certification:	This paper reports on original research I conducted during the period of my Higher Degree by Research candidature and is not subject to any obligations or contractual agreements with a third party that would constrain its inclusion in this thesis. I am the primary author of this paper.		
Signature		Date	26/03/21

Co-Author Contributions

By signing the Statement of Authorship, each author certifies that:

i. the candidate's stated contribution to the publication is accurate (as detailed above);

ii. permission is granted for the candidate in include the publication in the thesis; and

iii. the sum of all co-author contributions is equal to 100% less the candidate's stated contribution.

Name of Co-Author	Yue Qu		
Contribution to the Paper	YQ assisted in the construction of *EXP7::GFP-AtCCC1* plants and performed several of the mentioned protein localisation attempts.		
Signature		Date	26/03/21

Name of Co-Author	Heather E. McFarlane		
Contribution to the Paper	HEM performed TEM imaging and analysis. HEM contributed to the design and analysis of trafficking assays and co-localisation assays. HEM commented on the manuscript		
Signature		Date	26/03/21

Name of Co-Author	Apriadi Situmorang		
Contribution to the Paper	AS cloned *EXP7::GFP-AtCCC1* and assisted with previous co-localisation attempts. AS commented on the manuscript		
Signature		Date	26/03/21

Name of Co-Author	Matthew Gilliham		
Contribution to the Paper	MG contributed to experimental design, data analysis and writing the manuscript		
Signature		Date	26/03/21

Name of Co-Author	Stefanie Wege		
Contribution to the Paper	SW led the project, performed expression analysis and contributed to phenotyping. SW contributed to experimental design, data analysis and writing the manuscript		
Signature		Date	26/03/21

Title

Plant Trans-Golgi Network/Early Endosome pH regulation requires Cation Chloride Cotransporter 1 (CCC1)

Authors

Daniel W McKay[1], Yue Qu[1], Heather E McFarlane[2,3], Apriadi Situmorang[1], Matthew Gilliham[1] and Stefanie Wege[1,*]

Affiliations

[1]ARC Centre of Excellence in Plant Energy Biology, PRC, School of Agriculture, Food and Wine, Waite Research Institute, University of Adelaide, Waite Campus, Glen Osmond 5064, South Australia, Australia

[2]School of Biosciences, University of Melbourne, Melbourne, VIC 3010, Australia

[3]Present address: Department of Cell and Systems Biology, University of Toronto, Toronto, ON, M5S 3G5, Canada

[*]Correspondence: stefanie.wege@adelaide.edu.au

Abstract

Plant cells maintain a low luminal pH in the Trans-Golgi-Network/Early Endosome (TGN/EE), the organelle in which the secretory and endocytic pathways intersect. Impaired TGN/EE pH regulation translates into severe plant growth defects. The identity of the proton pump and proton/ion antiporters that regulate TGN/EE pH have been determined, but an essential component required to complete the TGN/EE membrane transport circuit remains unidentified − a pathway for cation and anion efflux. Here, we have used complementation, genetically encoded fluorescent sensors, and pharmacological treatments to demonstrate that the TGN/EE localised Arabidopsis Cation Chloride Cotransporter (AtCCC1) is this missing component

necessary for regulating TGN/EE pH and function. Loss of AtCCC1 function leads to alterations in TGN/EE-mediated processes including endo- and exocytosis, and trafficking to the vacuole, consistent with the multitude of phenotypes observed in *Atccc1* knockout plants. This discovery places CCC1 as a central component of plant cellular function.

Introduction

The plant Trans-Golgi Network/Early Endosome (TGN/EE) has a complex cellular role. One of its key roles is sorting and delivering proteins to the apoplast, plasma membrane (PM) and vacuole (Dettmer et al., 2006; Viotti et al., 2010; Sze and Chanroj, 2018). This cellular function of the TGN/EE requires a finely tuned luminal pH (Luo et al., 2015; Reguera et al., 2015). Within the endomembrane system, the TGN/EE has the most acidic luminal pH, which is established by the TGN/EE-localised V-H^+-ATPase (Martinière et al., 2013, Luo et al., 2015). Plants with reduced V-H^+-ATPase activity (called *det3*) exhibit severe developmental growth defects and increased TGN/EE luminal pH, which is accompanied by alterations in exocytosis of PM proteins, such as BRI1, and defects in cell division and expansion (Schumacher et al., 1999, Dettmer et al., 2006, Brüx et al., 2008, Luo et al., 2015).

In addition to the V-H^+-ATPase, endomembrane luminal pH regulation is also dependent on the activity of cation/proton exchangers (antiporters), which provide a pathway for electroneutral proton efflux from, and cation import into, the TGN/EE lumen. The best characterised cation/proton exchangers in the TGN/EE are NHX5 and NHX6. Double *nhx5/nhx6* mutants have similar, but not identical, growth defects to *det3* (Bassil et al., 2011; Reguera et al., 2015), with reduced cell length and a large decrease to overall plant size. However, in contrast to *det3*, the *nhx5/nhx6* TGN/EE lumen is hyperacidic, consistent with the proposed role of NHX in exporting protons out of the TGN/EE (Luo et al., 2015; Reguera et al., 2015). As in *det3*, trafficking of BRI1 is also altered in *nhx5/nhx6*; however, only recycling is affected while secretion to the PM is not (Dragwidge et al., 2019). Similarly, the PM abundance of the membrane integrated proteins, PIN1 and PIN2, are reduced in *nhx5/nhx6* (Dragwidge et al., 2018). Moreover, the hyperacidity of *nhx5/nhx6* TGN/EE lumen results in mis-sorting of vacuolar proteins due to altered binding of targets by the Vacuolar Sorting Receptor VSR1;1 (Reguera et al., 2015).

In animals, chloride/proton antiporters of the CLC (Chloride Channel) protein family are important for lysosome acidification. This function is reliant on the coupled export of protons

and import of anions, as demonstrated through the use of a CLC variant that conducted uncoupled proton/anion transport that was unable to complement the increased lysosomal pH of a mouse *clc-5* knockout (Novarino et al., 2010). In plants, two members of the CLC family, CLCd and CLCf, are localised in the Golgi and TGN/EE (Marmagne et al., 2007; von der Fecht-Bartenbach et al., 2007). CLCd is important for pathogen resistance, with otherwise minimal developmental growth defects in the single *clcd* knockout (Guo et al., 2014). It has been suggested that CLCd and CLCf fulfil similar, partially redundant, roles to their animal homologues, but this remains to be tested as no *clcd/clcf* double knockout has so far been described (Sze and Chanroj, 2018).

Collectively, these observations demonstrate that a typical consequence of alterations in TGN/EE lumen pH regulation are defects in protein trafficking, particularly in protein exocytosis, and defects in cell elongation and division, resulting in severe impacts on plant growth. The current model of TGN/EE pH regulation, however, is incomplete; it contains a proton pump (V-H^+-ATPase) and anion- and cation-proton exchangers (CLC, NHX), but no transport protein that mediates either cation or anion efflux has yet been identified. Here, we have explored a lead that suggests CCC1 is localised to the TGN/EE endomembrane system, a result provided through heterologous expression studies and proteomics in Arabidopsis (Colmenero‐Flores et al., 2007; Nikolovski et al., 2012; Henderson et al., 2015). CCC1s mediate electroneutral cation and anion symport, and are therefore excellent candidates to provide an ion efflux mechanism (Colmenero‐Flores et al., 2007, Henderson et al., 2018). Arabidopsis contains only a single *CCC* gene, *AtCCC1*, whose knockout exhibits a complex and severe phenotype including large reductions in overall plant size, a bushy appearance characterised by increased axillary shoot outgrowth, frequent stem necrosis, very low fertility, alterations in pathogen response, and changes in cell wall composition (Johnson et al., 2004; Colmenero‐Flores et al., 2007; Henderson et al., 2018; Han et al., 2020).

Here, we demonstrate that the non-proton coupled ion transporter, AtCCC1, is required for the regulation of the TGN/EE luminal pH, for the efflux of ions, and that loss of AtCCC1 function leads to defects in TGN/EE-dependent processes. This includes alterations in exocytosis of the auxin transporter PIN2 and the PM marker LTI6b, and trafficking of endocytosed cargo to the vacuole. We propose that AtCCC1 impacts these processes because it is the missing core component of the ion- and pH regulating machinery of the TGN/EE.

Results

AtCCC1 *is ubiquitously expressed*

Previous reports on *AtCCC1* expression are contradictory. Promoter-GUS studies indicated that *AtCCC1* expression is restricted to specific tissues, such as root stele or hydathodes and pollen; while RNA transcriptomic studies, including single-cell RNAseq, suggest expression occurs in a broader range of cell types (Colmenero‐Flores et al., 2007, Wendrich et al., 2020). To clarify the tissue expression pattern of *AtCCC1*, we transformed Col-0 wildtype plants with a 2kb genomic DNA sequence upstream of the *AtCCC1* coding region driving the expression of nuclear-localised triple Venus (a bright variant of the yellow fluorescent protein) or β-glucuronidase (GUS), named *AtCCC1prom::Venus* and *AtCCC1prom::GUS*, respectively. Combined analysis of fluorescence and GUS-staining revealed that *AtCCC1* is expressed in all cell types, including all root cells, hypocotyl, leaf and stem epidermis, guard cells and trichomes, as well as mesophyll cells and all flower parts, with a particularly strong signal in stamen filaments (Fig. 1). *AtCCC1* promoter activity reported by Venus fluorescence, or by GUS-activity, was slightly different despite use of the identical promoter sequence. For instance, fluorescence was detectable in root cortex and epidermis cells, including root hairs, and in the gynoecium, while GUS staining did not indicate expression in these cells. This is likely due to the increased sensitivity of the Venus fluorescence method.

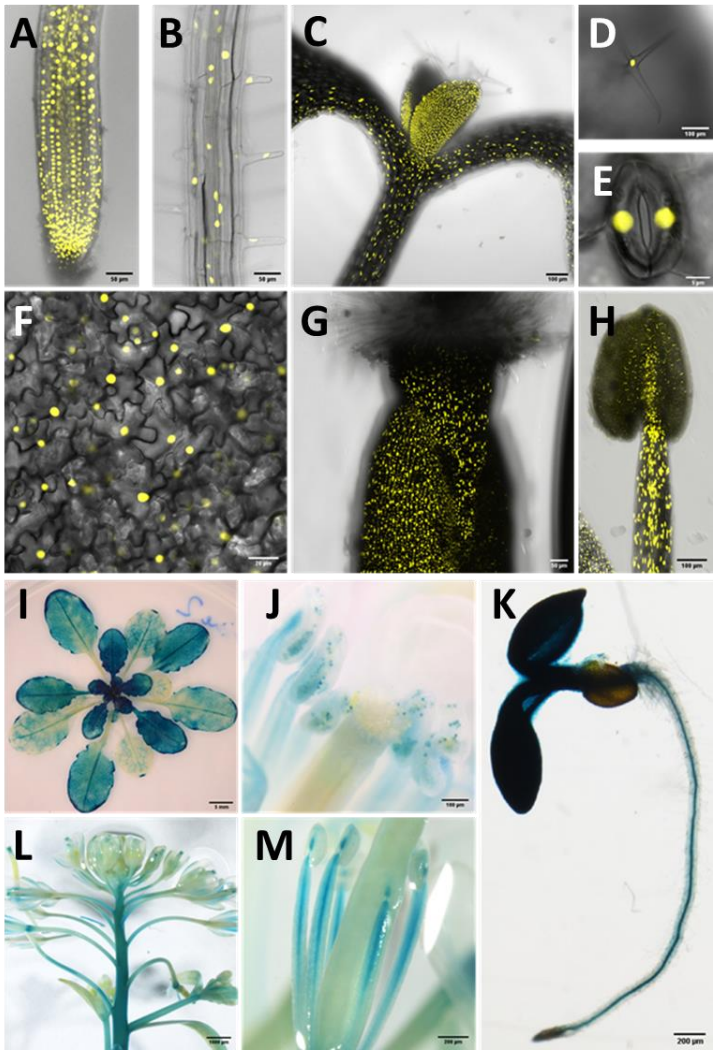

Figure 1. *AtCCC1* is expressed in most cell types. Expression of either 3×VenusNLS (bright YFP variant with a nuclear localisation signal) or β-glucuronidase (blue GUS staining). A–H) 3×VenusNLS expression indicating *AtCCC1* promoter activity in all root cells, including (A) the root tip, (B) root epidermal cells; (C) hypocotyl; all leaf cells including (D) trichomes, (E) guard cells, and (F) leaf epidermal and mesophyll cells; and reproductive organs (G) gynoecium and (H) stamen tissues. I–M) GUS staining indicating promoter activity predominantly in (I) younger leaves, (J) anthers, (K) root stele, (L) floral stem, and (M) stamen. Scale bars are 50 µm (images A, B, G), 100 µm (images C, D, H, J), 5 µm (image E), 20 µm (image F), 5 mm (image I), 200 µm (images K, M) and 1000 µm

Loss of AtCCC1 results in growth defects in root cells

Atccc1 knockout plants are severely affected in their growth, including a reduced shoot size and shorter primary roots (Fig. 2, and previously shown by Colmenero‐Flores et al., 2007; Henderson et al., 2015). We investigated the origin of the root phenotype of *Atccc1* at a cellular level and found that AtCCC1 function is required for cell elongation. Knockouts develop both shorter root epidermis cells, and shorter root hairs (Fig. 2). *Atccc1* knockouts also show a complete lack of collet hairs (Fig. 2), which are epidermal root hairs formed in some plant species in the transition zone between the root and the hypocotyl (Sliwinska et al., 2015). To

investigate the cause of the reduced root hair length in *Atccc1* plants, the elongation rates of wildtype and *Atccc1* root hairs were measured using time-lapse microscopy (Videos V1, V2). Measurements revealed that *Atccc1* root hairs grow for the same duration as wildtype hairs, but were shorter because they grow at a reduced speed. Between 50 and 100 min after elongation initiated, wildtype root hairs had an average elongation rate of 0.88 ± 0.27 µm min^{-1}, while *Atccc1* root hairs elongated at half that speed, at 0.47 ± 0.08 µm min^{-1} (Fig. 2). In addition, *Atccc1* root hairs also displayed branching and bulging, although, at a low frequency (Fig. S1). Ruptured root hairs were not observed (Fig. S1). Independent of the defect of root hair elongation, *Atccc1* plants frequently developed root hairs in cell files that usually exclusively contain atrichoblasts (non-root hair cells). The trichoblast marker *PRP3::H2B-2×mCherry* was used to confirm root hair cell identify and showed the frequent presence of multiple adjacent trichoblasts in *Atccc1*, which was absent from wildtype plants (Fig. S1).

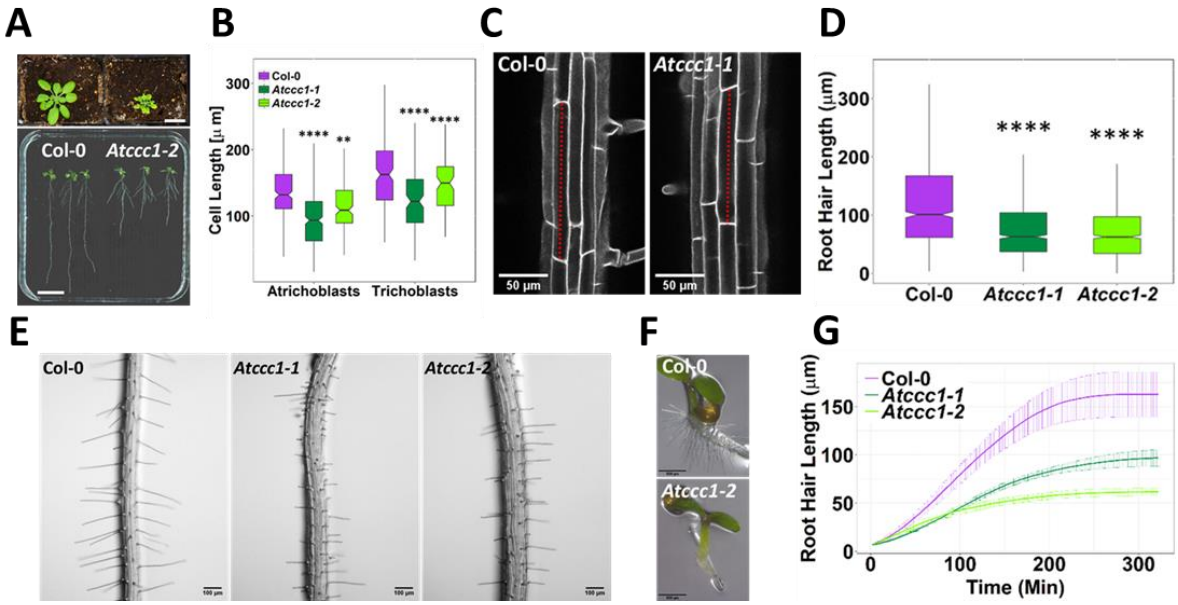

Figure 2. Severely phenotypically affected *Atccc1* plants show defects in cell elongation. A) Top image, *Atccc1* (right) have smaller shoots and deformed leaves compared to wildtype (left) plants. Plants grown 26 d in short day, scale bar is 2 cm. Bottom image, *Atccc1* (right) have shorter primary roots compared to wildtype (left) plants. Plants grown 14 d in long day, scale bar is 2 cm. B–C) Root epidermal cells are shorter in 2 *Atccc1* lines. n > 13 plants. Images are maximum intensity projections of cell wall autofluorescence. Scale bars are 50 µm.–D–E) *Atccc1* plants have shorter root hairs. n > 900 root hairs of > 30 plants. Scale bars are 100 µm. F) *Atccc1* plant do not develop collet hairs. Scale bars are 500 µm. G) *Atccc1* root hairs elongate more slowly (see Videos V1 and V2). Boxplots show range excluding outliers; median, 1st and 3rd quartile are indicated. Points represent individual measurements. Student's t-tests comparing *Atccc1* to wildtype. ** indicates

Functional GFP-AtCCC1 localises to the endomembrane system

We had previously localised AtCCC1-GFP to the Golgi and TGN/EE in transient expression assays in *Nicotiana benthamiana* (Henderson et al., 2015). In contrast, other studies have suggested that AtCCC1 might localise to the PM, which has led to multiple and conflicting interpretations of AtCCC1 function (Henderson et al., 2015; Wegner, 2017; Domingos et al., 2019). To clarify the subcellular localisation of AtCCC1, we generated plants that stably express N-terminally tagged GFP-AtCCC1, using the *EXP7* (*Expansin7*) trichoblast-specific promoter to express GFP-AtCCC1 in root epidermal cells. This approach was adopted after many attempts to generate plants with native *AtCCC1* promoter driven AtCCC1 expression, which did not produce any transformants. Approaches included the use of different protein linkers, different fluorescent proteins, smaller tags such as FLAG-tag, and different tag locations (N- and C-terminal, and internal). The difficulty in obtaining transformed plants might suggest that tagging interferes with AtCCC1 function in embryonic or meristematic tissue where it is highly expressed (Fig. 1); while internal tagging might have disrupted protein folding as transformants were recovered, but no fluorescence could be detected. We therefore decided to express GFP-AtCCC1 in a mature cell type, in which we had identified a clear phenotypic defect in *Atccc1* − trichoblasts. Expression in these epidermal cells was successful and importantly, complemented the short root hair phenotype of *Atccc1* knockout plants (Fig. 3).

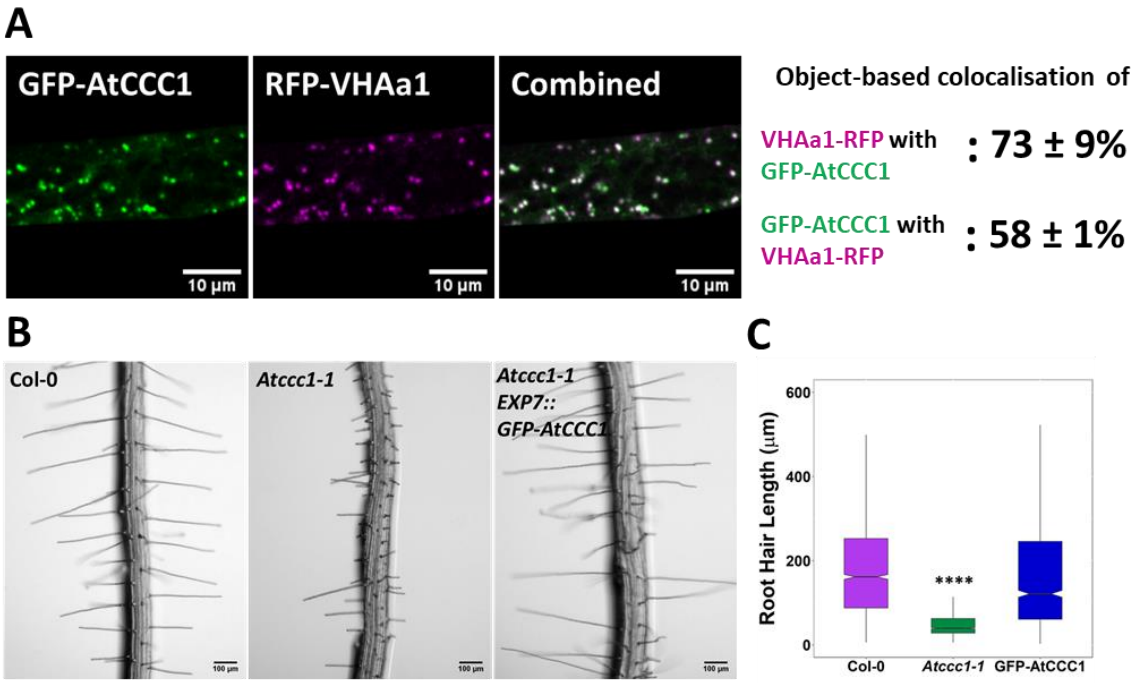

Figure 3. Stably expressed GFP-AtCCC1 is functional and localised in the TGN/EE. A) GFP-AtCCC1 (green) and VHAa1-RFP (magenta) co-localise. Colocalisation was calculated using DiAna object-based colocalisation plugin in ImageJ; Pearson's coefficient was also calculated as 0.86 ± 0.055. Error is standard deviation. n = 15 cells of 5 plants. Scale bars are 10 µm. Images are single representative optical sections from a stack. B–C) Expression of GFP-AtCCC1 rescues *Atccc1* root hair length defects. n > 1300 root hairs. Scale bars are 100 µm. Boxplot shows range excluding outliers; median, 1st and 3rd quartile are indicated. Student's t-tests comparing genotypes to

Stable expression of GFP-AtCCC1 in a native cell type revealed a similar pattern to what we previously observed in *Nicotiana benthamiana*, with the GFP signal localised to internal organelles (Henderson et al., 2015). Time-lapse imaging of the GFP-AtCCC1 movement was consistent with what could be expected for the Golgi or TGN/EE, however, GFP-AtCCC1 labelled organelles did not resemble the Golgi (Videos V3 and V4). To identify the observed GFP-AtCCC1 labelled compartments, we crossed the stably expressed marker, VHAa1-RFP, into plants expressing GFP-AtCCC1 (Fig. 3A). Colocalisation of GFP-AtCCC1 and VHAa1-RFP was measured using object-based colocalisation analysis, with the ImageJ plugin DiAna, which revealed that 73±9% of VHAa1-RFP colocalise with GFP-AtCCC1, while 58±11% of GFP-AtCCC1 colocalised with VHAa1-RFP. The asymmetrical colocalisation indicates that, in addition to the TGN/EE, AtCCC1 might also localise to additional organelles of the endomembrane system (Fig. 3), similar to NHX5 and NHX6 (Reguera et al., 2015). In addition, the Pearson correlation coefficient of pixel signal intensity for RFP and GFP channels was calculated, which gave a correlation value of 0.86±0.055. Pharmacological treatment further

confirmed the endosomal localisation. Treatment with the trafficking inhibitor, brefeldin-A (BFA), caused the GFP signal to accumulate in the centre of BFA bodies, consistent with a TGN/EE localisation (Fig. S2).

We then investigated if AtCCC1 might cycle between the TGN/EE and PM, but the signal intensity at the PM is too low to detect. Cases like this have been observed for other ion transporters that localise mainly in endosomes but function at the PM, such as the iron transporter, IRT1. PM localisation of IRT1 can be visualised using pharmacological treatment with TyrA23 (Tyrphostin A23; Barberon et al., 2011). For AtCCC1, no change in the subcellular localisation was observed after treatment with TyrA23, including no signal at the PM (Fig. S2). Similarly, an osmotic shock treatment, which can sometimes induce a change in protein localisation, did not lead to any observable changes in GFP-AtCCC1 localisation (Fig. S2). Combined, our results show very strong evidence that AtCCC1 functions in the TGN/EE.

Loss or knockdown of other TGN/EE-localised proteins, such as the H^+-V-ATPase, can affect the TGN/EE morphology (Dettmer et al., 2006). High-pressure freezing, freeze substitution, and transmission electron microscopy revealed that the lack of AtCCC1 did not lead to obvious morphological changes in the TGN/EE ultrastructure, and the appearances of all organelles was similar between *Atccc1* mutant and wildtype cells (Fig. S3). This suggests that the defects observed in *Atccc1* knockouts are probably connected to changes in TGN/EE luminal conditions.

AtCCC1 contributes to TGN/EE luminal pH regulation

After we confirmed TGN/EE localisation of AtCCC1, we hypothesised that the symporter might be part of the ion transport network regulating ion transport across the TGN/EE membrane, and may contribute to luminal pH regulation by affecting the activities of the cation- and anion-proton exchangers, and therefore ultimately the proton pump. To investigate this possible role of AtCCC1, we used a pharmacological treatment and a fluorescent pH sensor.

The ionophore monensin was utilised to assess if the loss of AtCCC1 results in changes to the ability of the TGN/EE to maintain a stable luminal environment. Monensin is a monovalent cation ionophore, acting as a membrane permeable ion exchanger, exchanging luminal protons for cations (Zhang et al., 1993). This rapid increase in osmotically active cations leads to observable TGN/EE swelling. The cation concentration gradient is likely to be an important factor determining the severity of monensin induced TGN/EE swelling, as the *nhx5/nhx6* mutants are less sensitive to monensin, despite a more acidic luminal pH (Dragwidge et al., 2019). We hypothesised that if AtCCC1 is important for ion efflux out of the TGN/EE, *Atccc1* TGN/EE might be hypersensitive to monensin-induced TGN/EE swelling. We assessed the susceptibility of *Atccc1* to monensin using live-cell imaging of VHAa1-RFP-labelled TGN/EE in wildtype and *Atccc1* root epidermal cells in the elongation zone, treated with 2.5 µM of monensin for 15 min. The average wildtype TGN/EE size increased by 28±13% while *Atccc1* TGN/EE size increased by 52±16%, revealing a highly increased susceptibility of *Atccc1* TGN/EE to osmotically induced swelling caused by cation accumulation (Fig. 4). This suggests that AtCCC1 mitigates the effect of monensin in wildtype cells, probably by effluxing K^+ and Cl^-, as anion and cation transport are stochiometrically linked in AtCCC1. We further suspected that TGN/EE pH could be altered as a consequence of altered cation and anion transport processes.

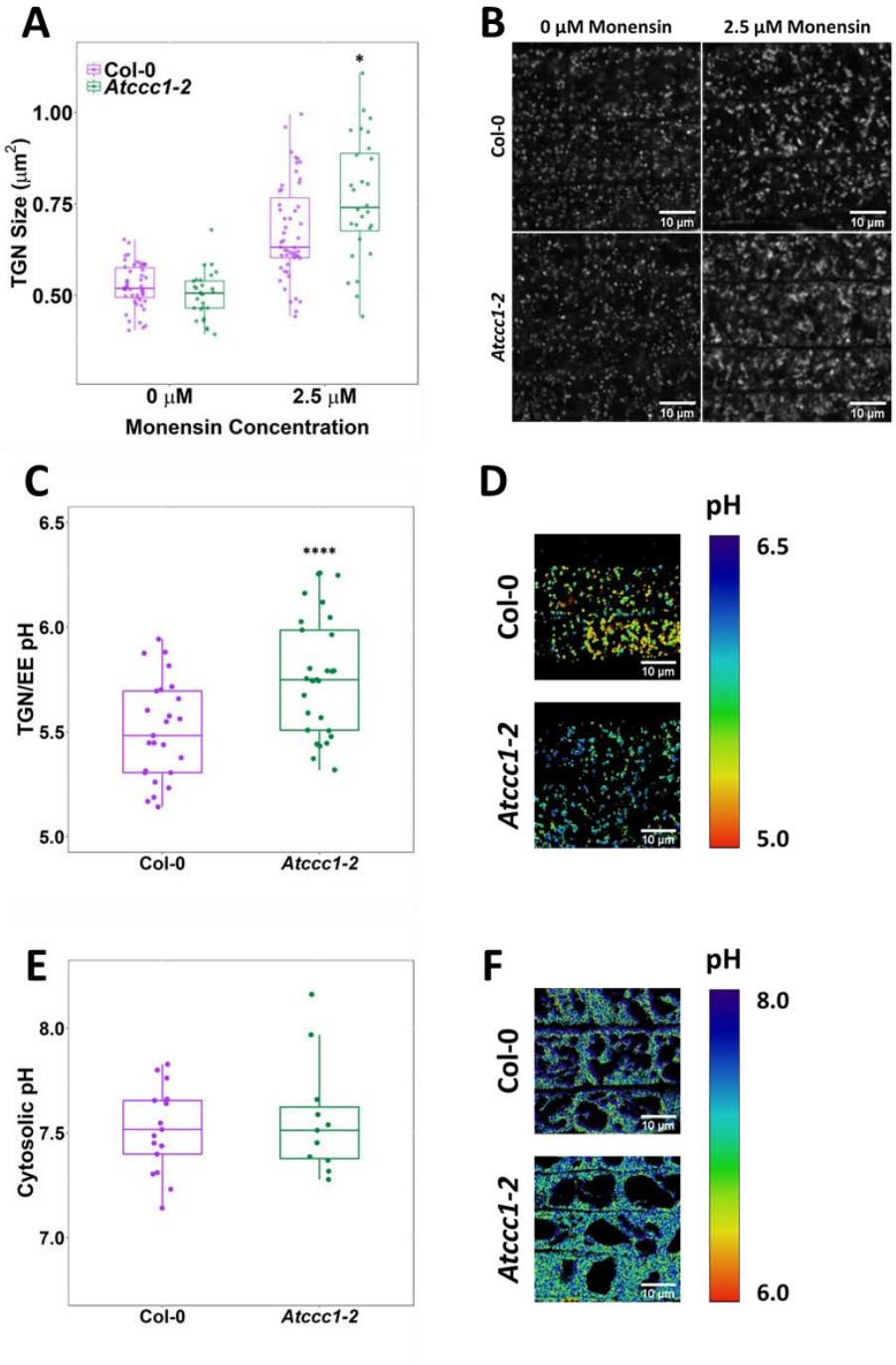

Figure 4. AtCCC1 is required for regulation of TGN/EE luminal conditions. A–B) Osmotically induced TGN/EE swelling due to cation influx is more severe in *Atccc1* epidermal root cells after 15 min of treatment with 2.5 µM monensin. TGN/EE are visualised through stable expression of VHAa1-RFP (white) in wildtype and *Atccc1* backgrounds. n > 28 plants. Scale bars are 10 µm. Images are single representative optical sections. C–D) Stable expression of the TGN/EE lumen pH sensor pHusion in wildtype and *Atccc1* backgrounds. The pH of *Atccc1* TGN/EE is 0.3 pH units higher compared to wildtype. E–F) Stable expression of the cytosolic pH sensor pHGFP in wildtype and *Atccc1* backgrounds. There is no significant pH difference between the two genotypes. pH with both sensors was calculated using calibration curves performed with each set of experiments. Images show the ratio of GFP/RFP of the pH-sensor SYP61-pHusion in the TGN/EE lumen and emission ratio for the pHGFP cytosolic sensor as a colour range, using the inverted "physics" look-up table in ImageJ. n > 26 plants for TGN/EE lumen pH measurements per genotype, and n = 11 plants for cytosolic pH measurements. Scale bars are 10 µm. Boxplots show range excluding outliers; median, 1st and 3rd quartile are indicated. Points represent individual measurements. Student's t-tests comparing *Atccc1* to wildtype. * indicates $P < 0.05$, **** indicates $P < 0.0001$.

To this end, we introduced the stably expressed TGN/EE localised pH-sensor, SYP61-pHusion (Luo et al., 2015), into *Atccc1* and investigated if defects in cation anion symport can impact pH regulation in the TGN/EE. Confocal imaging of epidermal cells in the root elongation zone revealed that luminal pH is more alkaline in *Atccc1*, with a pH of 5.8 ±0.05, compared to wildtype pH of 5.5 ±0.05, confirming our initial hypothesis that a non-proton transporting ion symporter can impact luminal pH (Fig. 4). We then investigated if loss of AtCCC1 might lead to a more general defect of cellular pH. Therefore, we measured cytosolic and vacuolar pH using the pH-sensor pHGFP and the pH sensitive dye, BCECF, respectively (Moseyko et al., 2001, Krebs et al., 2010). No difference was found between the genotypes, demonstrating that lack of AtCCC1 leads to spatially defined pH changes instead of a general effect (Fig. 4, S3).

Loss of AtCCC1 results in defects of endomembrane trafficking

Since pH and ion regulation are essential to TGN/EE function, we next investigated if there are defects in endomembrane trafficking in *Atccc1* cells, supporting the role of AtCCC1 in ion and pH regulation.

The rate of protein exocytosis, which is a combination of trafficking from secretion and recycling, was assayed using wildtype and *Atccc1* lines stably expressing PIN2-GFP. BFA treatment resulted in the accumulation of PIN2-GFP in the endomembrane system, measured as a strong increase in cytoplasm:PM signal ratio. This increase was more pronounced in *Atccc1* than in wildtype cells (Fig. 5). BFA treatment in Arabidopsis root cells leads to the formation of BFA bodies, which are an amalgamation of Golgi and TGN/EE (Geldner et al., 2001). Interestingly, BFA bodies in *Atccc1* were less dense, with a more diffuse GFP signal pattern, than the more compact and brighter, wildtype BFA bodies. Upon BFA washout, wildtype plants exhibited an almost complete recovery of the PIN2-GFP cytoplasm:PM signal ratio, suggesting that protein secretion and recycling had resumed. In contrast, *Atccc1* showed minimal recovery in the cytoplasm:PM signal ratio indicating a considerable decrease in PIN2-GFP exocytosis (Fig. 5).

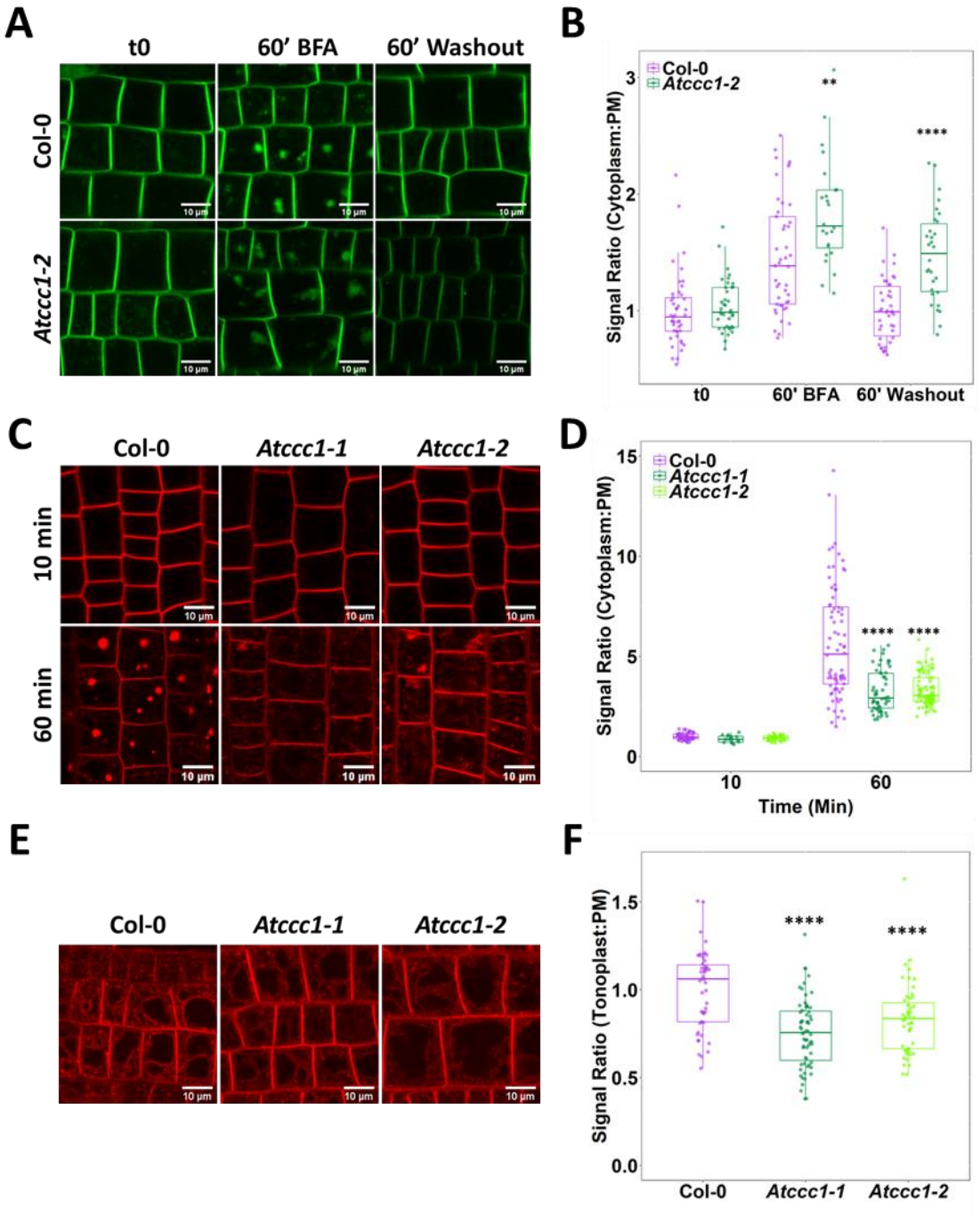

Figure 5. Loss of AtCCC1 leads to defects in endo- and exocytosis. A–B) *Atccc1* root epidermal cells show a reduced recovery of PIN2-GFP (green) cytoplasm:PM signal ratio after a 60 min treatment with 25 µM BFA. n > 24 cells, 3 cells measured per plant. C–D) Endocytosis of the membrane dye FM4-64 (red), measured as an increase in the cytoplasm:PM ratio, is reduced in *Atccc1* lines. Plants were kept in 25 µM BFA for the duration of the experiment. n > 56 cells of > 9 plants. E–F) Endocytosis and trafficking of FM4-64 (red) to the vacuole in the absence of BFA, measured as an increase of the tonoplast:PM signal ratio, is reduced in *Atccc1* lines. n > 51 cells of > 18 plants. Boxplots show range excluding outliers; median, 1st and 3rd quartile are indicated. Points represent individual measurements. All images are single representative optical sections. Student's t-tests comparing *Atccc1* to wildtype. ** indicates $P < 0.01$, **** indicates $P < 0.0001$. All scale bars are 10 µm.

Defects in TGN/EE luminal pH and the resulting defects in exocytosis are often accompanied by changes in endocytosis (Luo et al., 2015, Reguera et al., 2015, Dragwidge et al., 2018). Therefore, endocytosis was measured by internalisation of the endocytic tracer FM4-64, measured by an increase in the cytoplasm:PM signal ratio, both with and without BFA. After 60 min of treatment (10 min with FM4-64 & BFA, 50 min with BFA only), the fluorescence ratio was much lower in *Atccc1* than wildtype cells, consistent with a large reduction in the rate of endocytosis (Fig. 5). Like in the PIN2-GFP experiment, BFA bodies in *Atccc1* were more diffuse than in wildtype cells. The results of the two experiments indicate that the difference in BFA body morphology in wildtype and *Atccc1* is not the cause of the differences in signal internalisation in either experiment. In a second time course experiment, trafficking of FM4-64 to the vacuole was measured without the use of BFA. Labelling of the tonoplast with FM4-64 became visible in both wildtype and mutant cells after 3 h. The reduced ratio of tonoplast:PM signal in *Atccc1* compared with wildtype cells indicated a reduction in the trafficking of endocytosed FM4-64 to the vacuole (Fig. 5). The observed impact that loss of AtCCC1 has on both endo- and exocytosis, and its similarities to that which occurs in plants with loss of proton-transporting proteins localised in the TGN/EE, is consistent with AtCCC1 being part of the pH regulatory machinery of the TGN/EE.

Discussion

In the TGN/EE, both an increase or a decrease of luminal pH leads to changes in endomembrane trafficking, cell expansion, and cell wall formation, which implies that pH of the TGN/EE is finely regulated. Here, we show that AtCCC1 is localised in the TGN/EE in Arabidopsis, with no evidence found of PM localisation; and that loss of the cation anion symporter leads to defects in establishing the typical, low pH in TGN/EE lumen. This makes AtCCC1 the first TGN/EE-localised transporter important for pH regulation that does not directly transport protons. Our results show that AtCCC1 is important for counteracting the cation-induced osmotic swelling of TGN/EE by monensin (Fig. 4), consistent with the symporter being important for regulating luminal ion concentrations. pH measurements confirmed that *Atccc1* cells have a more alkaline pH in the TGN/EE lumen compared to wildtype. We therefore propose to extend the current model of pH regulation, containing the V-H^+-ATPase, NHX5 and NHX6, and CLCd (Sze et al., 2018) with CCC1 (Figure 6).

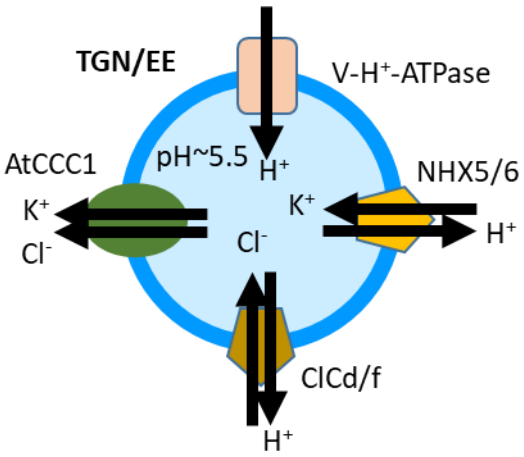

Figure 6: Proposed model of ion and pH regulation in the TGN/EE. The V-H$^+$-ATPase proton pump, the cation proton exchangers NHX5 and NHX6, and the anion proton exchanger CLCd have been previously shown or proposed to be important for pH regulation in the TGN/EE lumen. CCC1 is the first candidate for providing a cation and anion efflux mechanism, completing the regulatory transport circuit.

AtCCC1 is an electroneutral anion cation symporter, which fixes the stoichiometry of exported anions and cations at 1:1 (Colmenero‐Flores et al., 2007). This ion export ratio would therefore tightly connect the activities of the ion exchangers, and contribute to the strict regulation of pH. In addition, other transporters such as CLCf and the potassium efflux antiporters KEA4, KEA5 and KEA6 might also contribute to luminal pH regulation *in planta*; yet their roles are currently less understood since triple *kea4/kea5/kea5* knockouts show a much less severe phenotype compared to *nhx5/nhx6*, *det3*, or *Atccc1* (Dettmer et al., 2006, Colmenero‐Flores et al., 2007, Bassil et al., 2011, Zhu et al., 2018).

Functional endomembrane transport has a vital role in many cellular processes, including cell wall formation, nutrient acquisition and the establishment of hormone gradients (Guo et al., 2014, Adamowski and Friml, 2015, Sinclair et al., 2018). In agreement with this, *Atccc1* mutant plants display very severe phenotypic alterations compared to wildtype. We found that AtCCC1 is ubiquitously expressed, and its function is required for cell elongation, which might be the cause of the reduced overall growth of the mutants (Fig. 2, S1). Phenotypic defects in *Atccc1* are not restricted to cell elongation, and we found that also trichoblast patterning was altered in *Atccc1* roots (Fig. S1). *Atccc1* plants further exhibit highly increased shoot branching, which gives the knockout plants a bushy appearance (Henderson et al., 2018). One cause for this can be defects in auxin transport regulation in shoots, and we found alterations for PIN2

exocytosis in *Atccc1* roots, suggesting that similar defects could exist in shoot cells (Fig. 5). Additionally, *Atccc1* plants exhibit alterations in cell wall composition (Han et al., 2020).

Nutrient uptake and translocation have also been shown to be affected in *Atccc1* plants, with altered total shoot K^+, Na^+ and Cl^- accumulation compared to the wildtype (Colmenero‐Flores et al., 2007; Henderson et al., 2015). Furthermore, in a screen of the seed ionome, *Atccc1* seeds were identified as containing high concentrations of Fe, Ca and S, and low K and Na (McDowell et al., 2013). The alterations in Fe, Ca and S are of interest as these are not substrates of AtCCC1, which suggests loss of AtCCC1 function impacts the capacity of PM and/or tonoplast transport due to defects of TGN/EE function, most likely through impacts on trafficking.

Our research here demonstrates that CCC1 has a central role in cellular function, and fills a gap in our understanding of how endomembrane luminal pH is regulated through the identification of a novel ion efflux component of the TGN/EE membrane transport network.

Material and Methods

Plant material and growth conditions

Arabidopsis thaliana plants were all in the Columbia-0 (Col-0) background. Previously described T-DNA insertion lines in AT1G30450, *Atccc1-1* (SALK-048175), and *Atccc1-2* (SALK-145300) were used in this study (Colmenero‐Flores et al., 2007). *PIN2::PIN2-GFP, 35S::VHAa1-RFP, 35S::GFP-LTIB6 and 35s::SYP61-pHusion* plant lines were previously described (Cutler et al., 2000; Xu and Scheres, 2005; Dettmer et al., 2006; Luo et al., 2015).

Arabidopsis plants were grown on half strength Murashige and Skoog (1/2 MS) media containing 0.1% sucrose, 0.6% phytagel, pH 5.6 with KOH. Plants were sown on plates, incubated at 4 °C for at least 2 d and subsequently grown vertically at 21 °C and 19 °C in 16 h light and 8 h dark, respectively; or 8 h light and 16 h dark when short day is indicated. Plants were grown for different periods of time, as indicated below and in figure legends. Plants in pots (Fig. 2), were grown in Irish Peat soil.

Promoter activity analysis by GUS and Venus fluorescence

GUS staining was done according to Jefferson et al. (1987). In summary, plants were submerged in GUS-staining solution and stained (plant age and staining times indicated in figure legend). Image of the entire rosette was captured with a Nikon digital camera, flower and inflorescence images with a Nikon SMZ25 stereo microscope. Fluorescence of the nuclear localised NLS-Venus was imaged in plants ranging from 5–8 d to 8 weeks as indicated in figure legend. Excitation light wavelength was 514 nm, emission was detected at 520–560 nm, using either a Nikon A1R or an Olympus FV3000 Confocal Laser-Scanning Microscope; with the following objectives: 20× Plan Apo Lambda and 40× Apo LWD WI Lambda S (Nikon), and 10× UPSLAPO objective (Olympus).

Root hair length, root hair elongation rate

Light microscopy imaging of root hair length was performed using a Nikon SMZ25 stereo microscope with a 2× objective. For quantification of root hair length, images of roots were taken from above the maturation zone of 6 d plants. Each measurement was of a single root hair. Multiple root hairs were measured per plant. Root hair length was measured using FIJI (Schindelin et al., 2012). For time-lapse light microscopy of root hair elongation rate, plants were germinated in 2 mL of media placed in 1-well microscopy slides (Thermo Fisher) and grown vertically. Images of root hairs in the maturation zone were taken every 30 s for 6 h using a Nikon Diaphot 300. Measurements were taken from the beginning of root hair elongation, of root hairs that elongated beyond the initiation phase, until root hair growth ceased. For consistency, elongation rates of root hairs were only measured for root hairs where both initiation and cessation of growth could be observed in the time-lapse. A single root hair was measured per plant. Analysis and creation of videos was performed using FIJI.

Root morphology imaging

Root morphology images for epidermal cell length and ectopic root hairs were taken at the same Nikon confocal, using 6 d seedlings and root cell wall autofluorescence (excitation 404 nm, emission 425–475 nm). Each measurement for epidermal cell length was of a single cell. Multiple cells were measured per plant.

GFP-AtCCC1 cloning and expression

For stable expression of *AtCCC1* in root hairs, 1402 bp of the trichoblast-specific promoter *EXP7* (Marquès-Bueno et al., 2016) was first amplified from Col-0 genomic DNA, using the primers EXP7pro-HindIII_F (*tatacAAGCTTATTACAAAGGGGAAATTTAGGT*) and EXP7pro-KpnI_R (*cttatGGTACCTCTAGCCTCTTTTTCTTTATTC*), following a Phusion® PCR protocol (NEB). The PCR product and the binary plasmid pMDC43 were subsequently cut with the restriction enzymes *Hind*III-HF and *Kpn*I-HF to remove the *2×35S* promoter, and the digestion reactions were purified using illustra™ GFX™ PCR DNA and Gel Band Purification kits. Fragment ligation was performed using T4 DNA Ligase protocol (NEB) at 16 °C overnight. 2 µl of the ligation reaction was transformed into *E. coli* DB3.1 cells and after a sequencing verification, a plasmid was subsequently selected that showed the correct replacement of the *2×35S* promoter with the *EXP7* promoter. *AtCCC1* CDS (with stop codon) was then shuttled into the pMDC43EXP7 using LR clonase II enzyme, which creates N-terminally *GFP*-tagged *AtCCC1*. Correct plasmids were transformed into *Agrobacterium tumefaciens*, and heterozygous Arabidopsis plants (*Atccc1*$^{+/-}$) were floral dipped as the homozygous *Atccc1* knockout does not support floral dipping well. Floral dipping was performed according to Clough and Bent (1998), and transformants were selected on 1/2 MS plates with no sucrose, containing hygromycin for selection. Homozygous *Atccc1* knockouts expressing *GFP-AtCCC1* were selected, and phenotyped in the next generation.

Colocalisation

For colocalisation, 6 d plants expressing both *GFP-AtCCC1* (excitation 488 nm, emission 500–550 nm) and the TGN/EE marker VHAa1-RFP (excitation 561 nm, emission 570–620 nm) were imaged using Nikon A1R Confocal Laser-Scanning microscope, using a 60× Plan Apo VC WI objective with a numerical aperture of 1.2; pinhole set to of 1.2 AU. Five roots were imaged, with three images of three separate mature epidermal root cells being imaged per plant. Analysis was performed on image stacks with a step size of 0.45 µm. Colocalisation was assessed using the FIJI plugin DiAna (Gilles et al., 2017). In brief, segmentation was performed using the iterative segmentation function before the number of objects that overlap are counted. The percentage of overlapping objects is reported as the percentage of colocalisation.

Colocalisation with DiAna was supported by obtaining the Pearson's coefficient on the same stacks using JACoP (Bolte and Cordelieres, 2006).

TGN/EE swelling with monensin

TGN/EE swelling was induced using the ionophore, monensin (Sigma). 6 d plant roots expressing VHAa1-RFP (excitation 561 nm, emission 570–620 nm) were submerged in ½ MS solution with or without 2.5 µM monensin for 15 min before imaging. Imaging was performed on the Nikon A1R Confocal Laser-Scanning microscope and 60× objective described above. Images are single representative optical sections, taken of epidermal cells in the root elongation zone. A single measurement was taken per plant, which included multiple cells. Measuring was done using FIJI. TGN/EE were identified using VHAa1-RFP signal and segmented using the automatic threshold algorithm, "RenyiEntropy". The average size of the segmented TGN/EE was measured using "Analyse Particles".

TGN/EE and cytosolic pH measurements

The pH of the TGN/EE was measured as described in Luo et al. (2015). In brief, SYP61-pHusion (excitation 488 and 561 nm, emission 500–550 and 570–620 nm) was imaged in epidermal cells of the root elongation zone of 6 d plants on the Nikon A1R Confocal Laser-Scanning microscope and 60× objective described above, obtaining a single optical section. GFP/RFP intensity ratios were obtained from cells incubated in solutions of known pH to create a calibration curve. TGN/EE pH was measured by obtaining ratios from untreated plants. The calibration curve was created by measuring cells treated for 15 min with 50 mM MES-BTP (bis-tris-propane) or 50 mM HEPES-BTP with 50 mM ammonium acetate. Seven points between pH 5.0 and 8.0 were measured for the calibration curve. Six measurements were taken per point for calibration and a calibration was performed before every experiment. The curve was fit using a Boltzmann sigmoidal in GraphPad Prism 8.0. A single measurement was taken per plant, which included multiple cells. The GFP/RFP ratio was obtained in FIJI by firstly segmenting for TGN/EE using the automatic "RenyiEntropy" threshold on the RFP signal before measuring fluorescent intensity.

The cytosol was measured as described above for the measurement of the TGN/EE with some adjustments. The cytosolic pH sensor pHGFP (excitation 405 and 488 nm, emission 500–550

nm; Moseyko et al. 2001) was used. Sections of images used for measurement were manually cropped to remove any nuclei. pH measurements were obtained by acquiring a ratio of 488/405 nm signal intensity. Automatic thresholding in FIJI was performed using the "default" algorithm on the 488 nm channel.

Endo- and Exocytosis

Endocytosis was assayed in the root tips of 6 d plants using the fluorescent membrane stain FM4-64 (excitation 561 nm, emission 570–620 nm) and the endomembrane trafficking inhibitor brefeldin A (BFA). Plants were either incubated in 1/2 MS containing 4 µM FM4-64 and 25 µM BFA in the dark for 10 min before imaging or for 10 min in 1/2 MS with 4 µM FM4-64 and 25 µM BFA in the dark before washing and incubating in 1/2 MS with 25 µM BFA for 50 min before imaging. Images were single representative optical sections, taken of epidermal cells in the root elongation zone. A ratio of cytoplasm:PM signal was measured in ImageJ by using the polygon selection tool to measure the mean grey value of the entire interior of the cell and divide this by the PM mean grey value, acquired using the segmented line tool (width 1).

Trafficking of FM4-64 to the tonoplast was measured by incubating plants in 1/2 MS containing 4 µM FM4-64 for 10 min before washing and incubating in 1/2 MS for 3 h. Images were single representative optical sections taken of epidermal cells in the root elongation zone. A ratio of tonoplast:PM signal was acquired using the segmented line tool for both PM and tonoplast measurement.

Exocytosis was assayed in the root tips of 6 d old plants using PIN2-GFP or LTI6b-GFP in the epidermis. For the "t0" image point, plants were taken directly off growth media and immediately imaged. Otherwise, plants were treated with 25 µM BFA for 60 min, at which point some plants were imaged to obtain the "60' BFA" images. The rest were washed in liquid 1/2 MS and left to recover for 60 min in liquid 1/2 MS media before imaging for the "60' washout" images. Signal internalisation was measured as described for endocytosis. Imaging was done with the 60× objective and Nikon A1R Confocal Laser-Scanning microscope described above.

Cell types

Imaging for pH and monensin measurements, as well as for endo- and exocytosis, was done in epidermal cells in the root elongation zone; imaging of GFP-AtCCC1 for colocalisation was done in mature epidermis cells, specifically in trichoblasts.

Acknowledgments

We thank Melanie Krebs and Karin Schumacher for providing seeds expressing the TGN/EE pH sensor. Matthew Tucker for the 3×VenusNLS plasmid, Steve Tyerman for helpful discussions, Philip Brewer for *PIN2::PIN2-GFP* seeds, and Christian Luschnig for advice on genotyping. We thank Renée Philips and Marie Beillevert for assistance with lab and plant work. We thank Adelaide Microscopy, especially Gwen Mayo and Jane Sibbons, for support with microscopy; and we thank the University of Melbourne Advanced Microscopy Facility where electron microscopy was conducted. We thank the Australian Research Council for funding this work through DE170100054 to HEM, FT130100709 and CE140100008 to MG, and DE160100804 to SW; HEM is also supported in part by funding from the CRC program as the Canada Research Chair in Plant Cell Biology.

Author contributions

SW led the project; DWM, MG and SW designed experiments; DWM conducted most experiments with contributions from SW, HEM, YQ and AS; DWM, MG and SW wrote the paper, HEM, AS and YQ commented on the paper.

References

Adamowski M, Friml J (2015) PIN-dependent auxin transport: action, regulation, and evolution. Plant Cell **27:** 20-32

Barberon M, Zelazny E, Robert S, Conejero G, Curie C, Friml J, Vert G (2011) Monoubiquitin-dependent endocytosis of the IRON-REGULATED TRANSPORTER 1 (IRT1) transporter controls iron uptake in plants. Proceedings of the National Academy of Sciences of the United States of America **108:** E450-E458

Bassil E, Ohto M-a, Esumi T, Tajima H, Zhu Z, Cagnac O, Belmonte M, Peleg Z, Yamaguchi T, Blumwald E (2011) The Arabidopsis intracellular Na^+/H^+ antiporters NHX5 and NHX6 are endosome associated and necessary for plant growth and development. Plant Cell **23:** 224-239

Bolte S, Cordelieres FP (2006) A guided tour into subcellular colocalization analysis in light microscopy. Journal of Microscopy **224:** 213-232

Brüx A, Liu TY, Krebs M, Stierhof YD, Lohmann JU, Miersch O, Wastermack C, Schumacher K (2008) Reduced V-ATPase activity in the trans-Golgi network causes oxylipin-dependent hypocotyl growth inhibition in Arabidopsis. Plant Cell **20:** 1088-1100

Colmenero-Flores JM, Martínez G, Gamba G, Vázquez N, Iglesias DJ, Brumós J, Talón M (2007) Identification and functional characterization of cation–chloride cotransporters in plants. Plant Journal **50:** 278-292

Cutler S, R. , Ehrhardt D, W., Griffitts J, S., Somerville C, R. (2000) Random GFP::cDNA fusions enable visualization of subcellular structures in cells of *Arabidopsis* at a high frequency. Proceedings of the National Academy of Sciences **97:** 3718-3723

Dettmer J, Hong-Hermesdorf A, Stierhof Y-D, Schumacher K (2006) Vacuolar H^+-ATPase activity is required for endocytic and secretory trafficking in *Arabidopsis*. Plant Cell **18:** 715-730

Domingos P, Dias PN, Tavares B, Portes MT, Wudick MM, Konrad KR, Gilliham M, Bicho A, Feijó JA (2019) Molecular and electrophysiological characterization of anion transport in *Arabidopsis thaliana* pollen reveals regulatory roles for pH, Ca^{2+} and GABA. New Phytologist **223:** 1353-1371

Dragwidge JM, Ford BA, Ashnest JR, Das P, Gendall AR (2018) Two endosomal NHX-Type Na^+/H^+ antiporters are involved in auxin-mediated development in *Arabidopsis thaliana*. Plant and Cell Physiology **59:** 1660-1669

Dragwidge JM, Scholl S, Schumacher K, Gendall AR (2019) NHX-type $Na^+(K^+)/H^+$ antiporters are required for TGN/EE trafficking and endosomal ion homeostasis in *Arabidopsis thaliana*. Journal of Cell Science **132**

Geldner N, Friml J, Stierhof YD, Jurgens G, Palme K (2001) Auxin transport inhibitors block PIN1 cycling and vesicle traficking. Nature **413:** 425-428

Gilles JF, Dos Santos M, Boudier T, Bolte S, Heck N (2017) DiAna, an ImageJ tool for object-based 3D co-localization and distance analysis. Methods **115:** 55-64

Guo W, Zuo Z, Cheng X, Sun J, Li H, Li L, Qiu J-L (2014) The chloride channel family gene *CLCd* negatively regulates pathogen-associated molecular pattern (PAMP)-triggered immunity in *Arabidopsis*. Journal Of Experimental Botany **65:** 1205-1215

Han BD, Jiang YH, Cui GX, Mi JN, Roelfsema MRG, Mouille G, Sechet J, Al-Babili S, Aranda M, Hirt H (2020) CATION-CHLORIDE CO-TRANSPORTER 1 (CCC1) Mediates Plant Resistance against *Pseudomonas syringae*. Plant Physiology **182:** 1052-1065

Henderson S, Wege S, Gilliham M (2018) Plant cation-chloride cotransporters (CCC): evolutionary origins and functional insights. International Journal of Molecular Sciences **19:** 492

Henderson SW, Wege S, Qiu J, Blackmore DH, Walker AR, Tyerman SD, Walker RR, Gilliham M (2015) Grapevine and Arabidopsis cation-chloride cotransporters localize to the Golgi and trans-Golgi network and indirectly influence long-distance ion transport and plant salt tolerance. Plant Physiology **169:** 2215-2229

Jefferson RA, Kavanagh TA, Bevan MW (1987) GUS fusions: beta-glucuronidase as a sensitive and versatile gene fusion marker in higher plants. EMBO Journal **6:** 3901-3907

Johnson M, Zhou Q, Smith E (2004) Arabidopsis *hapless* mutations define essential gametophytic functions. Genetics **168:** 971-982

Krebs, M, Beyhl, D, Görlich, E, Al-Rasheid, KAS, Marten, I, Stierhof, YD, Hedrich, R, Schumacher, K (2010) Arabidopsis V-ATPase activity at the tonoplast is required for efficient nutrient storage but not for sodium accumulation. Proceedings of the National Academy of Sciences **107:** 3251-3256

Luo Y, Scholl S, Doering A, Zhang Y, Irani NG, Rubbo SD, Neumetzler L, Krishnamoorthy P, Van Houtte I, Mylle E, Bischoff V, Vernhettes S, Winne J, Friml J, Stierhof Y-D, Schumacher K, Persson S, Russinova E (2015) V-ATPase-activity in the TGN/EE is required for exocytosis and recycling in *Arabidopsis*. Nature Plants **1:** 15094

Marmagne A, Vinauger-Douard M, Monachello D, de Longevialle AF, Charon C, Allot M, Rappaport F, Wollman FA, Barbier-Brygoo H, Ephritikhine G (2007) Two members of the Arabidopsis CLC (chloride channel) family, AtCLCe and AtCLCf, are associated with thylakoid and Golgi membranes, respectively. Journal of Experimental Botany **58:** 3385-3393

Martinière A, Bassil E, Jublanc E, Alcon C, Reguera M, Sentenac H, Blumwald E, Paris N (2013) In vivo intracellular pH measurements in tobacco and *Arabidopsis* reveal an unexpected pH gradient in the endomembrane system. Plant Cell **25:** 4028-4043

McDowell SC, Akmakjian G, Sladek C, Mendoza-Cozatl D, Morrissey JB, Saini N, Mittler R, Baxter I, Salt DE, Ward JM, Schroeder JI, Guerinot ML, Harper JF (2013) Elemental concentrations in the seed of mutants and natural variants of *Arabidopsis thaliana* grown under varying soil conditions. Plos One **8**

Moseyko, N, Feldman, L.J (2001) Expression of pH-sensitive green fluorescent protein in *Arabidopsis thaliana*. Plant, Cell & Environment **24:** 557-563

Nikolovski N, Rubtsov D, Segura MP, Miles GP, Stevens TJ, Dunkley TPJ, Munro S, Lilley KS, Dupree P (2012) Putative glycosyltransferases and other plant Golgi apparatus proteins are revealed by LOPIT proteomics. Plant Physiology **160:** 1037-1051

Novarino G, Weinert S, Rickheit G, Jentsch TJ (2010) Endosomal chloride-proton exchange rather than chloride conductance is crucial for renal endocytosis. Science **328:** 1398-1401

Reguera M, Bassil E, Tajima H, Wimmer M, Chanoca A, Otegui MS, Paris N, Blumwald E (2015) pH regulation by NHX-type antiporters is required for receptor-mediated protein trafficking to the vacuole in Arabidopsis. Plant Cell **27:** 1200-1217

Schindelin J, Arganda-Carreras I, Frise E, Kaynig V, Longair M, Pietzsch T, Preibisch S, Rueden C, Saalfeld S, Schmid B, JTinevez e-Y, White DJ, Hartenstein V, Eliceiri K, Tomancak P, Cardona A (2012) Fiji: an open-source platform for biological-image analysis. Nature Methods **9:** 676-682

Schumacher K, Vafeados D, McCarthy M, Sze H, Wilkins T, Chory J (1999) The Arabidopsis *det3* mutant reveals a central role for the vacuolar H^+-ATPase in plant growth and development. Genes & Development **13:** 3259-3270

Sinclair R, Rosquete MR, Drakakaki G (2018) Post-Golgi Trafficking and Transport of Cell Wall Components. Frontiers in Plant Science **9**

Sliwinska E, Mathur J, Bewley JD (2015) On the relationship between endoreduplication and collet hair initiation and tip growth, as determined using six *Arabidopsis thaliana* root-hair mutants Journal Of Experimental Botany **66:** 3285-3295

Sze H, Chanroj S (2018) Plant endomembrane dynamics: studies of K^+/H^+ antiporters provide insights on the effects of pH and ion homeostasis. Plant Physiology **177:** 875-895

Viotti C, Bubeck J, Stierhof YD, Krebs M, Langhans M, van den Berg W, van Dongen W, Richter S, Geldner N, Takano J, Jurgens G, de Vries SC, Robinson DG, Schumacher K (2010) Endocytic and secretory traffic in Arabidopsis merge in the Trans-Golgi Network/Early Endosome, an independent and highly dynamic organelle. Plant Cell **22:** 1344-1357

von der Fecht-Bartenbach J, Bogner M, Krebs M, Stierhof Y-D, Schumacher K, Ludewig U (2007) Function of the anion transporter AtCLC-d in the *trans*-Golgi network. Plant Journal **50:** 466-474

Wegner LH (2017) Cotransport of water and solutes in plant membranes: The molecular basis, and physiological functions. Aims Biophysics **4:** 192-209

Wendrich JR, Yang B, Vandamme N, Verstaen K, Smet W, Van de Velde C, Minne M, Wybouw B, Mor E, Arents HE, Nolf J, Van Duyse J, Van Isterdael G, Maere S, Saeys Y, De Rybel B (2020) Vascular transcription factors guide plant epidermal responses to limiting phosphate conditions. Science **370:** eaay4970

Xu J, Scheres B (2005) Dissection of Arabidopsis ADP-RIBOSYLATION FACTOR 1 function in epidermal cell polarity. Plant Cell **17:** 525-536

Zhang GF, Driouich A, Staehelin LA (1993) Effects of monensin on plant Golgi: re-examination of monensin-induced changes in cisternal architecture and functional activities of the Golgi apparatus of sycamore suspension-cultured cells. Journal of Cell Science **104:** 819-831

Zhu X, Pan T, Zhang X, Fan L, Quintero FJ, Zhao H, Su X, Li X, Villalta I, Mendoza I, Shen J, Jiang L, Pardo JM, Qiu QS (2019) K^+ Efflux Antiporters 4, 5 and 6 mediate pH and K^+ homeostasis in endomembrane compartments. Plant, Cell & Environment **178**: 1657-1678

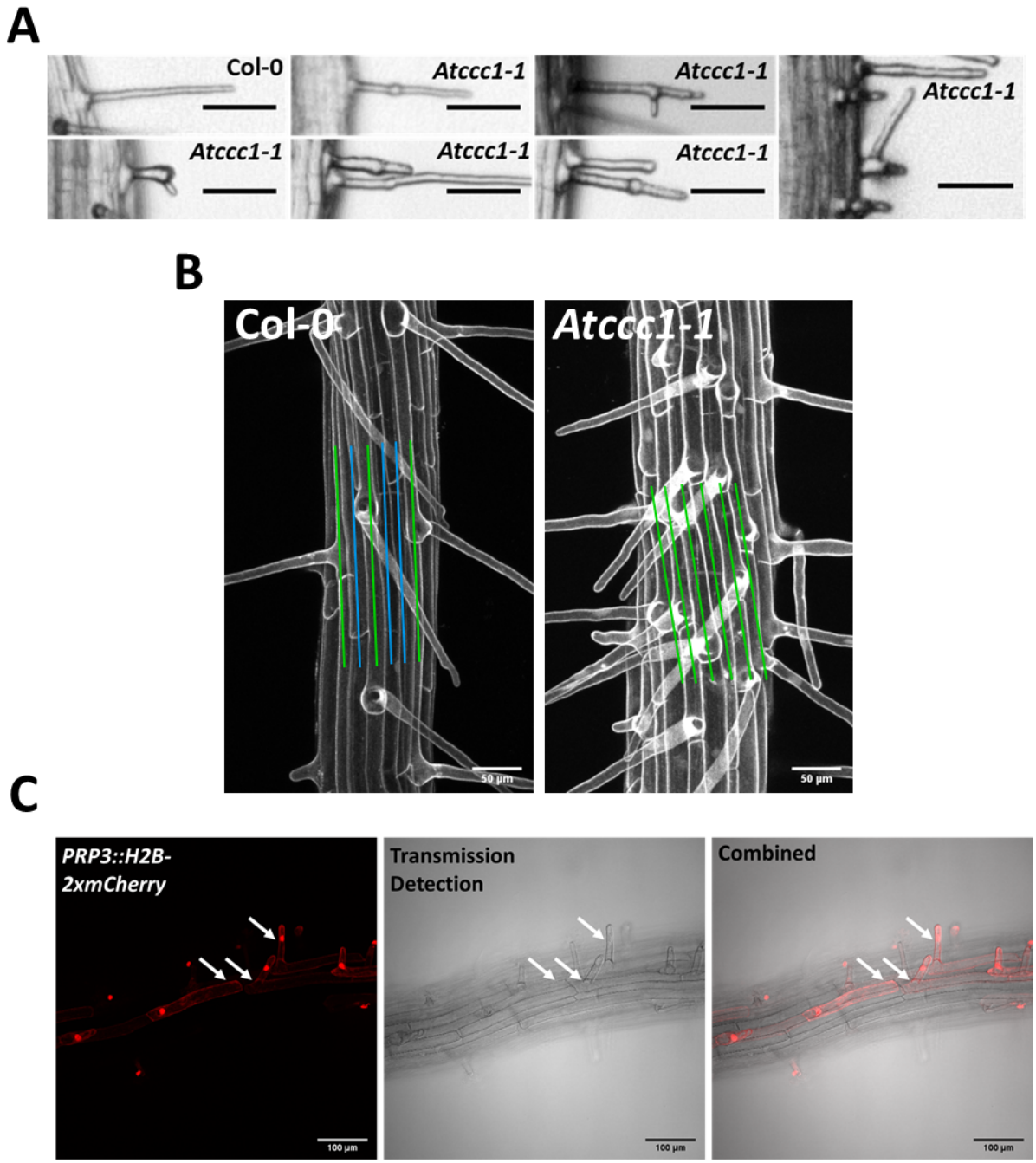

Figure S1. AtCCC1 is important for normal trichoblast development. A) A small number of *Atccc1* root hairs display forking and branching. Scale bars are 50 µm. B) *Atccc1* roots do not exhibit the classic cell file patterning of trichoblast and atrichoblast cell files observed in Arabidopsis. Cell files containing root hairs are marked with green while those that do not have root hairs are marked with blue. Images are of a maximum intensity projection, imaging cell wall autofluorescence. Scale bars are 50 µm. C) The trichoblast marker *PRP3::H2B-2xmCherry* (mCherry in red) confirms the appearance of adjacent trichoblasts in *Atccc1*. Arrows point to epidermal root cells in *Atccc1* which are of different files which are all expressing the trichoblast marker. Scale bars are 100 µm.

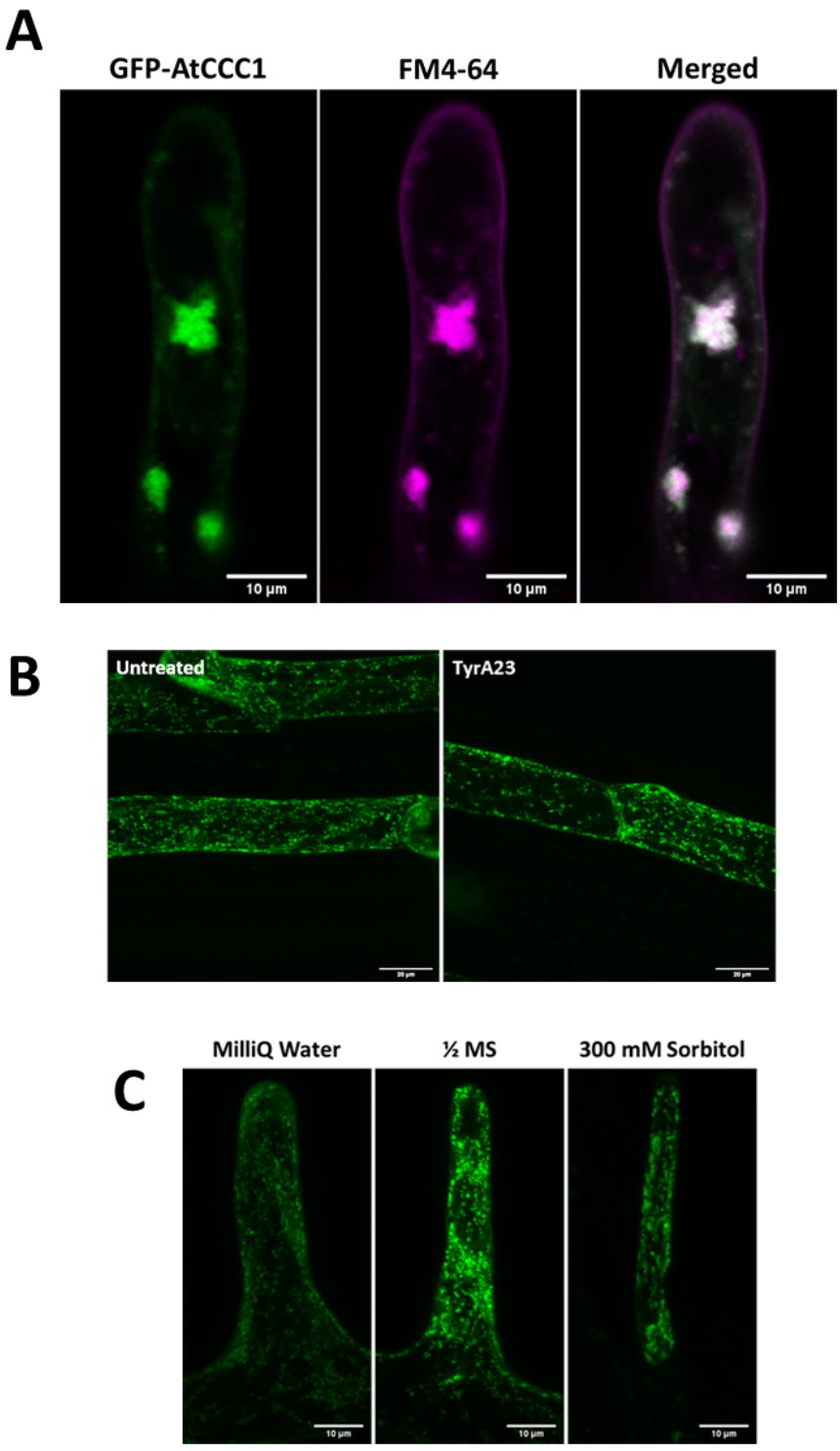

Figure S2. GFP-AtCCC1 is localised to the endomembrane system and does not cycle to the PM. A) After treating root hairs with 4 µM FM4-64 (magenta) for 5 min and 25 µM BFA for 1 h, GFP-AtCCC1 (green) and FM4-64 are both observed in the core of the BFA body. The image is a maximum intensity projection. Scale bars are 10 µm B) Treating roots with 50 µM of Tyrphostin A23(TyrA23) for 30 minutes, did not result in PM signal of GFP-AtCCC1 (green). Images are maximum intensity projections of mature root epidermal cells. Scale bars are 20 µm. C) Neither hyper- nor hypo-osmotic stress changed GFP-AtCCC1 localisation. Images are maximum intensity projections of root hairs equilibrated in 1/2 MS solution before being moved to MilliQ water or 300 mM sorbitol for 5 minutes. Scale bars are 10 µm.

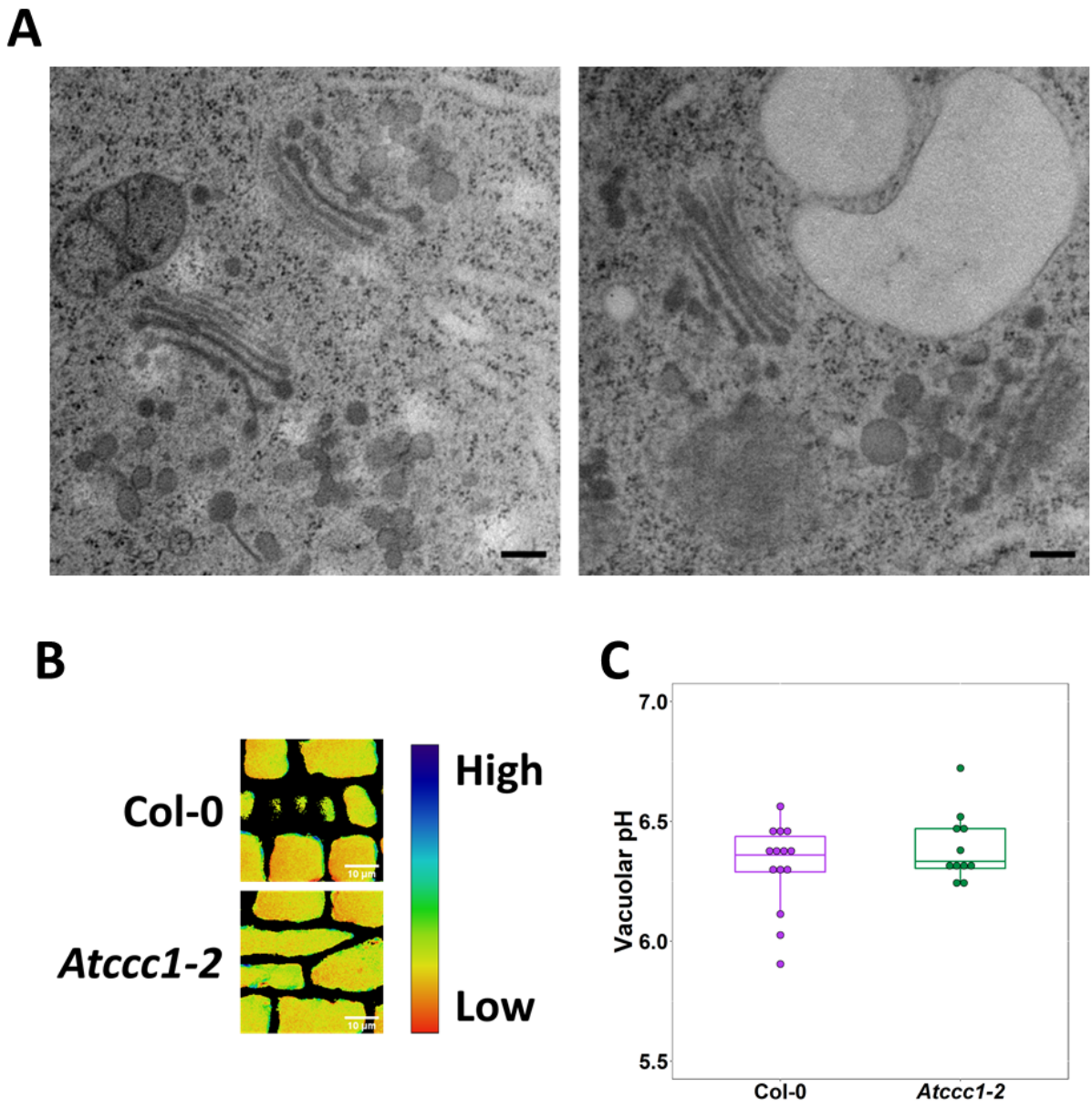

Figure S3. There are no obvious morphological alteration in *Atccc1* TGN/EE and AtCCC1 does not regulate vacuolar pH. A) Representative TEM images of highpressure frozen, freeze substituted early elongation zone root epidermal cells, showing Golgi and TGN/EE morphology in Col-0 wildtype (left) and *Atccc1* (right). Scale bars = 200 nm. B-C) The pH of *Atccc1* vacuoles is similar to wildtype in root epidermal cells, measured using the dye BCECF. Images show the ratio of the two BCECF excitations which were used to measure pH. n > 11 plants. Scale bars are 10 µm. Boxplot shows range excluding outliers; median and 1st and 3rd quartile are indicated. Points represent individual measurements. Students t-tests comparing *Atccc1* to wildtype. * < 0.05

Supplementary Material and Methods

Root morphology imaging

Root morphology images for epidermis cell length and root hair cell files were taken at a Nikon A1R Confocal Laser-Scanning microscope, using 6 d old seedlings and root cell wall autoflourescence (excitation = 404 nm, emission = 425-475 nm). Adjacent trichoblasts were also imaged in root epidermal cells of the maturation zone of *Atccc1* plants expressing the trichoblast marker *PRP3::H2B-2xmCherry* (excitation = 561 nm, emission = 570–620 nm; Marques-Bueno et al. 2016).

GFP-AtCCC1 imaging

6 d old plants expressing GFP-AtCCC1 (excitation = 488 nm, emission = 500–550 nm) driven by the *EXP7* promoter were imaged on a Nikon A1R Confocal Laser-Scanning microscope. For observation of GFP-AtCCC1 within BFA bodies, roots were first incubated in 1/2 MS with 4 µM FM4-64 (excitation = 561 nm, emission = 570–620 nm) for 5 min before being washed and incubated in 1/2 MS with 25 µM BFA for 1 h. Stacks were taken of elongating root hairs. For observing if GFP-AtCCC1 cycles to the PM, plants were incubated for 30 min in 1/2 MS with or without 50 µM tyrphostinA23. Stacks were taken of mature root epidermal cells. For observing if osmotic shock can induce a change of localisation of GFP-AtCCC1, plants were incubated in 1/2 MS solution for 1 h before being transferred to milliQ water, 1/2 MS solution or 1/2 MS solution containing 300 mM sorbitol for 5 min before imaging. Stacks were taken of elongating root hairs.

High-pressure freezing and transmission electron microscopy (TEM)

Wild type and *Atccc1* mutant seeds were grown on 1/2 MS plates with 1% sucrose in long-day conditions for 5 d. Roots tips were excised using a sharp razor then cryofixed according to McFarlane et al. (2008), with modifications. Cryofixation was performed using a Leica EM-ICE high pressure freezer, type A carriers (Leica), and 1-hexadecene (Sigma) as a cryoprotectant. Roots were freeze substituted in a Leica AFS2 at -85 °C over 5 d in a mixture of 2% osmium tetroxide (Electron Microscopy Sciences) and 8% 2,2-dimethoxypropane

(Sigma) in anhydrous acetone. Samples were warmed to room temperature over 2 d, then slowly infiltrated with Spurr's resin over 5 d (Spurr, 1969). Samples were polymerized for 36 h at 70 °C, then sectioned to ~70 nm (silver) on a Leica UC7 microtome using a DiATOME knife. Sections were placed onto copper fine-bar grids (Gilder) coated with 0.3% formvar, then post-stained with 1% aqueous uranyl acetate (Polysciences) for 10 min and triple lead (sodium citrate, lead acetate, lead citrate from BDH, lead nitrate from Fisher; Sato, 1968) for four min. Samples were viewed using a Phillips CM120 BioTWIN transmission electron microscope with tungsten filament at an accelerating voltage of 120 kV and a Gatan MultiScan 791 CCD camera.

Vacuole pH measurements

The pH of the vacuole was measured using BCECF-AM (Invitrogen) as described by Luo et al. (2015). In brief, 6 d old plants were incubated in the dark for 1 h in a 1/2 MS solution containing 10 µM BCECF and 0.02% pluronic F-127 (Invitrogen). Plants were washed before being imaged at the excitations 404 nm and 488 nm, both emissions were collected at 500–550 nm. The ratio between 404 and 488 is used to measure pH. A calibration curve was created by measuring cells treated for 15 min with 50 mM MES-BTP (bis-tris-propane) or 50 mM HEPES-BTP with 50 mM ammonium acetate. Seven points between pH 5.0 and 8.0 were measured for the calibration curve. Six measurements were taken per point for calibration and a calibration was performed before every experiment. The curve was fit using a Boltzmann sigmoidal in GraphPad Prism 8.0. A single measurement was taken per plant which included multiple cells. The 404/488 ratio was obtained in ImageJ by firstly segmenting using the automatic "default" threshold on the 488 nm channel before measuring fluorescent intensity.

Marques-Bueno MM, Morao AK, Cayrel A, Platre MP, Barberon M, Caillieux E, Colot V, Jaillais Y, Roudier F, Vert G (2016) A versatile Multisite Gateway-compatible promoter and transgenic line collection for cell type-specific functional genomics in Arabidopsis. Plant Journal 85: 320-333

McFarlane H, Young R, Wasteneys G, Samuels A (2008) Cortical microtubules mark the mucilage secretion domain of the plasma membrane in *Arabidopsis* seed coat cells. Planta **227:** 1363-1375

Sato T (1968) A modified method for lead staining of thin sections. Journal of Electron Microscopy **17:** 158-159

Spurr AR (1969) A low-viscosity epoxy resin embedding medium for electron microscopy. Journal of Ultrastructure Research **26:** 31-43

Chapter 3

Osmotic Stress Rescues Phenotypes of *Atccc1* Knockouts and AtCCC1 is Required for Dynamic Regulation of TGN/EE Luminal pH in Response to Salt and Osmotic Stress

3.1 Introduction

Salinity stress represents a major constraint on agricultural production in many parts of the world, including Australia. Salt stress leads to nutrient imbalance, the induction of multiple signalling pathways, reactive oxygen species (ROS) accumulation, reduced gas exchange, reduced plant growth and, when extreme, plant death (Isayenkov and Maathuis, 2019; van Zelm et al., 2020). The major stressors that plants face when challenged with saline conditions can be simplified into two components; ion toxicity and osmotic stress. The ion toxicity is caused by excessive sodium (Na^+) and chloride (Cl^-) accumulation in plant tissues, particularly the shoots. Excessive Na^+ competes with potassium (K^+) for uptake, and can induce loss of K^+ from tissues (Assaha et al., 2017). Plants need to maintain a pool of K^+ in the cytosol and so excluding Na^+ and maintaining K^+ specific uptake are important components of salt tolerance in plants. The second component, osmotic stress, is the result of an elevated osmolality in the surrounding soil. Plants typically establish and maintain a higher cellular osmolality in their roots comparative to the surrounding soils (van Zelm et al., 2020). This elevated osmolality is vital for water uptake and cell elongation. To mitigate osmotic stress, plants increase uptake of osmolytes and synthesise others such as proline and glycine betaine (Shabala and Lew, 2002; Sharma et al., 2019). The activation of the above salt tolerance mechanisms involves complex signalling pathways and secondary messengers including the hormone abscisic acid (ABA), calcium (Ca^{2+}) waves and ROS production, which result in the modification of the activity of proteins at membranes such as the plasma membrane (PM) and tonoplast (van Zelm et al., 2020). It has been implicated that other endomembrane compartments, such as the Trans-Golgi Network/Early Endosome (TGN/EE), may be important for response to salt stress too, however, the role of these compartments requires better characterisation (Bassil et al., 2011; Yu et al., 2016; Rosquete et al., 2018).

The TGN/EE is a hub for endomembrane trafficking and is involved in both the delivery of proteins and cell wall material. The trafficking of proteins entails both the delivery of newly synthesised proteins and recycling of existing PM proteins, a mechanism which can regulate PM protein abundance. The TGN/EE does, therefore, impact protein abundance and localisation. In response to salt or osmotic stress, both protein localisation and abundance of many proteins are altered to adapt to the new conditions. For example, PM aquaporins such

Arabidopsis thaliana PIP2;1 are removed from the PM and internalised in response to osmotic stress (Boursiac et al., 2008).

Two TGN/EE localised transporters and a proton pump have previously been implicated in salt tolerance. The TGN/EE V-H^+-ATPase pumps protons into the lumen (Luo et al., 2015). Arabidopsis V-H^+-ATPases localise to the both the TGN/EE and tonoplast. A weak mutant in the V-H^+-ATPase, *det3*, results in an increased pH in the TGN/EE but not the vacuole (Dettmer et al., 2006; Luo et al., 2015). Both *det3* plants and RNAi induced knockdowns of the TGN/EE V-H^+-ATPase are salt sensitive, with plants displaying a stronger reduction of primary root growth in response to 50 mM NaCl compared to wildtype plants (Batelli et al., 2007; Krebs et al., 2010). The two Arabidopsis TGN/EE NHX proteins, NHX5 and 6, are K^+/H^+ antiporters, and the transport direction is assumed to be import of K^+ into the lumen. Double knockouts of *nhx5* and *nhx6* are also salt sensitive. When transferred to media containing 100 mM NaCl, *nhx5/nhx6* plants exhibited severe reductions in plant growth in contrast to wildtype while germination of *nhx5/nhx6* was almost completely abolished on media containing 100 mM NaCl (Bassil et al., 2011). In addition, overexpression of the Arabidopsis NHX5 in paper mulberry (*Broussonetia papyrifera* L. Vent) plants resulted in plants with improved salt and drought tolerance (Li et al., 2011). The TGN/EE V-H^+-ATPase and NHXs are required for the establishment and maintenance of the acidic TGN/EE pH. The pH of the TGN/EE is vital for the organelles function and defects in pH regulation result in alterations to endomembrane trafficking (Luo et al., 2015; Reguera et al., 2015; Dragwidge et al., 2019). The current model of TGN/EE pH regulation also includes the Cl^-/H^+ antiporter CLCd (Sze and Chanroj, 2018). Unlike *det3* and *nhx5/nhx6* double mutants, Arabidopsis *clcd* knockouts do not have severe growth phenotypes and the salt tolerance of these plants is unknown (von der Fecht-Bartenbach et al., 2007; Guo et al., 2014). A second CLC, CLCf, is also localised to the TGN/EE and so may, like the NHXs, play a partially redundant role (Marmagne et al., 2007). We show that AtCCC1 is involved in the regulation of the TGN/EE luminal pH (Chapter 2, Fig. 4), where it likely plays a role in ion efflux. *Atccc1* knockouts have protein trafficking defects, severe growth phenotypes and a higher TGN/EE pH (Chapter 2, Fig. 2, 4 and 5) (Colmenero-Flores et al., 2007). In addition to the severe growth defects, *Atccc1* plants also display alterations in ion accumulation and distribution. *Atccc1* plants contain increased levels of all ions measured, Na^+, K^+ and Cl^-, in shoots of hydroponically grown plants under salt (50 mM NaCl) conditions (Henderson et al., 2015). Soil grown *Atccc1* plants grown in 50 mM Cl^-, salts also display

increased shoot, and decreased root, Cl^- accumulation (Colmenero-Flores et al., 2007). Interestingly, *Atccc1* seeds from plants grown under non-stressed conditions have increased amounts of Ca and S with decreased amounts of K and Na (McDowell et al., 2013). Knockouts of the rice (*Oryza sativa)* homolog of *AtCCC1*, *Osccc1.1*, have a decreased accumulation of Cl^- and K^+ in roots and shoots with an increased accumulation of Na^+ in addition to decreased root cell osmolality (Chen et al., 2016). Collectively, this suggests that AtCCC1 has a role in salt tolerance responses. The implication of the TGN/EE pH regulating pumps and transporters, V-H^+-ATPase, AtCCC1, NHX5 and NHX6, in salt tolerance, suggests that the TGN/EE pH may be important for salt stress responses in plants.

Here, we investigate the possible role of the TGN/EE luminal pH in the salt and osmotic stress response and how defects in luminal pH regulation translate into phenotypic alterations in *Atccc1* mutants. We therefore measured pH under stress conditions and assessed salt and osmotic sensitivity of *Atccc1*. In response to both salt and osmotic stress, TGN/EE luminal pH was increased in wildtype plants. The TGN/EE luminal pH of *Atccc1* plants was not responsive to salt or osmotic stress and remained elevated, like under control conditions. *Atccc1* plants have a reduced rate of root hair elongation which we show is rescued by osmotic stress. Germination of *Atccc1* is more tolerant to osmotic stress, and plasmolysis of *Atccc1* root cells requires a higher osmolality. These changes are not due to an elevated osmolality in *Atccc1* roots. We further investigated the internalisation of PIP2;1-GFP in response to salt and osmotic stress root epidermal cells, and found internalisation is reduced in *Atccc1*.

3.2 Results

The luminal pH of the TGN/EE increases in response to salt and osmotic stress

Arabidopsis wildtype plants maintain a low luminal pH in the TGN/EE under standard growth conditions. To determine if the TGN/EE luminal pH is responsive to environmental changes such as osmotic or salt stress, we used plants stably expressing the TGN/EE pH sensor SYP61-pHusion (Luo et al., 2015). The luminal pH of epidermal root cells of the elongation zone was quantified by imaging plants following a 15 min exposure to 200 mM NaCl or 400 mM mannitol which was compared to the pH of plants exposed to just the 1/2 MS control solution. In response to both NaCl and mannitol, the pH of the TGN/EE increased from 5.7 ± 0.04 (SEM)

under control conditions to 6.0 ± 0.09 and 6.0 ± 0.07 respectively (Fig. 1). Mannitol and NaCl both elicited the same pH response from plants demonstrating that the pH change is not exclusively connected to an increase in external ion concentrations but rather, occurs under an elevated external osmolality as well.

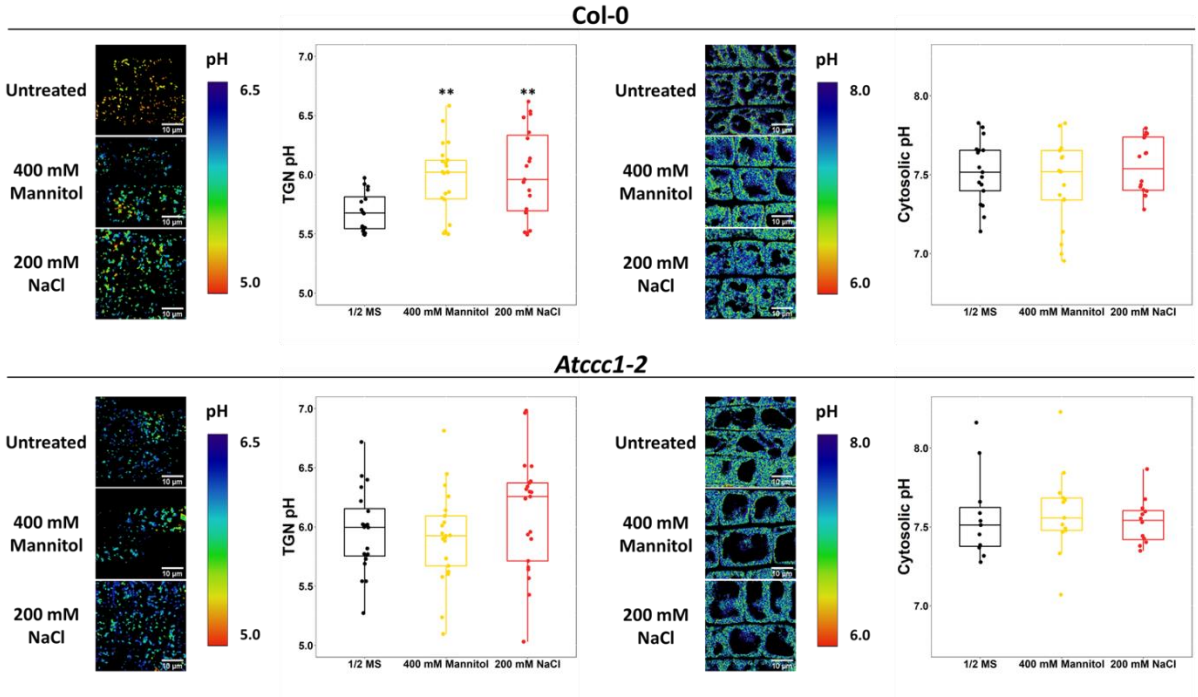

Figure 1. TGN/EE pH is increased in wildtype in response to salt and osmotic stress, but not in *Atccc1*. The pH of TGN/EE of epidermal root cells of the elongation zone was measured using the stably expressed pH sensor, SYP61-pHusion, in wildtype and *Atccc1*. The pH of cytosols was measured using pHGFP. pH was measured after 15 min treatment with 1/2 MS solution (control), 400 mM mannitol or 200 mM NaCl. The pH of wildtype TGN/EE increased by 0.3 units in response to salt and osmotic stress in wildtype plants. The pH of *Atccc1* TGN/EE was already 0.4 units higher than wildtype in control treated plants and did not increase further with stress treatment. For the TGN/EE, n > 16, for the cytosol, n > 12. Scale bars are 10 µM. ** indicates P < 0.01

Osmotic stress triggers an array of responses at the PM that can result in membrane depolarisation and depletion of cellular ATP (Che-Othman et al., 2017). Such events may impact proton transport across multiple membranes and as such, pH changes under osmotic stress may not be exclusive to the TGN/EE lumen. To assess this, the pH of the cytosol was measured using the sensor pHGFP (Moseyko and Feldman, 2001). Changes to cytosolic pH in response to salt have previously been investigated using the genetically encoded sensor pHluorin, at the root tissue level where it was found that salt causes a transient decrease in pH followed by an increase but it is unclear if nuclear signals were excluded from measurements

(Gao et al., 2004). The pH of the nucleus differs from that of the cytosol and may also differ in changes in response to stress (Shen et al., 2013). In contrast, no change in response to salt was found when the dye BCECF was used to measure cytosolic pH in root hairs (Halperin et al., 2003). Both previous studies used a widefield microscope for imaging. Using the genetically encoded and stably expressed pHGFP, confocal imaging at the cell level and specifically excluding nuclei from measurements, we found that neither NaCl nor mannitol treatment for 15 min, induced significant changes in cytosolic pH. Under control conditions, the pH of the cytosol was 7.5 ± 0.05. Almost identical pH values of 7.5 ± 0.07 under NaCl treatment and 7.6 ± 0.04 under mannitol treatment were obtained.

Previously, we found that the TGN/EE of *Atccc1* epidermal cells have a luminal pH of 6.0 (Chapter 2, Fig. 4), which was the same pH as detected here in wildtype TGN/EE in response to osmotic stress. We therefore used *Atccc1* to investigate if the pH increases further when *Atccc1* are exposed to the same osmotic stress. Under control conditions, *Atccc1* mean luminal pH was 6.0 ± 0.08, as expected. When treated with NaCl or mannitol, no significant change in luminal pH was detected with mean luminal pH values of 6.1 ± 0.11 (SEM) and 5.9 ± 0.08 respectively. Collectively, these results suggest that *Atccc1* plants do not further increase the pH of their TGN/EE. This might implicate that the pH is set to 6.0 in response to stress; and/or that pH 6 may be an upper limit for the TGN/EE.

Cytosolic pH was also measured for *Atccc1*. Like wildtype, no significant difference was observed between control conditions and NaCl or mannitol treatments. For *Atccc1*, cytosolic pH under control conditions was 7.5 ± 0.12. When treated with NaCl, the pH was 7.6 ± 0.08 and when treated with mannitol the cytosol pH was 7.5 ± 0.04.

Atccc1 *root hair elongation is rescued by hyperosmotic stress*

The TGN/EE pH regulating proteins, V-H^+-ATPase and NHX5 and NHX6 have previously been shown to be important for salt tolerance, while AtCCC1 has been implicated in root to shoot ion transport, but the salt tolerance of knockouts has not been further explored (Krebs et al., 2010; Bassil et al., 2011; Henderson et al., 2015). TGN/EE pH is altered in response to both salt and osmotic stress suggesting that TGN/EE pH regulation may be important for

response to osmotic stress and is not specific to ionic stress. Therefore, the osmotic stress tolerance of *Atccc1* was investigated to further explore how the TGN/EE may be important for osmotic stress tolerance.

We first assayed germination of *Atccc1* on media with a high osmotic strength. Wildtype and *Atccc1* seeds were germinated on media containing 0 to 600 mM of mannitol (Fig. 2). *Atccc1* seeds typically germinated slightly earlier than wildtype seeds so germination of seeds was not assessed until 6 d after imbibition. Under control conditions, over 85% of wildtype, *Atccc1-1* and *Atccc1-2* seeds germinated. The germination rate of all genotypes decreased with higher mannitol concentrations, yet, this decrease was much smaller in the *Atccc1* genotypes than wildtype. 75% of wildtype seeds germinated on 300 mM mannitol while 94% of *Atccc1-1* and 88% of *Atccc1-2* seeds germinated. On 600 mM mannitol, 0% of the wildtype seeds germinated, while 40% of *Atccc1-1* and 20% of *Atccc1-2* seeds were able to germinate in this condition. The greatest difference was seen on media containing 450 mM mannitol where 23% of wildtype seeds germinated compared with 86% of *Atccc1-1* and 53% of *Atccc1-2*. This suggests that the elevated pH of *Atccc1* TGN/EE alters germination under osmotic stress.

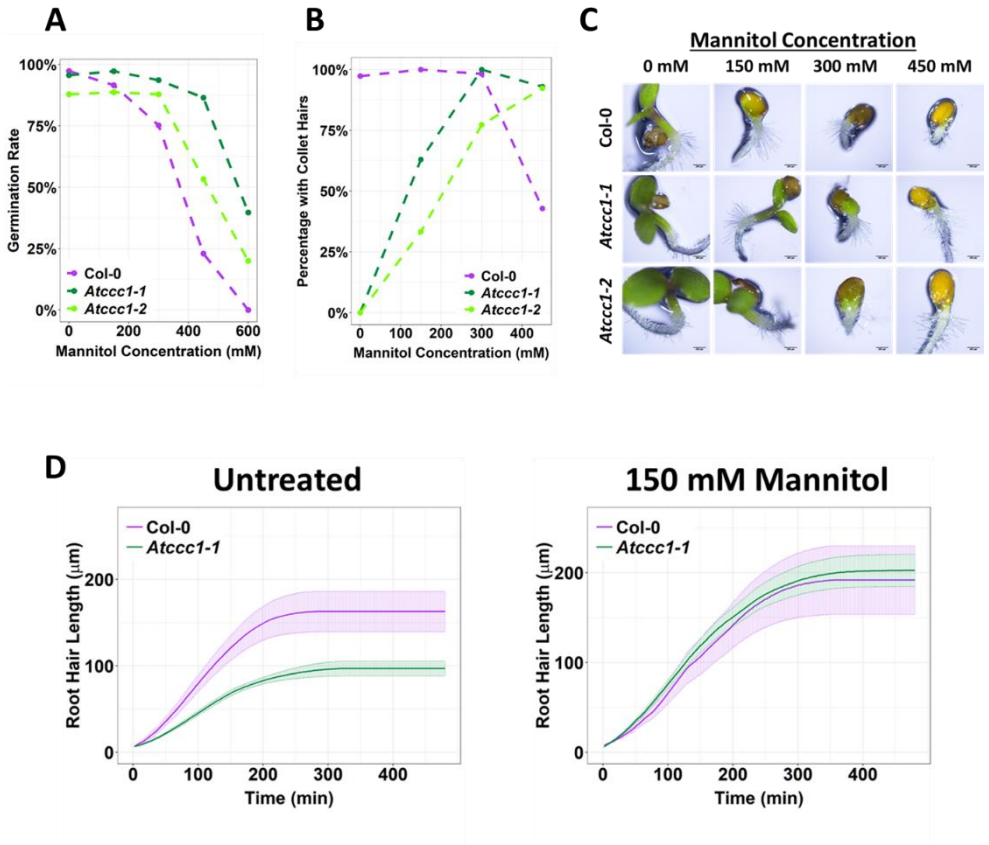

Figure 2. Increased external osmolality rescues cell elongation defects in *Atccc1.* A) A higher percentage of *Atccc1* seeds germinate on media with a higher osmolality, adjusted with increasing mannitol concentrations. Number of germinated seeds assessed 6 d after imbibition. n > 30. B-C) Collet hair formation in *Atccc1* is fully rescued on media with a higher osmolality. For 450 mM mannitol, n > 7, for all other concentrations of mannitol, n > 44. Scale bars are 200 µM. D) The slower rate of root hair elongation in *Atccc1* is rescued when grown in media with 150 mM mannitol. The 'Untreated' plot contains data also displayed in Chapter 2 (Fig. 2).

As *Atccc1* was able to germinate on media with a higher osmolality, we investigated if defects in the *Atccc1* plants might be alleviated when grown in environments with a higher external osmolality. We therefore assessed the presence of collet hairs, which are abolished in *Atccc1* plants under control conditions (Chapter 2, Fig. 2). This was done on the same plants as the germination assay. At 0 mM mannitol, over 90% of wildtype seedlings had collet hairs while they were present in 0% of *Atccc1* seedlings of either genotype, consistent with previous observations. Interestingly, at higher concentrations of mannitol, collet hair development in *Atccc1* was rescued. Collet hairs were observed in 63% of *Atccc1-1* seedlings and 30% of *Atccc1-2* seedlings grown on 150 mM mannitol. Over 97% of *Atccc1-1* and *Atccc1-2* seedlings grown on 300 or 450 mM mannitol had collet hairs (Fig. 2). In wildtype, there was instead a steady decrease of plants with collet hair outgrowth, decreasing to only 43% of seedlings grown on 450 mM mannitol.

As collet hair formation was rescued when exposed to high osmolality, we speculated that a higher osmolality may also rescue the reduced root hair elongation rate previously observed in *Atccc1* (Chapter 2, Fig. 2). To investigate this, plants were grown in media containing 150 mM mannitol. Only root hairs that elongated beyond 50 µm in length were measured. This excludes root hairs which formed but did not elongate and make it difficult to acquire an accurate measurement of elongation rate. Such root hairs are particularly common in plants grown in media with mannitol. Under control conditions, *Atccc1* root hairs elongated at almost half the rate of wildtype (Fig. 2). Strikingly, when grown in media with 150 mM mannitol, the elongation rate of *Atccc1* root hairs was the same as wildtype.

Atccc1 cells do not have higher cell sap osmolality but do have a reduced rate of plasmolysis

Atccc1 root hair elongation is rescued when grown on media with an elevated osmolality. This could conceivably be caused by an increased osmolality in *Atccc1* cells. Therefore, cell sap osmolality in wildtype and *Atccc1* roots was measured; however, cell sap osmolality was not higher in *Atccc1* compared to wildtype. Instead it might be potentially lower, as one allele was significantly different from wildtype, however, not the other; in general, individual measurements showed a high variance in all three genotypes (Fig. 3).

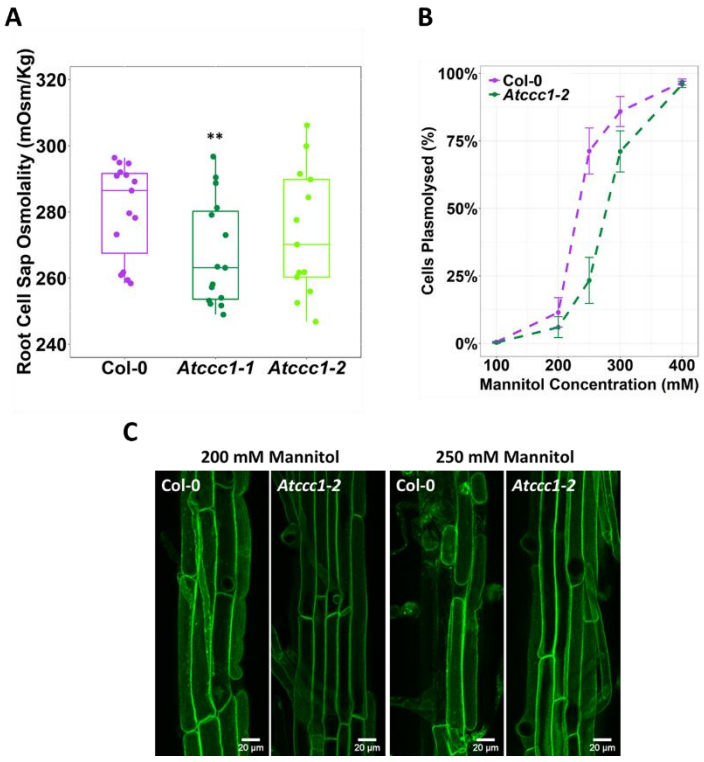

Figure 3. *Atccc1* root cells do not have a higher osmolality but are more tolerant to plasmolysis. A) The cell sap osmolality of whole root fluid, was measured using a freeze point osmomemter; no difference between wildtype and *Atccc1-2* cell sap was found, while *Atccc1-1* cells had a significantly lower cell sap. n = 13. B-C) *Atccc1* root epidermal cells require a higher external mannitol concentration to induce incipient plasmolysis. Plasmolysed cells were counted 1 h after treatment. The PM of cells was visualised with the PM marker, GFP-LIT6b (Green). 40 cells were assessed per plant, 12 plants were counted for each genotype/treatment. Scale bars are 20 µM. ** indicates $P < 0.01$

In addition to differences in cell sap osmolality, other factors could contribute to the improved growth of *Atccc1* plants on media with high osmotic strength such as altered osmoregulatory capacity. To explore this, the point of incipient plasmolysis was determined for wildtype and *Atccc1* epidermal root cells. This determines the external osmotic strength required to induce plasmolysis in 50% of the cells. Plasmolysis of mature epidermal root cells was induced by submerging roots in liquid media containing high concentrations of mannitol for 30 min after which plamolysed cells were observed using plants that stably express the plasma membrane marker GFP-LTI6b (Cutler et al., 2000). Fewer plasmolysed *Atccc1* cells were observed at all but the highest mannitol concentration (Fig. 3). The greatest difference was observed at 250 mM mannitol, where 71% ± 9% (SEM) of wildtype cells were plasmolysed compared to only 23% ± 9% of *Atccc1* cells at the same concentration. The estimated mannitol concentration for incipient plasmolysis was determined using a fitted curve (Boltzmann sigmoid). For wildtype, 50% of cells are estimated to plasmolyse at 232 mM mannitol, while plasmolysis of 50% of

Atccc1 root cells was estimated to require a mannitol concentration of 277 mM, 45 mM higher than that of the wildtype.

Trafficking of PIP2;1 in response to osmotic shock is reduced

Cell sap measurements did not indicate a higher internal osmolality in *Atccc1*, but cells required a higher osmotic strength to induce plasmolysis. We therefore investigated if other processes are responsible for these observations. We had previously shown that *Atccc1* exhibit alterations in endo- and exocytosis (Chapter 2, Fig. 5). In response to osmotic stress, aquaporins are removed from the PM (Boursiac et al., 2008; Hachez et al., 2014). The aquaporin PIP2;1 cycles between the PM and TGN/EE and is internalised in response to osmotic stress (Luu et al., 2012). We investigated osmotically induced internalisation of stably expressed PIP2;1-GFP in *Atccc1* and wildtype plants. Wildtype and *Atccc1* roots were treated with 100 mM NaCl or 200 mM mannitol for 30 min before internalisation of PIP2;1-GFP was measured by obtaining the ratio of fluorescent signal on the PM to signal inside the cell. In both wildtype and *Atccc1* roots, PIP2;1-GFP remained localised to the PM when treated with only 1/2 MS (Fig. 4). When treated with NaCl or mannitol, both genotypes internalised PIP2;1-GFP, but the relative portion of PIP2;1-GFP internalisation was lower in *Atccc1* than wildtype.

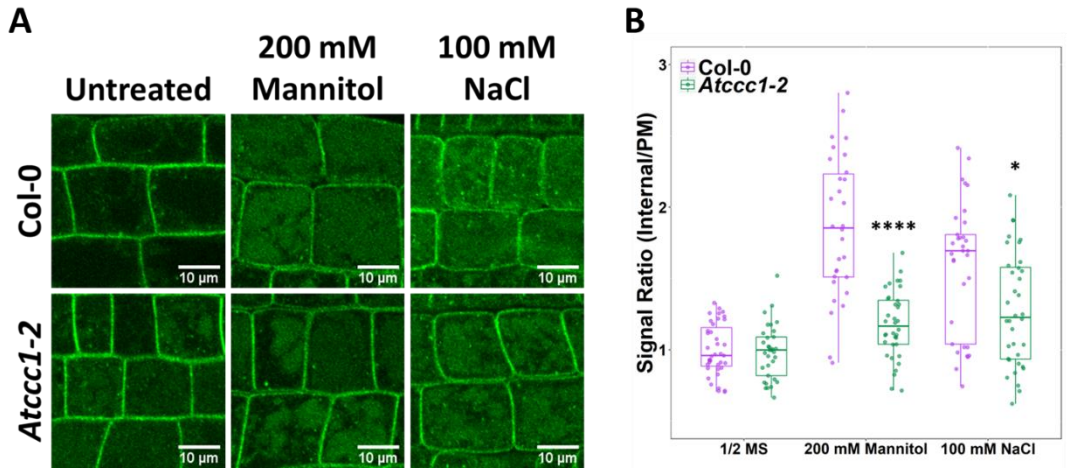

Figure 4. Osmotic and salt shock induced PIP2;1 internalisation is reduced in *Atccc1.* The internalisation of PIP2;1-GFP in response to osmotic (200 mM mannitol) and salt (100 mM NaCl) shock treatment was assayed in root epidermal cells of the elongation zone. Plants were imaged 30 min after treatment. A signal ratio of internal and PM signal was used to measure internalisation. n > 45. Scale bars are 10 µM. * indicate P < 0.05, **** indicates P < 0.0001

3.3 Discussion

Here, we show for the first time that the plant TGN/EE luminal pH is dynamic in response to environmental conditions. We also found that osmotic stress elevates TGN/EE pH but does not impact cytosolic pH in the conditions tested here. Some previous studies report that salt, but not osmotic stress, causes changes in cytosolic pH however, these studies have differed in plant species/cultivar and timing of stress application (Kader and Lindberg, 2010). In Arabidopsis roots, NaCl was reported to induce a rapid transient decrease in cytosolic pH when measured using widefield microscopy to image the ratiometric, genetically encoded pH sensor Phluorin at the tissue level. The pH change was then reversed to an increased cytosolic pH after 10-15 min (Gao et al., 2004). This is in contrast to other reports in Arabidopsis root hairs using the dye BCECF and wildfield microscopy, which show that NaCl treatment did not impact cytosolic pH of root cells after either 20 min or 6 d (Halperin et al., 2003). In rice leaf protoplasts, the response of cytosolic pH to NaCl was dependant on the cultivar, with a salt sensitive cultivar showing a decrease in cytosolic pH when measured with BCECF and widefield microscopy, while a pH increase was found in the salt tolerant cultivar (Kader et al., 2007). Our results using stably expressed pHGFP, confocal microscopy and specific selection of cytosolic signal with exclusion of nuclei, show that the cytosolic pH of Arabidopsis cells in the root elongation zone is unaltered after 15 min treatment with either 200 mM NaCl or 400 mM mannitol. This finding may reflect the precise timing of stress treatment or the impact of nuclei on pH measurements. Our finding indicates that the TGN/EE pH is more responsive to salt and osmotic treatments than that of the cytosol which implies that the TGN/EE plays an important role in modifying adaptation to these stresses.

Previous studies have obtained varying TGN/EE luminal pH values including 6.4, 6.2, 6.1, 5.6 and 5.5 under standard conditions (Chapter 2, Fig. 4)(Martinière et al., 2013; Shen et al., 2013; Luo et al., 2015; Reguera et al., 2015; Zhu et al., 2018). Further highlighting the dynamic changes in TGN/EE pH and potential adaptation to minute environmental changes, we obtained slightly different average pH values between the experiments performed here and in Chapter 2 (Fig. 4), while the difference between the wildtype and the mutant remained the same. The average value of both the wildtype and *Atccc1* luminal pH was 0.2 units higher here. Such variance in TGN/EE pH suggests that there might be environmental impacts on luminal pH, which can be observed even when plants were grown under identical temperature and light

conditions. Such variation is surprising considering differences as small as 0.3 pH units result in altered sorting of protein cargo (Reguera et al., 2015). Furthermore, pH appears to be important for the rate of endomembrane trafficking. The pH of *det3* TGN/EE is 0.4 units higher, *Atccc1* is 0.3 units higher and *nhx5/nhx6* is 0.3 units lower (Chapter 2, Fig. 4)(Luo et al., 2015; Reguera et al., 2015). All three mutants display reductions in the rate of trafficking (Chapter 2, Fig. 5)(Luo et al., 2015; Dragwidge et al., 2019). It is likely that the reduced rate of trafficking in *Atccc1* causes the reduced ability of *Atccc1* to internalise PIP2;1 following an osmotic shock. PIP2;1 allows the movement of water through the PM (Chaumont and Tyerman, 2014). Therefore, removal of PIP2;1 from the PM will decrease the water permeability. It is interesting to note here, that reduced internalisation of PIP2;1-GFP in *Atccc1* plants likely results in a higher PM water permeability than in wildtype. An increased PM water permeability alone would result in an increased susceptibility to osmotically induced water loss, yet, incipient plasmolysis of *Atccc1* epidermal root cells requires a higher external osmolality than wildtype. This suggests that factors other than PM water permeability are the likely cause for the observed differences in onset of incipient plasmolysis.

Several proteins are involved in the regulation of the TGN/EE luminal pH including the TGN/EE V-H^+-ATPase, NHX5 and 6, CLCd and AtCCC1. Of these, the V-H^+-ATPase and NHXs have been shown to be important for tolerance to salt stress with *nhx5/nhx6* knockouts as well as the V-H^+-ATPase defective, *det3*, being salt sensitive (Bassil et al., 2011; Luo et al., 2015). It was previously shown that the primary roots of *Atccc1* mutants are shorter than wildtype on both control and saline media (Henderson et al., 2015). Intriguingly, here we show that *Atccc1* has root-based phenotypes that are more tolerant to higher osmotic conditions. For instance, we show that *Atccc1* knockouts germinate under higher osmotic conditions than wildtype and withstand greater external osmolality before plamolysing. Whilst *Atccc1* plants lack collet hairs and have reduced root hair elongation under control conditions, both of these phenotypes are rescued by osmotic stress. In fact, collet hair growth is maintained at higher osmolality than wildtype, while root hair growth occurs equally well under osmotic stress.

Conditional phenotypic complementation of *Atccc1*, where under standard conditions the *Atccc1* root hairs are unable to grow properly, but normal root hair growth is restored when external osmotic conditions are elevated, suggests that the role of AtCCC1 in regulating

TGN/EE luminal conditions, differentially affects cellular function at different external osmolality. AtCCC1 is suggested to efflux ions from the TGN/EE, and therefore, loss of function plants might accumulate more ions in the TGN/EE compared to wildtype. Such accumulation may be important in cells challenged with osmotic stress but not required otherwise, resulting in AtCCC1 being important for efflux under normal conditions but not when the external osmolality is increased.

Our research here demonstrates that TGN/EE pH is dynamic and is adjusted in response to luminal conditions. It further highlights the role regulation of TGN/EE luminal conditions has in osmotic tolerance in plants. This work identifies a new mechanism by which salt tolerance in plants may be addressed.

3.4 Materials and Methods

Plant material and growth conditions

All plants used were *Arabidopsis thaliana* in the Columbia-0 (Col-0) background. The previously described AT1G30450 T-DNA insertion lines, *Atccc1-1* (SALK-048175) and *Atccc1-2* (SALK-145300) were used (Colmenero-Flores et al., 2007). Also used were the previously described lines *35S::SYP61-Phusion, 35S::pHGFP, and 35S::GFP-LTI6b* (Cutler et al., 2000; Moseyko and Feldman, 2001; Luo et al., 2015). *UBQ10::PIP2;1-GFP* plants were kindly provided by Chuang Wang. Plants were grown on media containing half strength Murashige and Skroog (1/2 MS), 0.1% sucrose, 0.6% phytagel and pH 5.6 adjusted with KOH. Plants were sown on plates, incubated at 4^{o}C for 2 d before being grown vertically at 21°C and 19°C in 16 h light and 8 h dark, respectively.

TGN/EE and cytosol pH measurements

pH measurements of the TGN/EE were measured as specified in chapter 2. Briefly, a calibration curve of the dual fluorescence TGN/EE pH sensor, SYP61-pHusion (excitation 488 and 561 nm, emission 500 – 550 and 570 – 620 nm) was performed for each genotype at the beginning of each experiment. pH was measured in epidermal root cells in the elongation zone of 6 d old plants by taking the ratio of GFP/RFP signal. Samples were submerged in 1/2 MS

liquid media containing 200 mM NaCl or 400 mM mannitol 15 min before imaging on a Nikon A1R confocal laser scanning microscope with a 60x Plan Apo VC WI objective. Image analysis was performed using FIJI (Schindelin et al., 2012).

Germination and collet hairs

Seed germination and collet hair formation in response to osmotic stress was assayed on the same seeds. Seeds were germinated on 1/2 MS media containing the indicated concentration of mannitol. 6 d after imbibition, the percentage of seeds that had germinated were counted with radicle emergence being used as the indicator for germination. On the same day, for all plants that had developed to the point where collet hairs should be visible, the percentage with properly developed collet hairs was determined. Development of collet hairs was scored as seedlings with a ring of collet hairs that spread around the hypocotyl as normally observed in wildtype. A seedling with a few, sparse, elongated collet hairs was considered to not have developed collet hairs.

Root hair elongation rate

Time lapse light microscopy was used to measure root hair elongation rate. Plants were germinated within 2 mL of media placed in 1-well microscopy slides (Thermo Fisher) and grown vertically. Images of root hairs in the maturation zone were taken every 30 s for 6 h using an inverted Nikon Diaphot 300, with slides placed horizontally. Measurements were taken from the beginning of root hair elongation, of root hairs that elongated beyond the initiation phase, until root hair growth ceased. For consistency, elongation rates of root hairs were only measured for root hairs where both initiation and cessation of growth could be observed in the time lapse. A single root hair was measured per plant. Analysis and creation of videos was performed using FIJI. The result displaying elongation rate in “untreated” conditions is also presented in chapter 2 (Fig. 2). This was done at the same time as the results presented here and is the control for this experiment.

Plasmolysis

Mannitol was used to induce plasmolysis of plants grown for 6 d on 1/2 MS without mannitol. The mannitol concentration at which root cells plasmolysed was determined using epidermal cell without root hairs, in plants expressing the PM marker GFP-LTI6b. Plants were transferred from the growth media to a liquid 1/2 MS solution containing different concentrations of mannitol, as indicated in Fig. 3, 1 h before counting. Plasmolysed and non-plasmolysed cells were counted under a Nikon Ni-E widefield microscope. From each root, the plasmolysis state of 40 cells was assessed. Cells which had root hairs were not included. A cell was considered as plasmolysed if the corners of the cell had detached/curved. Only cells past the maturation zone of the plant were included. The estimated concentration at which 50% of cells would plasmolyse for each genotype was determined by fitting a Boltzmann sigmoid curve in Graphpad Prism 9 to obtain the 'V50'.

Root cell sap osmolality

For each sample, seeds (approx.. 50 per plate) were placed in a row at the top of a 1/2 MS media plate. After 12 d, roots were cut from the shoots and all roots from the same plate placed together in tubes with 100 µL of water. The sealed tubes were heated to 85^{o}C for 20 min. Tubes were cooled before osmolality was measured with a Friske 210 micro-sample osmometer. Final displayed osmolalitywas adjusted for the fresh weight of the input material.

Trafficking of PIP2;1-GFP

Internalisation of PIP2;1-GFP in response to osmotic stress was measured in epidermal root cells of the elongation zone of 6 d old plants. Plants were transferred from 1/2 MS media to liquid 1/2 MS containing 100 mM NaCl or 200 mM mannitol 30 min before imaging, or control 1/2 MS. Imaging was performed using a Nikon A1R confocal laser scanning microscope with a 60x Plan Apo VC WI objective. A ratio of PIN2;1-GFP (excitation = 488 nm, emission = 500 – 550 nm) at the PM and inside the cell was determined by measuring the signal intensity at the PM and inside the cell with FIJI. All results were normalised to wildtype median signal ratio under control conditions.

3.5 References

Assaha, D.V.M., Ueda, A., Saneoka, H., Al-Yahyai, R., and Yaish, M.W. (2017). The role of Na^+ and K^+ transporters in salt stress adaptation in glycophytes. Frontiers in Physiology **8,** 509.

Bassil, E., Ohto, M.A., Esumi, T., Tajima, H., Zhu, Z., Cagnac, O., Belmonte, M., Peleg, Z., Yamaguchi, T., and Blumwald, E. (2011). The Arabidopsis intracellular Na^+/H^+ antiporters NHX5 and NHX6 are endosome associated and necessary for plant growth and development. Plant Cell **23,** 224-239.

Batelli, G., Verslues, P.E., Agius, F., Qiu, Q., Fujii, H., Pan, S., Schumaker, K.S., Grillo, S., and Zhu, J.K. (2007). SOS2 promotes salt tolerance in part by interacting with the vacuolar H^+-ATPase and upregulating its transport activity. Molecular and Cellular Biology **27,** 7781-7790.

Boursiac, Y., Boudet, J., Postaire, O., Luu, D.T., Tournaire-Roux, C., and Maurel, C. (2008). Stimulus-induced downregulation of root water transport involves reactive oxygen species-activated cell signalling and plasma membrane intrinsic protein internalization. Plant Journal **56,** 207-218.

Chaumont, F., and Tyerman, S.D. (2014). Aquaporins: highly regulated channels controlling plant water relations. Plant Physiology **164,** 1600-1618.

Che-Othman, M.H., Millar, A.H., and Taylor, N.L. (2017). Connecting salt stress signalling pathways with salinity-induced changes in mitochondrial metabolic processes in C3 plants. Plant Cell and Enviroment **40,** 2875-2905.

Chen, Z.C., Yamaji, N., Fujii-Kashino, M., and Ma, J.F. (2016). A cation-chloride cotransporter gene is required for cell elongation and osmoregulation in rice. Plant Physiology **171,** 494-507.

Colmenero-Flores, J.M., Martínez, G., Gamba, G., Vázquez, N., Iglesias, D.J., Brumós, J., and Talón, M. (2007). Identification and functional characterization of cation-chloride cotransporters in plants. Plant Journal **50,** 278-292.

Cutler, S.R., Ehrhardt, D.W., Griffitts, J.S., and Somerville, C.R. (2000). Random GFP::cDNA fusions enable visualization of subcellular structures in cells of Arabidopsis at a high frequency. Proceedings of the National Academy of Sciences **97,** 3718-3723.

Dettmer, J., Hong-Hermesdorf, A., Stierhof, Y.D., and Schumacher, K. (2006). Vacuolar H^+-ATPase activity is required for endocytic and secretory trafficking in Arabidopsis. Plant Cell **18,** 715-730.

Dragwidge, J.M., Scholl, S., Schumacher, K., and Gendall, A.R. (2019). NHX-type $Na^+(K^+)/H^+$ antiporters are required for TGN/EE trafficking and endosomal ion homeostasis in *Arabidopsis thaliana*. Journal of Cell Science **132**.

Gao, D., Knight, M.R., Trewavas, A.J., Sattelmacher, B., and Plieth, C. (2004). Self-reporting Arabidopsis expressing pH and Ca^{2+} indicators unveil ion dynamics in the cytoplasm and in the apoplast under abiotic stress. Plant Physiology **134,** 898-908.

Guo, W., Zuo, Z., Cheng, X., Sun, J., Li, H., Li, L., and Qiu, J.L. (2014). The chloride channel family gene CLCd negatively regulates pathogen-associated molecular pattern (PAMP)-triggered immunity in Arabidopsis. Journal of Experimental Botany **65,** 1205-1215.

Hachez, C., Veljanovski, V., Reinhardt, H., Guillaumot, D., Vanhee, C., Chaumont, F., and Batoko, H. (2014). The Arabidopsis abiotic stress-induced TSPO-related protein reduces cell-surface expression of the aquaporin PIP2;7 through protein-protein interactions and autophagic degradation. Plant Cell **26,** 4974-4990.

Halperin, S.J., Gilroy, S., and Lynch, J.P. (2003). Sodium chloride reduces growth and cytosolic calcium, but does not affect cytosolic pH, in root hairs of *Arabidopsis thaliana* L. Journal of Experimental Botany **54,** 1269-1280.

Henderson, S.W., Wege, S., Qiu, J., Blackmore, D.H., Walker, A.R., Tyerman, S.D., Walker, R.R., and Gilliham, M. (2015). Grapevine and Arabidopsis cation-chloride cotransporters localize to the

Golgi and trans-Golgi network and indirectly influence long-distance ion transport and plant salt tolerance. Plant Physiology **169,** 2215-2229.

Isayenkov, S.V., and Maathuis, F.J.M. (2019). Plant salinity stress: many unanswered questions remain. Frontiers in Plant Science **10,** 80.

Kader, M.A., and Lindberg, S. (2010). Cytosolic calcium and pH signaling in plants under salinity stress. Plant Signaling & Behaviour **5,** 233-238.

Kader, M.A., Lindberg, S., Seidel, T., Golldack, D., and Yemelyanov, V. (2007). Sodium sensing induces different changes in free cytosolic calcium concentration and pH in salt-tolerant and -sensitive rice (Oryza sativa) cultivars. Physiologia Plantarum **130,** 99-111.

Krebs, M., Beyhl, D., Görlich, E., Al-Rasheid, K.A., Marten, I., Stierhof, Y.D., Hedrich, R., and Schumacher, K. (2010). Arabidopsis V-ATPase activity at the tonoplast is required for efficient nutrient storage but not for sodium accumulation. Proceedings of the National Academy of Sciences **107,** 3251-3256.

Li, M., Li, Y., Li, H., and Wu, G. (2011). Overexpression of AtNHX5 improves tolerance to both salt and drought stress in Broussonetia papyrifera (L.) Vent. Tree physiology **31,** 349-357.

Luo, Y., Scholl, S., Doering, A., Zhang, Y., Irani, N.G., Rubbo, S.D., Neumetzler, L., Krishnamoorthy, P., Van Houtte, I., Mylle, E., Bischoff, V., Vernhettes, S., Winne, J., Friml, J., Stierhof, Y.D., Schumacher, K., Persson, S., and Russinova, E. (2015). V-ATPase activity in the TGN/EE is required for exocytosis and recycling in Arabidopsis. Nature Plants **1,** 15094.

Luu, D.T., Martinière, A., Sorieul, M., Runions, J., and Maurel, C. (2012). Fluorescence recovery after photobleaching reveals high cycling dynamics of plasma membrane aquaporins in Arabidopsis roots under salt stress. Plant Journal **69,** 894-905.

Marmagne, A., Vinauger-Douard, M., Monachello, D., de Longevialle, A.F., Charon, C., Allot, M., Rappaport, F., Wollman, F.A., Barbier-Brygoo, H., and Ephritikhine, G. (2007). Two members of the Arabidopsis CLC (chloride channel) family, AtCLCe and AtCLCf, are associated with thylakoid and Golgi membranes, respectively. Journal of Experimental Botany **58,** 3385-3393.

Martinière, A., Bassil, E., Jublanc, E., Alcon, C., Reguera, M., Sentenac, H., Blumwald, E., and Paris, N. (2013). In vivo intracellular pH measurements in tobacco and Arabidopsis reveal an unexpected pH gradient in the endomembrane system. Plant Cell **25,** 4028-4043.

McDowell, S.C., Akmakjian, G., Sladek, C., Mendoza-Cozatl, D., Morrissey, J.B., Saini, N., Mittler, R., Baxter, I., Salt, D.E., Ward, J.M., Schroeder, J.I., Guerinot, M.L., and Harper, J.F. (2013). Elemental concentrations in the seed of mutants and natural variants of *Arabidopsis thaliana* grown under varying soil conditions. PloS One **8,** e63014.

Moseyko, N., and Feldman, L.J. (2001). Expression of pH-sensitive green fluorescent protein in *Arabidopsis thaliana*. Plant Cell and Enviroment **24,** 557-563.

Reguera, M., Bassil, E., Tajima, H., Wimmer, M., Chanoca, A., Otegui, M.S., Paris, N., and Blumwald, E. (2015). pH regulation by NHX-type antiporters is required for receptor-mediated protein trafficking to the vacuole in Arabidopsis. Plant Cell **27,** 1200-1217.

Rosquete, M.R., Davis, D.J., and Drakakaki, G. (2018). The plant trans-Golgi network: not just a matter of distinction. Plant Physiology **176,** 187-198.

Schindelin, J., Arganda-Carreras, I., Frise, E., Kaynig, V., Longair, M., Pietzsch, T., Preibisch, S., Rueden, C., Saalfeld, S., Schmid, B., Tinevez, J.Y., White, D.J., Hartenstein, V., Eliceiri, K., Tomancak, P., and Cardona, A. (2012). Fiji: an open-source platform for biological-image analysis. Nature Methods **9,** 676-682.

Shabala, S.N., and Lew, R.R. (2002). Turgor regulation in osmotically stressed Arabidopsis epidermal root cells. Direct support for the role of inorganic ion uptake as revealed by concurrent flux and cell turgor measurements. Plant Physiology **129,** 290-299.

Sharma, A., Shahzad, B., Kumar, V., Kohli, S.K., Sidhu, G.P.S., Bali, A.S., Handa, N., Kapoor, D., Bhardwaj, R., and Zheng, B. (2019). Phytohormones regulate accumulation of osmolytes under abiotic stress. Biomolecules **9**.

Shen, J., Zeng, Y., Zhuang, X., Sun, L., Yao, X., Pimpl, P., and Jiang, L. (2013). Organelle pH in the Arabidopsis endomembrane system. Molecular Plant **6,** 1419-1437.

Sze, H., and Chanroj, S. (2018). Plant endomembrane dynamics: studies of K^+/H^+ antiporters provide insights on the effects of pH and ion homeostasis. Plant Physiology **177,** 875-895.

van Zelm, E., Zhang, Y., and Testerink, C. (2020). Salt tolerance mechanisms of plants. Annual Reviews in Plant Biology **71,** 403-433.

von der Fecht-Bartenbach, J., Bogner, M., Krebs, M., Stierhof, Y.D., Schumacher, K., and Ludewig, U. (2007). Function of the anion transporter AtCLC-d in the trans-Golgi network. Plant Journal **50,** 466-474.

Yu, F., Lou, L., Tian, M., Li, Q., Ding, Y., Cao, X., Wu, Y., Belda-Palazon, B., Rodriguez, P.L., Yang, S., and Xie, Q. (2016). ESCRT-I component VPS23A affects ABA signaling by recognizing ABA receptors for endosomal degradation. Molecular Plant **9,** 1570-1582.

Zhu, X., Pan, T., Zhang, X., Fan, L., Quintero, F.J., Zhao, H., Su, X., Li, X., Villalta, I., Mendoza, I., Shen, J., Jiang, L., Pardo, J.M., and Qiu, Q.S. (2018). K^+ efflux antiporters 4, 5, and 6 mediate pH and K^+ homeostasis in endomembrane compartments. Plant Physiology **178,** 1657-1678.

Chapter 4

Polysaccharide Accumulation and Auxin Signalling are Altered in *Atccc1* Knockouts

4.1 Introduction

Plant cells are delineated by two important boundaries; the cell wall and plasma membrane (PM). Intracellularly derived proteins and polysaccharides are essential for the role of both. Transporters at the PM can mediate uptake of nutrients and receptors perceive external signals such as hormones. Hormones such as auxin drive plant growth, development and response to environmental conditions. The polysaccharide composition of the cell wall adjusts cell growth, shape and can alter pathogen resistance (Molina et al., 2021). Most proteins that are integrated into the PM are synthesised in the Endoplasmic Reticulum (ER); while many of the cell wall polysaccharides (excluding cellulose and callose, which are synthesised at the PM) are synthesised in the Golgi (Brandizzi, 2018; Sinclair et al., 2018). Proteins and polysaccharides therefore require delivery to the PM and apoplast, which is mediated by the endomembrane system. The hub for this trafficking system is the Trans-Golgi Network/Early Endosome (TGN/EE), the intersection between secretory and endocytic trafficking pathways as well as the intersection for cell surface and vacuolar delivery routes (Dettmer et al., 2006). Defects in endomembrane trafficking commonly result in alterations to auxin signalling and cell wall composition (Rogers et al., 2005; McFarlane et al., 2013; Dragwidge et al., 2018; Rosquete et al., 2018; Sinclair et al., 2018).

Cell wall

The cell wall is primarily composed of cellulose fibres embedded in a cell wall matrix. The cell wall can be dynamically modified to increase extensibility, fortified to increase pathogen resistance or lignified to provide structural strength and impermeability (Cosgrove, 2016; Bacete and Hamann, 2020). The broad role of the TGN/EE in trafficking of a variety of cargo makes it important for many aspects of cell wall formation. Cell wall matrix polysaccharides such as pectin, xyloglucan and hemicellulose are synthesised in the Golgi and therefore require secretion to the apoplast (Driouich et al., 2012). Likewise, glycoproteins are synthesised into the Endoplasmic Reticulum and are thought to traffic to the apoplast through the TGN/EE (Sinclair et al., 2018). Cellulose and callose are synthesised at the PM by the cellulose synthase complex and glucan synthase-likes respectively. Both cellulose synthase complexes and glucan synthase-likes are reliant on TGN/EE mediated trafficking for normal function (Drakakaki et al., 2012; Bashline et al., 2014).

Regulation of the cell wall rigidity is vital to enabling cell growth and shape (Cosgrove, 2016). Cell wall rigidity is regulated by the cell wall matrix, specifically, by the pectin composition. The most common of the different types of pectins in Arabidopsis is homogalacturonan, which carries methyl-ester groups, altering the bonding properties of the polysaccharide and therefore the strength of the cell wall matrix (Cosgrove, 2016; Amos and Mohnen, 2019). De-methyl-esterified pectin forms additional cross links with cell wall matrix polysaccahrides in the presence of Ca^{2+}, stiffening the cell wall (Wu et al., 2018). Homogalacturonan pectin is, by default, synthesised with attached methyl-ester groups. Once integrated into the cell wall, methyl ester groups are be removed by PECTIN METHYL-ESTERASE's (PME's) to increase cell wall rigidity. In pollen tubes, PMEs are predominantly localised at the shanks of the cell while the negative regulators of PMEs, PME INHIBITORS (PMEI) are found at the growing tip (Röckel et al., 2008). It has been postulated that a similar distribution is likely to mediate tip growth in root hairs (Mendrinna and Persson, 2015).

In Arabidopsis, large quantities of pectin are deposited in the seed coat. When mature seeds are imbibed, the pectin is hydrated resulting in rapid expansion of a pectineus gel that ruptures the outside of the seed coat and surrounds the seed (Voiniciuc et al., 2015). Arabidopsis seed mucilage is primarily composed of pectin, which is synthesised in the Golgi and deposited in the apoplast of the seed coat cells in a specific pattern prior to seed maturation and cessation of growth. Mucilage is deposited in a ring around a large central pillar of secondary cell wall called the columella (Fig. 1) (Haughn and Western, 2012). The accumulation of mucilage and subsequent formation of the columella results in displacement of the cytoplasm. The large accumulation of polysaccharides in mucilage and the conspicuousness of mucilage excretion have led to suggestions that mucilage is an ideal model for studying polysaccharide synthesis (Arsovski et al., 2010; Haughn and Western, 2012; Griffiths and North, 2017). Like cell wall integrated pectin, mucilage pectin is synthesised in the Golgi and requires TGN/EE mediated secretion to be deposited in the apoplast. Reduced mucilage excretion has been observed in trafficking mutants such as the TGN/EE protein mutant *echidna* and the exocyst complex mutant *exo70A1*, which is required for reception of vesicles at the PM (Kulich et al., 2010; McFarlane et al., 2013).

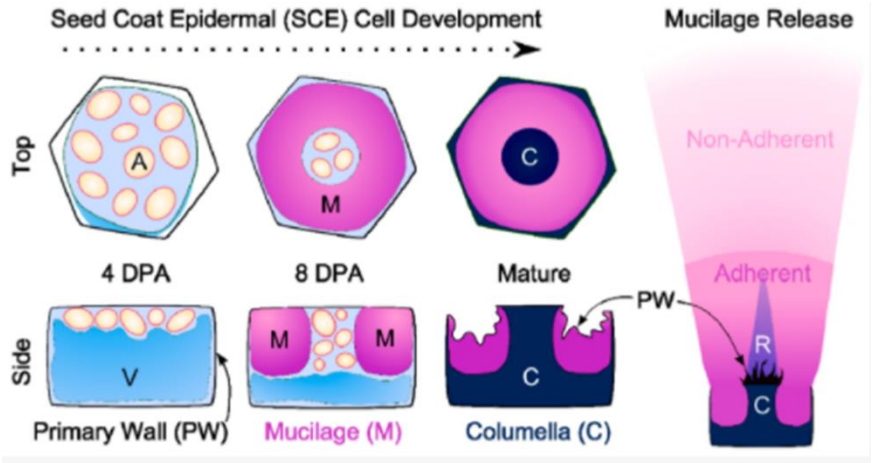

Figure 1. Development of mature seed coat cells in Arabidopsis. As seed coat cells mature, cytoplasm, vacuole (V) and amyloplasts (A) are displaced by apoplastic deposits of mucilage (M). The mucilage is deposited in a ring. After mucilage deposition, an intracellular cell wall forms, the columella (C). Image from Voiniciuc et al. (2015).

Auxin

Auxin is a plant hormone with an important role in plant growth and development. Auxin can impact and regulate cell division, cell expansion, cell differentiation, lateral root formation and flowering (Leyser, 2018). Auxin synthesis is not ubiquitous throughout the plant, rather, the majority of synthesis occurs in specific tissue such as apical meristems (Ljung et al., 2005). Therefore, directed transport of auxin from source tissue is a key component of auxin signalling. This transport is mediated by proteins from the PIN-FORMED (PIN) family (Zwiewka et al., 2019). PM localised PIN proteins export auxin from cells. Polar localisation of PIN proteins to just one side of a cell results in directional efflux of auxin. This creates a flow of auxin through tissue and enables the distribution of auxin throughout the plant (Fig. 2) (Adamowski and Friml, 2015). Therefore, regulation of the localisation of PIN proteins plays a large role in determining auxin distribution and subsequently plant growth, development and shape (Vieten et al., 2005; Adamowski and Friml, 2015). Localisation and degradation of PM PIN proteins is reliant on the endomembrane system. It is therefore, unsurprising that defects in endomembrane trafficking result in changes to auxin distribution. The mutant, *nhx5/nhx6*, has a decreased TGN/EE pH, reduced abundance of PIN1 and PIN2 in roots and an altered distribution of auxin in roots (Dragwidge et al., 2018).

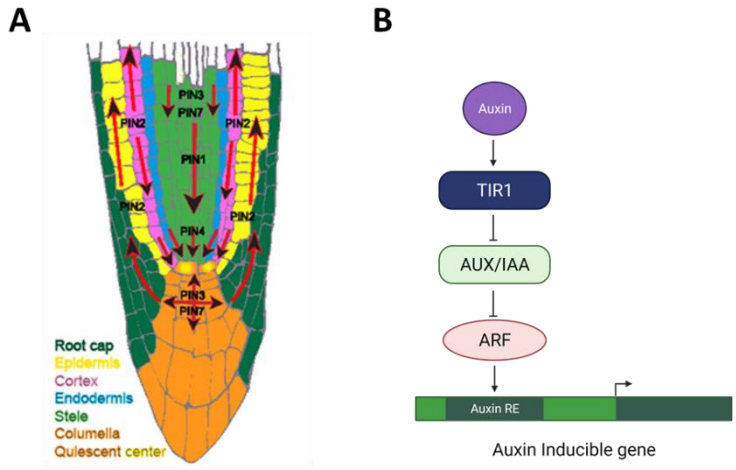

Figure 2. Auxin transport and signalling in Arabidopsis roots. A) Directional auxin flow through plant tissue is dependent on polar localised PIN auxin transporters. Specific PIN expression and polarity is cell type specific. Image from Feraru et al. (2008). B) Auxin triggers transcriptional changes in cells mediated through the physical interaction between TIR1 and the DII domain of AUX/IAA proteins. Interaction between TIR1 and AUX/IAA results in ubiquitination and subsequent degradation of AUX/IAA proteins. This results in the release of ARF proteins which interact with auxin response elements (RE) to alter expression of downstream genes.

Auxin is detected intracellularly and results in the degradation of AUXIN ALTERED GENE EXPRESSION/INDOLEACETIC ACID-INDUCED PROTEINs (AUX/IAA) (Zenser et al., 2001). Necessary and sufficient for this is domain II (DII). AUX/IAA proteins bind and repress the activity of the AUXIN RESPONSE FACTOR (ARF) transcription factors (Li et al., 2016). DII mediated AUX/IAA degradation results in the activation of ARF transcription factors that target auxin response elements to alter gene expression (Fig. 2). DII and auxin response elements are, therefore, commonly utilised to assay auxin content in cells. Fluorescent proteins fused with DII will be degraded in response to auxin (Brunoud et al., 2012). Auxin can also be assayed with the *DR5* promoter, a construct consisting of seven consecutive auxin response elements resulting in upregulation of the *DR5* driven reporter in response to auxin (Ulmasov et al., 1997).

We have characterised a novel endomembrane ion regulatory protein, CATION CHLORIDE COTRANSPORTER (AtCCC1) (Chapters 2 and 3), and found that the Cl^- and Na^+/K^+ symporter likely exports ions from the TGN/EE lumen into the cytosol. The transport activity of AtCCC1 is required for pH regulation of the TGN/EE lumen (Chapter 2, Fig. 4). Importantly, we further demonstrated that AtCCC1 is required for normal endomembrane trafficking (Chapter 2, Fig. 5). Here, to further assess the role of AtCCC1 in endomembrane trafficking,

we investigated if *Atccc1* has defects in pectin secretion and auxin distribution. We found that *Atccc1* seeds exude less mucilage than wildtype. In addition, the polysaccharide composition of cell walls in leaves was assayed showing mild differences between *Atccc1* and wildtype. The signal intensity of PIN1-GFP and PIN2-GFP in *Atccc1* was assayed and suggested a lower abundance of both PIN1 and PIN2 in *Atccc1* compared to wildtype. Auxin distribution was assayed using both DII and *DR5* reporters. Results obtained with the two reporters indicate that there are alterations in auxin signalling and/or distribution.

4.2 Results

Mucilage excretion and seed coat formation are altered in Atccc1

To investigate if the endomembrane trafficking defects in *Atccc1* lead to defects in pectin secretion, mucilage release from *Atccc1* seeds was visualised with the dye, ruthenium red. This revealed a reduction in mucilage expelled from *Atccc1* seeds (Fig. 3). *Atccc1* seeds were, on average, larger than wildtype seeds and so the mucilage expelled was normalised to the seed size. After normalisation, the two *Atccc1* genotypes had on average a 30% decrease in mucilage released compared to wildtype. The pattern of expulsion was also perturbed with wildtype mucilage forming a uniform and complete ring around the seed while *Atccc1* seed mucilage was unevenly distributed around the seed. The central columella of seed coat cells is observable in imbibed, ruthenium red treated, cells with a stereo microscope and it appears as dark structure in the centre of each seed coat cell (Fig 3.). Columella cells are also visible in dry, untreated seeds using a laser scanning microscope such as a confocal, due to high level of autofluorescence from the cell wall of the columella (Fig. 3). While a columella is visible at the centre of every seed coat cell in wildype, they do not appear in every cell of *Atccc1* seed coats. The seed coats of *Atccc1* were frequently patchy which may indicate the lack of the intracellular secondary cell wall that is the columella.

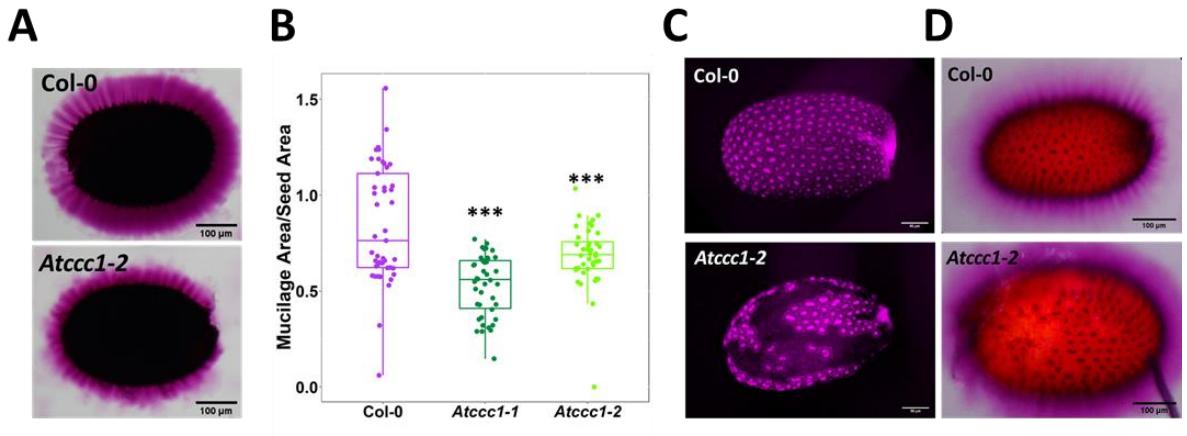

Figure 3. Mucilage excretion is reduced and seed coat cell development is altered in *Atccc1* seeds. A-B) Seed mucilage stained with ruthenium red (magenta) exhibits uneven excretion in *Atccc1* seeds. Total mucilage excretion is reduced. C) Ruthenium red staining and D) cell wall autofluorescence enabled the visualisation of seed coat cell wall features such as the central columella of seed coat cells. *Atccc1* seed coats have a patchy appearance with some cells lacking the columella. Scale bars are 100 µm (A and C) and 50 µm (D). *** indicates P < 0.001

Loss of AtCCC1 results in altered polysaccharide composition in young leaves

Reduced mucilage excretion and missing columella indicate issues with polysaccharide delivery or synthesis in *Atccc1*. To determine if the cell wall polysaccharide accumulation was altered in *Atccc1*, a monosaccharide analysis was performed on leaves of *Atccc1* and wildtype plants. This analysis quantifies the simple sugars from the insoluble part of the cell (Fig. 4). The analysis does not include any sugars from cellulose which is not degraded in this experiment, neither does it include sugars that are already soluble in the tissue and are removed by a 70% ethanol wash and were measured separately (Fig.4). For Arabidopsis, the primary monosaccharides of pectin are galacturonic acid, rhamnose and arabinose. Pectin is important in primary cell walls for regulating cell wall expansion. *Atccc1* has defects in cell elongation, particularly of root hairs (Chapter 2, Fig. 2). This may be a result of reduced amounts of pectin in primary cell walls. To more specifically address this, the chosen tissue type for the analysis, leaves, were separated into two groups, young and mature. In young leaves, xylose, arabinose and fucose were consistently higher in both *Atccc1* mutant alleles compared with wildtype (Fig. 4). Wildtype leaves contained 1.0% xylose (w/w of dry weight), 1.4% arabinose and 0.17% fucose compared with 1.2% xylose, 1.9% arabinose and 0.21% fucose in *Atccc1*. This is in contrast to mature leaves where no consistent alterations in the levels of any sugar were detected between *Atccc1* and wildtype.

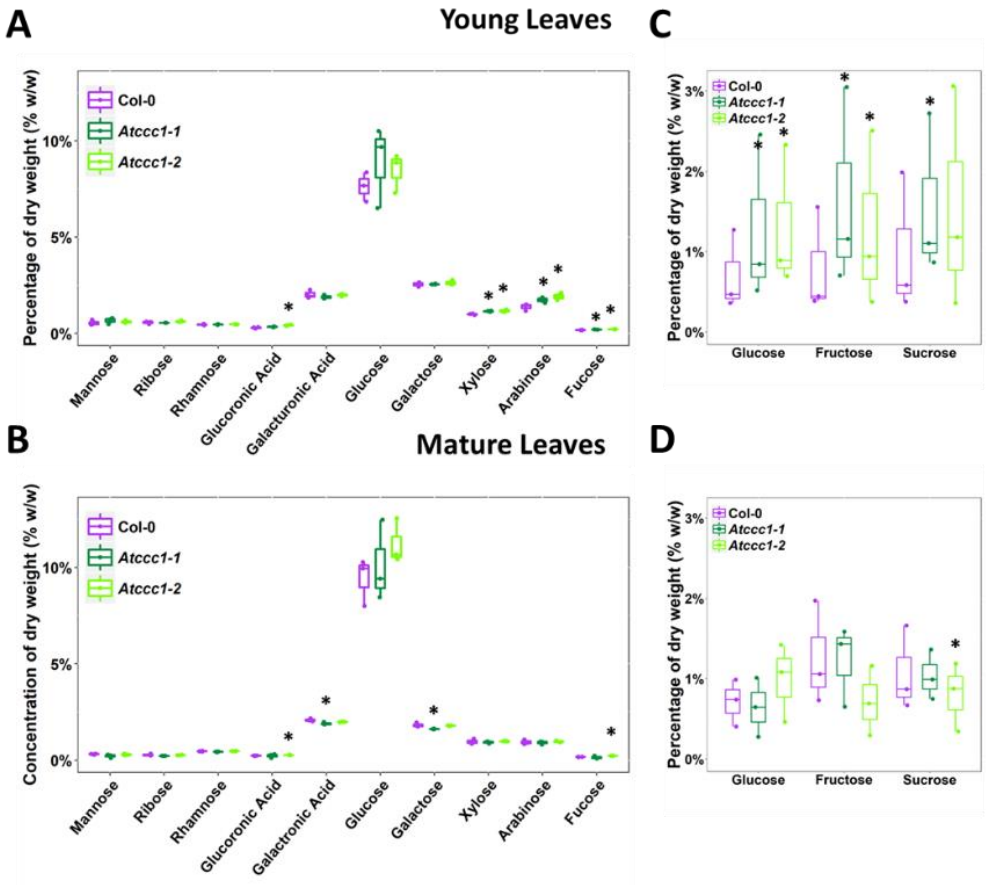

Figure 4. The cell wall composition of young leaves is altered in *Atccc1*. A-B) The composition of insoluble monosaccharides from cell walls from ground A) young and B) mature leaf material of 6 week old plants. C-D) The percentage (w/w dry weight) of soluble monosaccharides from ground C) young or D) mature leaves. * indicates $P < 0.05$

For each sample, a soluble fraction was also obtained. The levels of glucose, fructose and sucrose were measured from the soluble fractions. In young leaves, glucose and fructose were almost doubled in both mutants (Fig. 4). Wildtype plants contained 1.6% glucose and 0.5% fructose compared with 2.7% glucose and 1.0% fructose in *Atccc1-1* and 2.6% glucose and 1.0% fructose in *Atccc1-2*. Combining the three sugars, *Atccc1* plants showed a significantly higher amount of soluble sugar in young leaves. In wildtype plants, the three soluble sugars accounted for 2.5% of the dry weight of young leaves whereas the three sugars accounted for 4.5% and 4.1% of the dry weight of *Atccc1-1* and *Atccc1-2* respectively. No differences in the levels of soluble sugar was detected in mature leaves (Fig. 4).

Fluorescence of PIN1-GFP and PIN2-GFP is reduced in Atccc1 *roots*

It was previously found that the PM abundance of PIN1 and PIN2 is lower in *nhx5/nhx6* roots (Dragwidge et al., 2018). We therefore investigated PIN1 and PIN2 abundance at the PM in *Atccc1*. *pPIN1::PIN1-GFP* and *pPIN2::PIN2-GFP* were expressed in wildtype and *Atccc1* plants. The polarity of both PIN1-GFP and PIN2-GFP was unaltered in *Atccc1* (Fig. 5). The signal intensity was measured at the apical side of stele cells and the basal side of epidermal cells of the elongation zone for PIN1-GFP and PIN2-GFP respectively. The signal intensity was lower for both PIN1-GFP and PIN2-GFP in *Atccc1*. For PIN1-GFP, the signal intensity was 40% lower in *Atccc1* compared with wildtype while for PIN2-GFP, the signal intensity was 26% lower in *Atccc1*. The reduced PM signal intensity of PIN1-GFP and PIN2-GFP may indicate a reduced abundance of PIN1 and PIN2 at the PM in *Atccc1*.

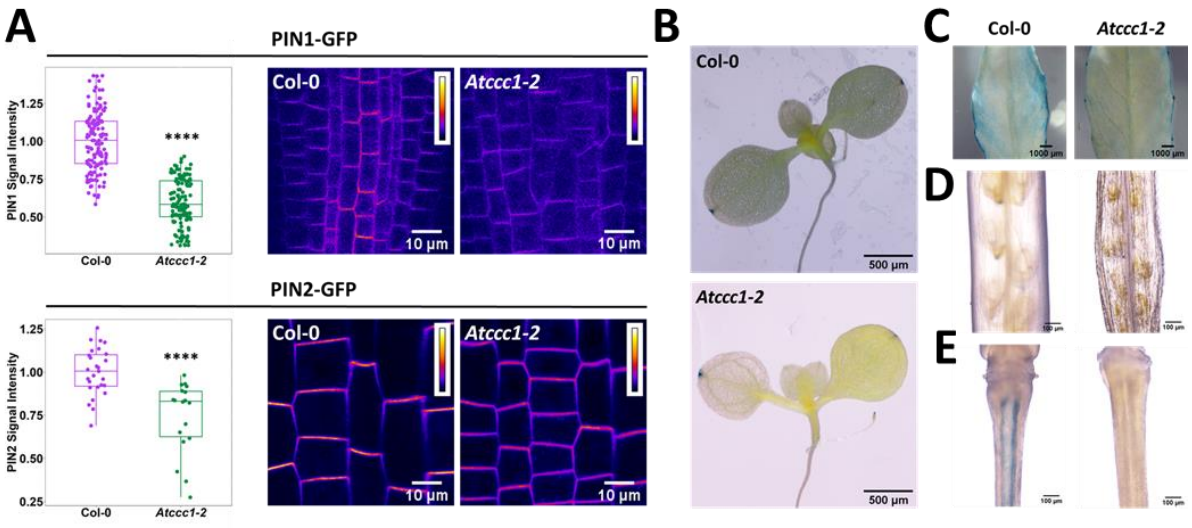

Figure 5. Fluorescence of PIN1-GFP and PIN2-GFP is reduced in *Atccc1*. A) The total signal intensity of PIN1-GFP and PIN2-GFP was measured in the root stele and epidermal cells of the root elongation zone respectively. PIN1-GFP is displayed as a maximum intensity projection of several optical sections, while PIN2-GFP is a single optical section. B-E) *DR5* promoter activity indicated by GUS staining (blue) of B) 6 d old seedlings, and C) leaves and D-E) siliques of 4 week old plants. Staining was performed overnight. Scale bars are A) 10 µm, B) 500 µm, C) 1000 µm or D-E) 100 µm. **** indicates $P < 0.0001$

AtCCC1 is important for root auxin detection

As there are likely differences in PIN1 and PIN2 abundance in *Atccc1*, we assayed if auxin distribution was perturbed in *Atccc1*. We used genetically encoded markers and sensors to assess auxin distribution. Auxin distribution was first assayed at the tissue level using β-glucuronidase (GUS) driven by the auxin induced promoter, *DR5*. GUS staining was identical in wildtype and *Atccc1*, in roots and first true leaves, while the staining pattern differed in more developmentally advanced leaves (Fig. 5). A different GUS staining pattern between wildtype and *Atccc1* was also observed in the vasculature in the pedicel, and in the funiculus, where the seed connects to silique. As differences in auxin distribution were observed at the tissue level and PIN abundance might be reduced in roots, we sought to further investigate auxin distribution in *Atccc1* at the cellular level. To achieve this, we expressed the ratiometric auxin sensor, R2D2, in wildtype and *Atccc1* plants. R2D2 expression is driven by the *RPS5A* promoter, and the sensor is therefore expressed only in dividing cells (Liao et al., 2015). R2D2 revealed no difference in root tip auxin accumulation between wildtype and *Atccc1* (Fig. 6). Both the signal pattern and the relative auxin quantity was the same. To confirm the efficacy of the sensor in the two genotypes, relative auxin concentration was measured after a 30 min treatment with 10 µM IAA. The result was a 28% increase in wildtype as expected, but only a 2% increase in *Atccc1*. This result suggested that *Atccc1* cells may be less responsive to auxin induced degradation of DII domain proteins, as IAA is membrane permeable when protonated (external media pH set to 5.6) and the high concentration ensured that IAA will increase in the cytosol, despite lower PIN abundance in *Atccc1* (Yang et al., 2006). A second auxin reporter was used as well, with which similar results were obtained. The auxin reporter DII-3xVENUS (expression driven by the *35s* promoter) was crossed into *Atccc1*, and signal intensity of the fluorescent reporter was lower in *Atccc1* compared to wildtype (Fig. 6). As this sensor is not ratiometric, lower signal may indicate increased auxin, increased auxin independent protein degradation or decreased expression.

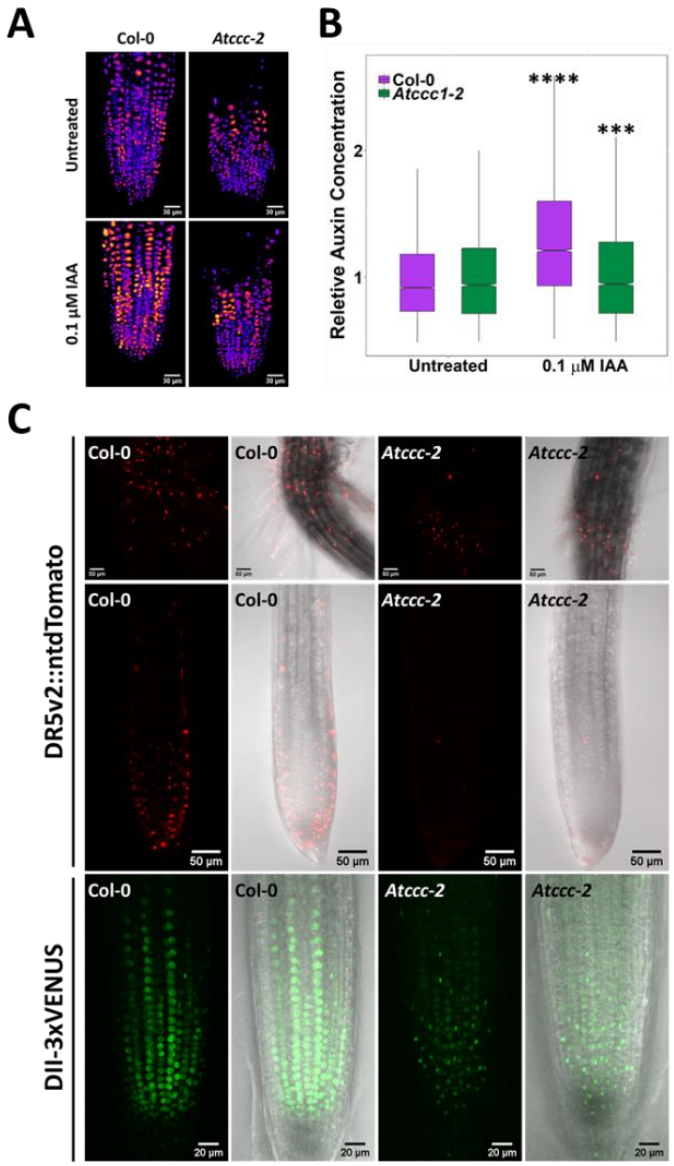

Figure 6. Auxin signalling is altered in *Atccc1* plants. Root auxin content was assayed using A-B) the ratiometric auxin sensor, R2D2, or C) the auxin reporters *DR5v2::ntdTomato* and *2x35S::DII-3xVENUS*. A-B) The relative auxin content of wildtype and *Atccc1* root tips is assayed in control conditions and in response to 30 min IAA treatment. C) Auxin is assayed with nuclear localised fluorescent protein ntdTomato (red) driven by the auxin responsive *DR5v2* promoter in hypocotyls or root tips. DII-3xVENUS (green) is degraded in response to auxin. Imaging performed in root tips. Scale bars are 30 µm (R2D2), 50 µm (ntdTomato) and 20 µm (DII-3xVENUS). All images are maximum intensity projections of several optical sections. *** indicates $P < 0.001$, **** indicates $P < 0.0001$

To further investigate auxin response, the auxin reporter, *DR5v2::ntdTomato,* was used (red fluorescent protein with a nuclear localisation signal). *DR5v2*, is a promoter downstream of DII regulated transcription factors and is upregulated by auxin. If degradation of the DII proteins, AUX/IAA, is impaired in *Atccc1* then *DR5v2* activation should be reduced in *Atccc1* plants. In wildtype root tips, ntdTomato was detected in epidermal cells while the marker was almost never detected in any cells of *Atccc1* root tips (Fig. 6). The marker was, however, present and observable in the hypocotyl of both wildtype and *Atccc1* plants. This might be consistent with an impaired degradation of DII containing proteins in *Atccc1*, resulting in reduced AUX/IAA degradation and reduced ARF mediated *DR5v2* activation. Differences in auxin signalling may not have been detected with GUS staining due to the lower sensitivity of the method (see also

Chapter 2, Fig. 1). These results indicate that in addition to reduced PIN abundance and trafficking of PIN2, *Atccc1* plants may have defects in auxin signalling.

Atccc1 *roots detect and respond to IAA*

To investigate if the potentially disturbed auxin signalling on the cellular level translates into changes in auxin response on the plant level, wildtype and *Atccc1* seedlings were grown and transferred to media supplemented with IAA for 24h. IAA treatment is known to increase both the number and length of root hairs in wildtype plants (Vissenberg et al., 2020). We could confirm this in our assay, with wildtype seedlings on media containing 0.03 µM or 0.2 µM (Fig. 7). IAA did increase root hair initiation in *Atccc1*, however, did not result in longer root hairs compared with untreated plants. The short root hairs of *Atccc1* may be due to other factors and cannot be rescued by IAA. The increase in root hair initiation sites, however, suggests that *Atccc1* roots could detect and respond to IAA.

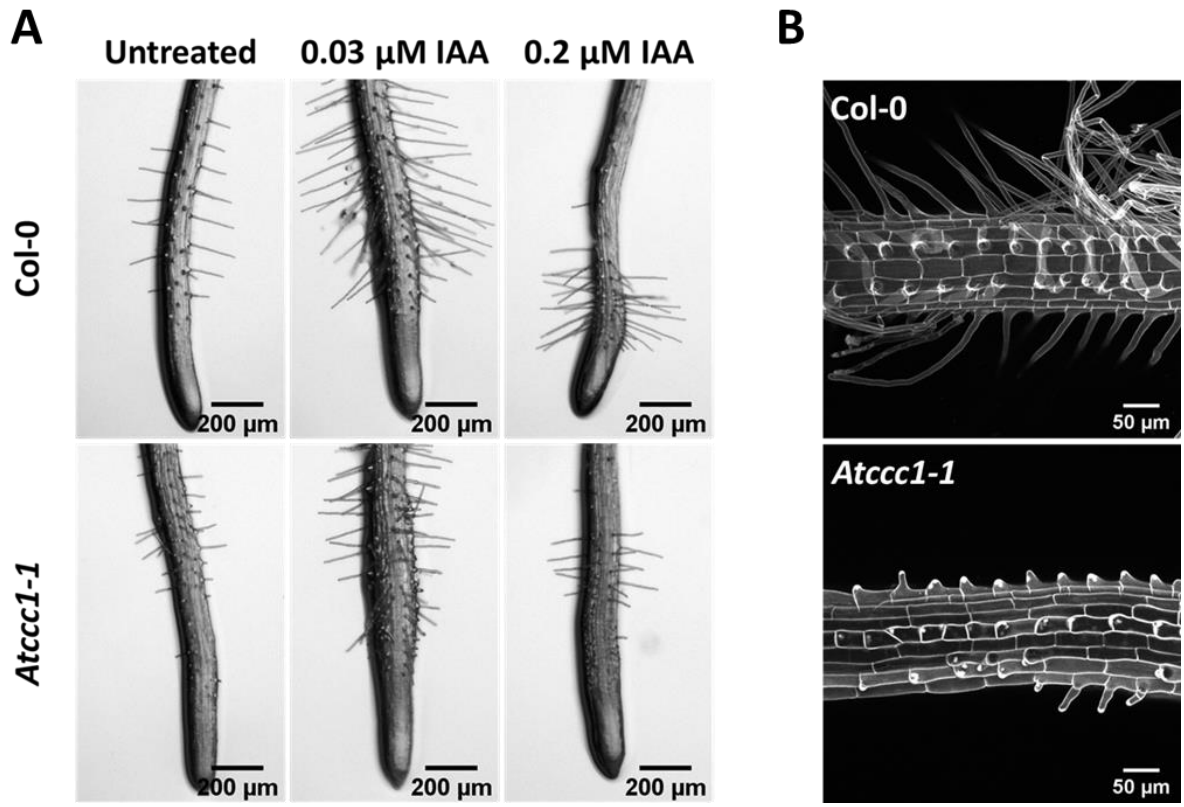

Figure 7. *Atccc1* roots are responsive to auxin. 24 h IAA treatment of wildtype and *Atccc1* roots of 6d old. A) IAA treatment induced root growth arrest and initiation of root hairs. B) Maximum intensity projections of optical sections, cell wall autofluorescence is shown in white. Plants treated with 0.2 µM IAA show increased root hair initiation. Root hairs are elongated in wildtype cells. Bumps on *Atccc1* roots are initiated root hairs, suggesting responsiveness to the IAA treatment.

4.3 Discussion

Atccc1 knockouts have severe phenotypic defects, which indicates that core processes are impaired in these plants. Here, we addressed two major aspects that can be affected in plants with altered endomembrane trafficking: cell wall composition and auxin distribution.

We observed a reduction in seed mucilage, altered seed coats and changes to monosaccharide accumulation in *Atccc1*. Altered monosaccharide accumulation was observed in young leaves, while mature leaves had monosaccharide levels comparable to wildtype. This suggests that the differences in cell wall composition may be more pronounced in growing cells. Supporting our data, a recent study by Han et al. (2020), published after the experiments described here were performed, found changes in monosaccharide composition. The tissue assayed is not specified and may be either hypocotyls or leaves. Similar to the results obtained here in young leaves, they show an increased accumulation of arabinose, fucose and xylose. In addition, they also show an increase in rhamnose, galactose and galacturonic acid to have an increase in all non-cellulosic polysaccharides assayed. They also measured the abundance of cellulose and found a reduction in *Atccc1* cell walls. Interestingly, *det3* plants also exhibit a reduction in cell wall cellulose and an increase in fucose, rhamnose and xylose in stems (Rogers et al., 2005).

The abundance of three soluble monosaccharides, glucose, sucrose and fructose, was measured in leaves. This revealed an increase in the total sugar in the younger leaves of *Atccc1* plants. Multiple factors could be contributing to this increase such as an overall reduction in plant growth, resulting in reduced energy requirements usage and therefore reduced breakdown of sugars. It could also indicate defects in shoot to root transport of sugars. Interestingly, however, is the implication of the increased sugar accumulation for osmolality in young leaves. With approximately double the amount of sugar in the developing leaves of *Atccc1*, there may be significant impacts to osmolality. The soluble sugar could be replacing other osmolytes that are missing in leaves. Previous work shows that hydroponically grown *Atccc1* plants accumulate more Cl^- under control conditions and more K^+, Na^+ and Cl^- in shoots of salt (50 mM NaCl) treated plants (Henderson et al., 2015). Similarly, soil grown *Atccc1* accumulates more Cl^- in leaves when grown with added Cl^- salts (50 mM Cl^-)(Colmenero-Flores et al., 2007). This potentially indicates that *Atccc1* plants have increased, not decreased accumulation of ions in shoots. Previous results (Chapter 3, Fig. 3), did not reveal changes in the cell sap

osmolality of whole roots, however, it is possible that only specific cell types, such as growing cells, might have an altered osmolality. Consistent with this, an increase in soluble sugar was only observed in young leaves and not mature leaves. In roots, elongation of the rapid growing root hairs is rescued by growing plants on media with higher osmolality which might help to reduce the difference in osmolality between the cell and external media (Chapter 3, Fig. 2). This could be rescuing root hairs if the internal osmolality is too high resulting in an elevated stress on the cell wall, being mitigated by increasing the rigidity of the cell wall. If there is a difference in the osmolality of a small subset of cells, the actively growing cells, then the whole root osmolality assay may not be sensitive enough to detect it. Sugar may accumulate in growing cells of *Atccc1* due to defects in the regulation of PM sugar transporters. Degradation of PM sugar transporters plays a role in their regulation and therefore *Atccc1* may impact sugar accumulation in specific cell types if trafficking to the vacuole or recycling of such transporters is impaired (Krügel and Kühn, 2013).

Mucilage quantity was reduced in *Atccc1* seeds. This suggests impaired excretion and trafficking in *Atccc1* resulting in decreased deposition of the required constituents of mucilage in the apoplastic space. The seed coats of *Atccc1* appear patchy when observed with both ruthenium red staining and auto-fluorescence. The spots in the middle of seed coat cells is likely the columella and therefore patchy *Atccc1* seeds are lacking these structures. Columella are likely not formed in *Atccc1* cells due to defects in the secretion of the cell wall material. This could be further addressed in the future through cross section imaging of seed coat cells during different stages of development to determine why columella are not forming.

Here, we use both DII and the *DR5v2* promoter to assay auxin content in the root tip. The DII containing R2D2 showed no difference in relative root tip auxin concentrations between *Atccc1* and wildtype plants. The sensor, however, was unresponsive to high external IAA application in *Atccc1* roots. *DR5v2* showed a decrease in auxin response in root tips. This may suggest auxin mediated degradation of DII containing proteins is reduced. Such a reduction in DII degradation will result in ARFs remaining bound to AUX/IAA proteins and therefore the *DR5v2* promoter not being activated (Li et al., 2016).

We also observed a reduction in the abundance of PIN1-GFP and PIN2-GFP in *Atccc1* roots. The reduced signal could be caused by reduced expression of the protein, increased internalisation or increased degradation. The internalisation of PIN2-GFP was observed in chapter 2 (Fig. 5) and does not show a difference between wildtype and *Atccc1*, indicating that internalisation of the protein is not the cause of the reduced PM abundance. It has been suggested that TRANSPORT INHIBITOR RESPONSE 1 (TIR1) impacts PIN abundance through ARF mediated transcriptional regulation. Alternatively, it may be possible that PIN abundance is altered due to defects in sorting, secretion or recycling of PIN proteins in *Atccc1*.

TIR1, AUX/IAAs and ARFs are primarily nuclear localised, and are unlikely to be directly impacted by changes in the TGN/EE lumen (Dharmasiri et al., 2005). This suggests that the impacts of *Atccc1* and the TGN/EE on cellular processes can result in broad downstream changes. Interestingly, auxin insensitivity seemed to be isolated to the root tip with root hair initiation being auxin responsive and hypocotyl *DR5v2::ntdTomato* signal being normal in *Atccc1*. Overall, these results indicate that AtCCC1 function is important for auxin signalling and polysaccharide accumulation, which further supports its role in endomembrane trafficking.

4.4 Materials and Methods

Plant material and growth conditions

All plants were *Arabidopsis thaliana* in the Columbia-0 (Col-0) background. The previously described AT1G30450 T-DNA insertion lines, *Atccc1-1* (SALK-048175) and *Atccc1-2* (SALK-145300) were used (Col 2007 REF). Also used were the previously described lines, *pPIN1::PIN1-GFP*, *pPIN2::PIN2-GFP*, *DR5::GUS*, R2D2, *DR5v2::ntdTomato* and *35s::DII-3xVENUS* (Benková et al., 2003; Xu and Scheres, 2005; Brunoud et al., 2012; Liao et al., 2015). Plants were grown on media containing half strength Murashige and Skroog (1/2 MS), 0.1% sucrose, 0.6% phytagel and pH 5.6 adjusted with KOH. Plants were sown on plates, incubated at 4ºC for 2 d before being grown vertically at 21°C and 19°C in 16 h light and 8 h dark, respectively. For GUS staining and the monosaccharide analysis, plants were transferred from plates to pots at 2 weeks old and grown at 21°C and 19°C in 16 h light and 8 h dark for the GUS staining and 9 h light and 15 h dark for the monosaccharide analysis.

Mucilage staining and seed coat imaging

Mucilage and seed coats were stained using ruthenium red and EDTA as described in McFarlane et al. (2014). Imaging of ruthenium red stained seeds was performed on a Nikon SMZ25 stereo microscope with a 2x objective. Dry, untreated seeds were imaged with a Nikon A1R confocal laser scanning microscope with a Plan Apo Lambda 20x objective. Imaging was performed using seed coat autofluorescence (excitation = 404 nm, emission = 425 – 475 nm).

Monosaccharide analysis

For the monosaccharide analysis, rosettes of 6 week old plants were separated from roots before the mature leaves were separated from the rest of the rosette. For each replicate, three plants were pooled together so that the mature and young leaves of the same three plants were pooled together. Plant material was freeze dried and ground before soluble sugars were washed out of the material by washing thrice with 70% ethanol. Ethanol from washes was collected, dried and then the soluble fractions were resuspended in water. The material remaining after washing with 70% ethanol was then washed with 100% ethanol and twice with acetone before being dried. The monosaccharide analysis was performed as described in Cowley et al. (2020). In brief, hydrolysis was performed in 5M H_2SO_4 at 100^{o}C for 3 h. Both monosaccharides released from hydrolysis and the soluble fractions were derivatised with 1-phenyl-3-methyl-5-pyrazoline (PMP) and separated by reverse phase high performance liquid chromatography (RP-HPLC).

Auxin markers and sensors

GUS staining was performed as described in Chapter 2 (Jefferson et al., 1987). In brief, plant tissue from 4 week old plants was collected and cleared in an ethanol:acetic acid solution (1:1) for 24 h before clearing in a Hoyers solution (100g chloral hydrate, 5mL glycerol in 100mL water) for 16 h. For the seedlings, plants were 6 d old and clearing was performed by washing plants with 50%, 70% then 100% ethanol. Tissue was then stained in GUS solution for 16 h before imaging. Imaging was performed using a Nikon SMZ25 stereo microscope. Growth, treatment and imaging of seedlings was performed by Stefanie Wege.

For *DR5v2::ntdTomato* (excitation = 561 nm, emission = 570 – 620 nm) and DII-3xVENUS (excitation = 488 nm, emission = 500 – 550 nm), images were taken on a Nikon A1R confocal laser scanning microscope using an Apo LWD 40x WI λS DIC N2 objective (Brunoud et al., 2012; Liao et al., 2015). Optical sections were obtained of the root tip or hypocotyl of 6 d old plants. The duel fluorescence sensor R2D2 (auxin sensitive excitation = 488 nm, emission = 500 – 550 nm; Expression control excitation = 561 nm, emission = 570 – 620 nm) was imaged using the Nikon confocal as described above (Liao et al., 2015). Quantification of R2D2 signal was performed in FIJI (Schindelin et al., 2012). First, the fluorescent intensity of the expression control was divided by the fluorescent intensity of the auxin sensitive DII-n3xVENUS channel before the intensity of each nucleus was measured.

IAA response assay

Plants were grown on 1/2 MS media as described above. At 6 d old, plants were transferred to 1/2 MS media containing the indicated concentration of IAA. After 24 h the plants were imaged with the Nikon SMZ25 stereo microscope or Nikon A1R confocal described above. Growth, treatment and imaging of plants imaged with the stereo microscope was performed by Stefanie Wege.

Signal intensity of PIN1 and PIN2

The methods used for PIN2-GFP imaging is described in chapter 2 (Fig. 5). The experiment for PIN1-GFP was performed the same way.

4.5 References

Adamowski, M., and Friml, J. (2015). PIN-dependent auxin transport: action, regulation, and evolution. Plant Cell **27,** 20-32.

Amos, R.A., and Mohnen, D. (2019). Critical review of plant cell wall matrix polysaccharide glycosyltransferase activities verified by heterologous protein expression. Frontiers in Plant Science **10,** 915.

Arsovski, A.A., Haughn, G.W., and Western, T.L. (2010). Seed coat mucilage cells of Arabidopsis thaliana as a model for plant cell wall research. Plant Signaling & Behaviour **5,** 796-801.

Bacete, L., and Hamann, T. (2020). The role of mechanoperception in plant cell wall integrity maintenance. Plants **9,** 574.

Bashline, L., Li, S., and Gu, Y. (2014). The trafficking of the cellulose synthase complex in higher plants. Annals of Botany **114,** 1059-1067.

Benková, E., Michniewicz, M., Sauer, M., Teichmann, T., Seifertová, D., Jürgens, G., and Friml, J. (2003). Local, efflux-dependent auxin gradients as a common module for plant organ formation. Cell **115,** 591-602.

Brandizzi, F. (2018). Transport from the endoplasmic reticulum to the Golgi in plants: Where are we now? Seminars in Cell and Developmental Biology **80,** 94-105.

Brunoud, G., Wells, D.M., Oliva, M., Larrieu, A., Mirabet, V., Burrow, A.H., Beeckman, T., Kepinski, S., Traas, J., Bennett, M.J., and Vernoux, T. (2012). A novel sensor to map auxin response and distribution at high spatio-temporal resolution. Nature **482,** 103-106.

Colmenero-Flores, J.M., Martínez, G., Gamba, G., Vázquez, N., Iglesias, D.J., Brumós, J., and Talón, M. (2007). Identification and functional characterization of cation-chloride cotransporters in plants. Plant Journal **50,** 278-292.

Cosgrove, D.J. (2016). Plant cell wall extensibility: connecting plant cell growth with cell wall structure, mechanics, and the action of wall-modifying enzymes. Journal of Experimental Botany **67,** 463-476.

Cowley, J.M., Herliana, L., Neumann, K.A., Ciani, S., Cerne, V., and Burton, R.A. (2020). A small-scale fractionation pipeline for rapid analysis of seed mucilage characteristics. Plant Methods **16,** 20.

Dettmer, J., Hong-Hermesdorf, A., Stierhof, Y.D., and Schumacher, K. (2006). Vacuolar H^+-ATPase activity is required for endocytic and secretory trafficking in Arabidopsis. Plant Cell **18,** 715-730.

Dharmasiri, N., Dharmasiri, S., Weijers, D., Lechner, E., Yamada, M., Hobbie, L., Ehrismann, J.S., Jürgens, G., and Estelle, M. (2005). Plant development is regulated by a family of auxin receptor F box proteins. Developmental cell **9,** 109-119.

Dragwidge, J.M., Ford, B.A., Ashnest, J.R., Das, P., and Gendall, A.R. (2018). Two endosomal NHX-type Na^+/H^+ antiporters are involved in auxin-mediated development in *Arabidopsis thaliana*. Plant Cell Physiology **59,** 1660-1669.

Drakakaki, G., van de Ven, W., Pan, S., Miao, Y., Wang, J., Keinath, N.F., Weatherly, B., Jiang, L., Schumacher, K., Hicks, G., and Raikhel, N. (2012). Isolation and proteomic analysis of the SYP61 compartment reveal its role in exocytic trafficking in Arabidopsis. Cell Research **22,** 413-424.

Driouich, A., Follet-Gueye, M.L., Bernard, S., Kousar, S., Chevalier, L., Vicré-Gibouin, M., and Lerouxel, O. (2012). Golgi-mediated synthesis and secretion of matrix polysaccharides of the primary cell wall of higher plants. Frontiers in Plant Science **3,** 79.

Feraru, E., and Friml, J. (2008). PIN polar targeting. Plant Physiology **147,** 1553-1559.

Griffiths, J.S., and North, H.M. (2017). Sticking to cellulose: exploiting Arabidopsis seed coat mucilage to understand cellulose biosynthesis and cell wall polysaccharide interactions. New Phytologist **214,** 959-966.

Han, B., Jiang, Y., Cui, G., Mi, J., Roelfsema, M.R.G., Mouille, G., Sechet, J., Al-Babili, S., Aranda, M., and Hirt, H. (2020). CATION-CHLORIDE CO-TRANSPORTER 1 (CCC1) mediates plant resistance against *Pseudomonas syringae*. Plant Physiology **182,** 1052-1065.

Haughn, G.W., and Western, T.L. (2012). Arabidopsis seed coat mucilage is a specialized cell wall that can be used as a model for genetic analysis of plant cell wall structure and function. Frontiers in Plant Science **3,** 64.

Henderson, S.W., Wege, S., Qiu, J., Blackmore, D.H., Walker, A.R., Tyerman, S.D., Walker, R.R., and Gilliham, M. (2015). Grapevine and Arabidopsis cation-chloride cotransporters localize to the Golgi and trans-Golgi network and indirectly influence long-distance ion transport and plant salt tolerance. Plant Physiology **169,** 2215-2229.

Jefferson, R.A., Kavanagh, T.A., and Bevan, M.W. (1987). GUS fusions: beta-glucuronidase as a sensitive and versatile gene fusion marker in higher plants. The EMBO Journal **6,** 3901-3907.

Krügel, U., and Kühn, C. (2013). Post-translational regulation of sucrose transporters by direct protein-protein interactions. Frontiers in Plant Science **4,** 237.

Kulich, I., Cole, R., Drdová, E., Cvrcková, F., Soukup, A., Fowler, J., and Zárský, V. (2010). Arabidopsis exocyst subunits SEC8 and EXO70A1 and exocyst interactor ROH1 are involved in the localized deposition of seed coat pectin. New Phytologist **188,** 615-625.

Leyser, O. (2018). Auxin signaling. Plant Physiology **176,** 465-479.

Li, S.B., Xie, Z.Z., Hu, C.G., and Zhang, J.Z. (2016). A review of auxin response factors (ARFs) in plants. Frontiers in Plant Science **7,** 47.

Liao, C.Y., Smet, W., Brunoud, G., Yoshida, S., Vernoux, T., and Weijers, D. (2015). Reporters for sensitive and quantitative measurement of auxin response. Nature Methods **12,** 207-210, 202 p following 210.

Ljung, K., Hull, A.K., Celenza, J., Yamada, M., Estelle, M., Normanly, J., and Sandberg, G. (2005). Sites and regulation of auxin biosynthesis in Arabidopsis roots. Plant Cell **17,** 1090-1104.

McFarlane, H.E., Gendre, D., and Western, T.L. (2014). Seed coat ruthenium red staining assay. Bio-protocol **4,** e1096.

McFarlane, H.E., Watanabe, Y., Gendre, D., Carruthers, K., Levesque-Tremblay, G., Haughn, G.W., Bhalerao, R.P., and Samuels, L. (2013). Cell wall polysaccharides are mislocalized to the Vacuole in echidna mutants. Plant Cell Physiology **54,** 1867-1880.

Mendrinna, A., and Persson, S. (2015). Root hair growth: it's a one way street. F1000prime reports **7,** 23.

Molina, A., Miedes, E., Bacete, L., Rodríguez, T., Mélida, H., Denancé, N., Sánchez-Vallet, A., Rivière, M.P., López, G., Freydier, A., Barlet, X., Pattathil, S., Hahn, M., and Goffner, D. (2021). Arabidopsis cell wall composition determines disease resistance specificity and fitness. Proceedings of the National Academy of Sciences **118**

Röckel, N., Wolf, S., Kost, B., Rausch, T., and Greiner, S. (2008). Elaborate spatial patterning of cell-wall PME and PMEI at the pollen tube tip involves PMEI endocytosis, and reflects the distribution of esterified and de-esterified pectins. Plant Journal **53,** 133-143.

Rogers, L.A., Dubos, C., Surman, C., Willment, J., Cullis, I.F., Mansfield, S.D., and Campbell, M.M. (2005). Comparison of lignin deposition in three ectopic lignification mutants. New Phytologist **168,** 123-140.

Rosquete, M.R., Davis, D.J., and Drakakaki, G. (2018). The plant trans-Golgi network: not just a matter of distinction. Plant Physiology **176,** 187-198.

Schindelin, J., Arganda-Carreras, I., Frise, E., Kaynig, V., Longair, M., Pietzsch, T., Preibisch, S., Rueden, C., Saalfeld, S., Schmid, B., Tinevez, J.Y., White, D.J., Hartenstein, V., Eliceiri, K., Tomancak, P., and Cardona, A. (2012). Fiji: an open-source platform for biological-image analysis. Nature Methods **9,** 676-682.

Sinclair, R., Rosquete, M.R., and Drakakaki, G. (2018). Post-Golgi trafficking and transport of cell wall components. Frontiers in Plant Science **9,** 1784.

Ulmasov, T., Murfett, J., Hagen, G., and Guilfoyle, T.J. (1997). Aux/IAA proteins repress expression of reporter genes containing natural and highly active synthetic auxin response elements. Plant Cell **9,** 1963-1971.

Vieten, A., Vanneste, S., Wisniewska, J., Benková, E., Benjamins, R., Beeckman, T., Luschnig, C., and Friml, J. (2005). Functional redundancy of PIN proteins is accompanied by auxin-dependent cross-regulation of PIN expression. Development **132,** 4521-4531.

Vissenberg, K., Claeijs, N., Balcerowicz, D., and Schoenaers, S. (2020). Hormonal regulation of root hair growth and responses to the environment in Arabidopsis. Journal of Experimental Botany **71,** 2412-2427.

Voiniciuc, C., Yang, B., Schmidt, M.H., Günl, M., and Usadel, B. (2015). Starting to gel: how Arabidopsis seed coat epidermal cells produce specialized secondary cell walls. International Journal of Molecular Sciences **16,** 3452-3473.

Wu, H.C., Bulgakov, V.P., and Jinn, T.L. (2018). Pectin methylesterases: cell wall remodeling proteins are required for plant response to heat stress. Frontiers in Plant Science **9,** 1612.

Xu, J., and Scheres, B. (2005). Dissection of Arabidopsis ADP-RIBOSYLATION FACTOR 1 function in epidermal cell polarity. Plant Cell **17,** 525-536.

Yang, Y., Hammes, U.Z., Taylor, C.G., Schachtman, D.P., and Nielsen, E. (2006). High-affinity auxin transport by the AUX1 influx carrier protein. Current Biology **16,** 1123-1127.

Zenser, N., Ellsmore, A., Leasure, C., and Callis, J. (2001). Auxin modulates the degradation rate of Aux/IAA proteins. Proceedings of the National Academy of Sciences **98,** 11795-11800.

Zwiewka, M., Bilanovičová, V., Seifu, Y.W., and Nodzyński, T. (2019). The nuts and bolts of PIN auxin efflux carriers. Frontiers in Plant Science **10,** 985.

Chapter 5

Discussion

5.1 The TGN/EE pH Regulatory Network

This thesis focused on elucidating the role that AtCCC1 fulfils within plants. Here, we have confirmed that AtCCC1 is localised in the TGN/EE and revealed that AtCCC1 is required for the maintenance of the acidic pH of the TGN/EE (Chapter 2, Fig. 3 and 4). AtCCC1 is likely to impact pH through regulation of the activity of the TGN/EE ion/proton antiporters and proton pump by providing an efflux pathway for, and manipulating the gradients of, K^+, Na^+ and Cl^- across the TGN/EE membrane, and not by directly transporting protons. *Atccc1* knockouts have a TGN/EE pH of 5.8 (Chapter 2, Fig. 4), which is 0.3 units higher than wildtype. This is similar to *det3* plants, which have reduced V-H^+-ATPase activity and a TGN/EE pH 0.4 units higher than wildtype (Luo et al., 2015). As V-H^+-ATPase is the primary source of acidification for the TGN/EE, it is probable that AtCCC1 activity is required for regulating V-H^+-ATPase function.

Our results are consistent with the regulation of ion concentrations in the TGN/EE lumen being essential for pH regulation. Experiments with monensin, which is a cationic ionophore, suggest that AtCCC1 effluxes ions from the TGN/EE (Chapter 2, Fig. 4). Ion efflux activity of AtCCC1 could be important for complementing the activity of the TGN/EE localised antiporters, the NHXs and CLCs. NHX5 and 6 import K^+ into the TGN/EE while CLCd and CLCf import Cl^- (Bassil et al., 2011; Scholl, 2017). Without AtCCC1, the TGN/EE may accumulate K^+ and Cl^- in the lumen, which reduces the ion gradient that the antiporters use for transport of ions into the lumen, to potentially beyond the limit of their transport capacity. Reduced antiporter activity results in reduced proton export through the antiporters, but importantly, it will also prevent the import of a countercharge. *nhx5/nhx6* knockouts have a lower luminal pH, likely due to the reduced proton efflux (Reguera et al., 2015). *clcd*/*clcf* double knockout plants are infertile but a *clcd* knockout with an inducible *clcf* knockdown has been used to characterise the role of the anion/proton antiporters in the TGN/EE (Scholl, 2017). The *clcd* knockout, *clcf* knockdown mutant does not exhibit severe growth defects and has no change in TGN/EE pH but does display reduced cell elongation and partial mislocalisation of the TGN/EE V-H^+-ATPase to the *trans*-Golgi. The lack of change in TGN/EE pH is of interest as the influx of inorganic anions such as Cl^- or NO_3^- must be essential for this system as they provide the necessary negative charge to balance the influx of positively charged H^+ and K^+ ions. The importance of the coupled anion/proton transport of CLC was shown through the function of

an animal, lysosomal localised CLC (Novarino et al., 2010). Therefore, reduced Cl^- influx through the CLCs should result in decreased V-H^+-ATPase activity resulting in an elevated TGN/EE pH. This pH increase may be offset by the loss of H^+ export in *clcd/cldf* mutants. Additional sources of anion influx may exist including transient cargo of the endomembrane system. It was recently found that vacuolar ATPases can contribute to the acidification of the TGN/EE as they transit through to the tonoplast (Lupanga et al., 2020).

If the reduced acidification of the TGN/EE in *Atccc1* is due to reduced V-H^+-ATPase activity, then the luminal pH of the *Atccc1* mutants should not be further changed by V-H^+-ATPase inhibition. ConcanamycinA (ConcA) is a pharmaceutical inhibitor of V-H^+-ATPases that results in an increase in TGN/EE pH (Luo et al., 2015). Measuring the TGN/EE pH of ConcA treated *Atccc1* plants would be able to determine if the luminal pH changes in *Atccc1* are due to an impact on V-H^+-ATPase activity.

Transport of cation and anions through AtCCC1 is stoichiometrically linked (Colmenero-Flores et al., 2007). Therefore, this provides a mechanism by which the activity of NHXs and CLCs are linked. Further understanding the mechanics of this system will require the measurement of Na^+, K^+ and Cl^- luminal ion concentrations in wildtype and knockouts. Guard cell cytosolic Cl^- and NO_3^- concentrations have previously been measured using the genetically encoded ratiometric sensor, ClopHensor (Demes et al., 2020). Very recently, a genetically encoded K^+ sensor was shown to work in Arabidopsis roots. This K^+ sensor was developed in animals cells and employs a bacterial K^+-binding protein domain with fluorescent proteins to create a Förster resonance energy transfer (FRET) sensor (Bischof et al., 2017; Wang et al., 2021). For use in the TGN/EE, it needs to be assessed whether the sensor is appropriate for assays at the single cell or organelle level.

5.2 Regulation of TGN/EE Osmolality and Ion Accumulation

Osmoregulation is vital for managing the size of organellular compartments and preventing their shrinkage or bursting. It is currently unknown how the osmolality of the TGN/EE is regulated. The transporters identified as part of the pH regulatory network may contribute to regulation of TGN/EE osmolality in addition to pH. NHXs import K^+ and CLCs import Cl^-,

therefore increasing the luminal osmolality while AtCCC1 effluxes K^+ and Cl^-, decreasing the osmolality (Marmagne et al., 2007; Bassil et al., 2011; Guo et al., 2014)(Chapter 2, Fig. 4). The TGN/EE V-H^+-ATPase provides the proton gradient required to mediate ion influx through NHXs and CLCs (Luo et al., 2015). As such, this network could have dual roles in the regulation of both pH and osmolality of the TGN/EE. Furthermore, pH changes in the TGN/EE will be tightly linked to ion transport and osmoregulation of the organelle. As the pH of the TGN/EE decreases, transport through NHX and CLC becomes more favourable and therefore ion influx may increase. Conversely, AtCCC1 activity may be modulated by luminal pH as ion accumulation in AtCCC1 expressing *Xenopus lavis* oocytes was greater at higher pH levels, suggesting that AtCCC1 might be more active as luminal pH increases (Colmenero-Flores et al., 2007). Therefore, decreasing V-H^+-ATPase activity in response to ion accumulation in the TGN/EE may signal an increase in AtCCC1 transport, to efflux ions and reduce the osmolality of the TGN/EE.

In Chapter 3 (Fig. 1), we show that the pH of the TGN/EE lumen is dynamically adjusted in response to external conditions. When challenged with either osmotic or salt shock, the pH of TGN/EE in root epidermal cells increases. As discussed above, pH may signal changes in ion transport to coordinate the osmoregulation of the TGN/EE. There are likely more conditions that feed into TGN/EE regulation as well, adding to the complexity of the regulation of luminal pH. The proposed role of the endomembrane pH is to mediate protein-protein interactions in a compartment specific manner to control where receptors such as VSR bind and dissociate with cargo (Robinson and Neuhaus, 2016). The strength of protein-protein binding is influenced by pH. The binding of the VSR, BP-80, to aleurain is strongest at pH 6 (Kirsch et al., 1994). As the pH increases to 7.5 or drops to 5.5, only 50% of BP-80 is ligand bound. Binding of cargo to VSRs may therefore occur in the ER and Golgi, but in the more acidic TGN/EE, the receptor and cargo dissociate. In addition to pH, protein-protein binding is also influenced by temperature and ionic conditions (Papaneophytou et al., 2014; He and Ma, 2016). Ionic conditions refers to both the concentration of ions and the specific ions that contribute to that concentration, eg. Na^+, Cl^- or K^+. Therefore, to maintain normal VSR binding/dissociation in the TGN/EE, the effects of pH, ionic conditions and temperature must be balanced. It is not yet known how temperature impacts TGN/EE pH or how these three factors are balanced but the proton pump and three transporters, V-H^+-ATPase, NHXs, CLCs and CCCs may together, be able to dynamically regulate the pH, osmolality and ionic conditions of the TGN/EE.

Characterising the role of temperature on TGN/EE pH and identifying how the activity of the TGN/EE transporters are regulated through cellular signalling can help to expand our understanding of this system and may uncover how the system reacts to developmental and environmental cues. Five phosphorylation sites have been identified in AtCCC1 and two identified in NHX5, however, neither the impact of phosphorylation nor the trigger for phosphorylation have been identified (Reiland et al., 2009; Roitinger et al., 2015; Bhaskara et al., 2017). The regulatory role of phosphorylation could be investigated through AtCCC1 harbouring phosphomimic amino acids at the identified sites. Expressing these constructs in heterologous systems to investigate transporter activity; and expression in Arabidopsis to investigate cellular effects, such as TGN/EE lumen pH, will help to understand how the transport network in the TGN/EE is regulated. Identification of environmental conditions that result in phosphorylation of AtCCC1 can be achieved through proteomics. Such identification could assist in understanding how AtCCC1 may adjust the luminal conditions of the TGN/EE in response to environmental stimuli. This can further be investigated by measuring the pH of the TGN/EE lumen in response to heat and cold treatments. This work will begin to characterise how the TGN/EE reacts to environmental conditions that may impact trafficking, such as temperature.

5.3 The Importance of TGN/EE Luminal Conditions

Mutants of the TGN/EE luminal regulatory network display reductions in the rate of endomembrane trafficking and frequently have reduced abundance of PM proteins (Luo et al., 2015; Dragwidge et al., 2018)(Chapter 2, Fig. 5 and chapter 4, Fig. 5). The cause of reduced trafficking and PM protein abundance is yet to be identified, however. *Atccc1* plants have reduced bulk endocytic trafficking, reduced internalisation of PIP2;1 and reduced exocytosis of PIN2 (Chapter 2, Fig. 5 and chapter 3, Fig. 4). *det3* plants exhibit reduced recycling and secretion of BRI1 in addition to reduced endocytic trafficking (Luo et al., 2015). *nhx5*/*nhx6* knockouts have reduced recycling and endocytic trafficking but have no identified defects in secretion (Bassil et al., 2011; Dragwidge et al., 2019). The ubiquitous trafficking defects between the three mutants is interesting as all three mutants are likely to have different TGN/EE luminal conditions. *det3* plants have a higher TGN/EE pH and likely accumulate less ions in the TGN/EE due to a decrease in the proton gradient required for antiporter activity (Table. 1) (Luo et al., 2015). *nhx5/nhx6* plants have a lower TGN/EE pH and are also likely to accumulate

less cations in the TGN/EE (Reguera et al., 2015). *Atccc1* plants have, like *det3*, a higher TGN/EE pH but unlike *det3*, are likely to accumulate more cations and anions in the TGN/EE (Chapter 2, Fig. 4). Therefore, changes in the rate of trafficking is unlikely to be specifically caused by an increase or decrease in pH or ion accumulation and rather, may be caused by deviations from ideal conditions in the mutant TGN/EE lumens or may have different base causes in the different mutants. The TGN/EE pH of *clcd* knockout/*clcf* knockdown plants does not differ from wildtype and plants do not have defects in the rate of trafficking (Scholl, 2017). This may suggest that pH is the crucial factor for the rate of trafficking. Interestingly, the pH of the TGN in mammals has been implicated as an important factor for vesicle formation. The mammalian TGN V-H^+-ATPase recruits proteins such as the guanine exchange factor, ARNO, and the ADP-ribosylation factors, ARF1 and ARF6, to endosomal compartments (Hurtado-Lorenzo et al., 2006). Recruitment of these proteins is required for vesicle budding and coating. V-H^+-ATPase mediated recruitment is pH sensitive. It has been postulated that luminal histidine residues of V-H^+-ATPase may be involved in the detection of luminal pH (Marshansky, 2007). The rate of trafficking may therefore be limited by V-H^+-ATPase in a pH sensitive manner. Investigating this in plants can determine if the plant TGN/EE V-H^+-ATPase also has a role in detecting luminal pH and transmitting signals to the cytosol. Such a mechanism in plants could result in decreased vesicle formation, and therefore reduced endomembrane trafficking from the TGN/EE if the luminal pH is altered. This would not, however, directly explain the reduction in endocytic trafficking. Although it is possible that reductions in exocytosis result in reciprocal reductions in endocytosis to balance the influx and efflux of membrane to and from the PM.

Table 1. Different TGN/EE transporter mutants have different luminal changes. The luminal pH of mutants have all been measured, however, there are not yet any tools to enable the measurement of ion concentrations in the TGN/EE. Therefore, changes in ion content of TGN/EE lumen in mutants is speculative at this time. Expansion of TGN/EE in response to monensin has been assayed in *nhx5/6* and *Atccc1* plants.

Transporter/ Pump	Mutant	Measured TGN/EE pH Change	Putative Ion Change	Monensin Tolerance
V-H^+-ATPase	*det3*	Increase	Decrease	Untested
NHX5/6	*nhx5/6*	Decrease	Decrease	Tolerant
AtCCC1	*Atccc1*	Increase	Increase	Sensitive

The abundance of several fluorescently tagged PM proteins is lower in mutants of the luminal regulatory network. For instance, in *Atccc1,* signal intensity of PIN1-GFP and PIN2-GFP is lower than wildtype (Chapter 4, Fig. 5). In *det3*, BRI1-GFP signal is reduced (Luo et al., 2015). In *nhx5/nhx6*, PIN1-GFP and PIN2-GFP signal is reduced, but BRI1-GFP signal is not (Dragwidge et al., 2018; Dragwidge et al., 2019). All mutants, therefore, exhibit decreases in the abundance of some PM proteins which could suggest that changes are not specifically related to acidification of the TGN/EE, although, the difference in BRI1-GFP signal between *det3* and *nhx5/nhx6* could indicate that the reduced abundance of proteins has different causes in the different mutants but with a similar observable outcome. It is not yet known just how many PM proteins may exhibit reduced abundance in these mutants, nor is it known if mutants also impact native proteins or just tagged proteins. Reductions in the abundance of PM proteins could be the result of missorting during secretory trafficking or defects in recycling that result in enhanced degradation of PM proteins.

To further our understanding of endomembrane trafficking and determine the role of luminal conditions in TGN/EE function, experiments investigating all three mutants, *Atccc1*, *det3* and *nhx5/nhx6* in parallel would be useful. Each mutant is speculated to have a different combination of changes to pH and ion accumulation and therefore, a focus of future work on assaying rates of recycling and secretion of proteins in the three mutants might help to determine the relative importance of TGN/EE acidification and ion accumulation in each process. In addition, Western blots can help to determine the PM abundance of specific proteins which would help confirm that the reduced GFP-signal of PIN2-GFP in *Atccc1* mutants is due to reduced protein abundance, and might extend to other PM proteins as well.

5.4 Endomembrane Trafficking Impacts Many Cellular Processes

In *Atccc1* plants, a variety of phenotypes have been observed both here and in previous work. These phenotypes include dwarfed growth, reduced fertility, stem necrosis, cell wall changes, seed coat defects, reduced pathogen resistance, reduced cell elongation, increased shoot branching and altered root to shoot ion transport (Colmenero-Flores et al., 2007; Henderson et al., 2015; Han et al., 2020)(Chapter 2, Fig. 2 and chapter 4, Fig. 3 and 4). It is likely that many of these phenotypes are the result of altered endomembrane trafficking. The broad range of

observed phenotypes for *Atccc1,* therefore, may reflect the diversity of cargo trafficking through the TGN/EE.

Atccc1 plants have an altered composition of cell walls (Chapter 4, Fig. 4) (Han et al. 2020). The precise compositional change may be dependent on the tissue type assayed. The largest changes were observed in Han et al. (2020), where they found an increase in several cell wall sugars including xylose, arabinose, fucose, galactose and arabinose. However, the tissue type analysed is not specified and might be either hypocotyl or leaves. In our analysis, we found no difference in mature leaves but a mild increase in xylose, arabinose and fucose in younger leaves. This may suggest that the changes are more severe in faster growing cells. Han et al. (2020) also performed a cellulose hydrolysis and found that total cell wall cellulose was greatly reduced. A reduction in total cell wall cellulose and increase in other monosaccharides was also observed in *det3* mutants (Rogers et al., 2005; Luo et al., 2015). In *det3*, there is reduced trafficking of the cellulose synthase complex (CSC) to the PM. CSCs are membrane integral complexes that synthesise cellulose at the PM and expel it into the apoplast (Sinclair et al., 2018). The reduction of cellulose in both *Atccc1* and *det3* suggests an importance of TGN/EE acidification for CSC trafficking. It is likely that the reduced cell wall cellulose in both *det3* and *Atccc1* is caused by a reduction in the abundance of CSCs, similar to what is observed with other PM proteins. Reduced cellulose synthesis could result in reduced cell expansion and therefore the reduced cell elongation observed in *Atccc1*.

Determining the PM abundance of CSCs in *Atccc1* can help to determine if reduced quantities of CSCs are the cause of reduced cell wall cellulose. In addition, trafficking of CSCs and the cell wall cellulose content can be analysed in *nhx5/nhx6* plants which can help to determine if TGN/EE acidification also impacts CSC localisation.

Atccc1 mutants have an increased susceptibility to infection by *pst.* DC3000, while at the same time, they exhibit an increase in early pathogen triggered immunity responses such as ROS production and an increase in salicylic acid (Han et al., 2020). These results might be caused by decreased endocytic trafficking of the pathogen receptor FLS2. Reduced endocytosis of FLS2 results in increased early immune responses, but decreased late responses and an

increased susceptibility to *pst.* DC3000 infection (Gu et al., 2017). Additionally, defects in vacuolar delivery of endocytic cargo may result in increased salicylic acid signalling. Plants lacking the ESCRT subunit, VPS2.1, exhibit increased susceptibility to powdery mildew and increased upregulation of typical salicylic acid marker genes (Katsiarimpa et al., 2013). *det3* plants also exhibit a change in pathogen resistance, however, unlike *Atccc1*, *det3* plants are more resistant to infection by *pst*. DC3000 (Rogers et al., 2005). Similarly, *clcd* mutants exhibit enhanced *pst.* DC3000 resistance and greater ROS production in response to pathogen detection (Guo et al., 2014). *det3* and *Atccc1* plants both have a higher luminal pH in the TGN/EE, but contrasting changes to pathogen resistance. This suggests that alkalisation of the TGN/EE alone is not the cause of the altered pathogen responses observed in *det3* or *Atccc1*. It is also unlikely that it is a result of the cell wall changes, which appear to be similar between the two mutants. The difference between the two mutants could be caused by changes in protein trafficking that result from altered TGN/EE ion accumulation.

Assaying the trafficking, particularly the pathogen signal induced internalisation, of fluorescently tagged FLS2 in *det3* and *Atccc1* could help elucidate the cause of the altered pathogen response in the mutants.

The quantity of seed mucilage and seed coat morphology were both altered in *Atccc1* knockouts (Chapter 4, Fig. 5). Reductions in seed mucilage have previously been observed in mutants of proteins important for trafficking such as the ECH/YIP complex subunit, *ech*, and the exocyst complex subunit, *exo70a1* (Kulich et al., 2010; McFarlane et al., 2013). In *ech* knockouts, pectin accumulates in the TGN/EE and is also found in the vacuole. Therefore, the reduction in mucilage is thought to be caused by defective secretion of pectin. *ech* mutants also display differences in seed coat morphology. At the centre of every seed coat cell is a pillar of secondary cell wall called the columella. In *ech* mutants, the columella is less pronounced and is not raised like in wildtype plants. Flattening of the columella is observed in several mutants with reduced mucilage and is thought to be caused by the changes in spatial arrangement that result from smaller mucilage stores (Western et al., 2001; Usadel et al., 2004; McFarlane et al., 2013). This might be the cause of the observed defects in *Atccc1*, however, not all cells are affected and as a consequence mucilage excretion is not severely reduced. Seed coat formation in *Atccc1* is therefore not uniform and columellae develop in some cells. Mucilage deposition

may be sufficiently large enough to result in normal columella formation in some cells but not others. Consistent with this, mucilage excretion around *Atccc1* seeds is not uniform.

SEM imaging *of Atccc1* seed coats and cross sections of seed coat cells at different developmental points would enable evaluation of the reason why columellae are not visible in some cells. Fixing, and immunolabelling of pectins in *Atccc1* seeds would further reveal altered trafficking of pectin may be the cause of the reduced mucilage as was previously observed in *ech* mutants (McFarlane et al., 2013).

Brassinosteroids are growth hormones that impact plant development, stress response and cell elongation (Nolan et al., 2020). Knockouts of the brassinosteroid receptor, BRI1, are severely dwarfed (Noguchi et al., 1999). Both *det3* and *nhx5/nhx6* plants have altered BRI1 trafficking. *det3* plants exhibit both reduced secretion and recycling of BRI1 resulting in a reduced abundance of PM BRI1 and brassinosteroid insensitivity (Luo et al., 2015). *nhx5/nhx6* have reduced recycling but normal secretion of BRI1 (Dragwidge et al., 2019). *nhx5/nhx6* plants are unlikely to be insensitive to brassinosteroids because, unlike *det3* they do not exhibit reduced PM abundance of BRI1. Given the reduced size of *Atccc1* shoots and reduced root length, it may be possible that brassinosteroid reception is also reduced and at least partly possible for the reduced plant size.

Cell elongation is reduced in *Atccc1* plants. We observed a reduction in the elongation rate of root hairs and shorter epidermal root cells while pollen tube elongation has recently been shown to be slower in *Atccc1* (Chapter 2, Fig. 2) (Domingos et al., 2019). Reductions in cell elongation have also been observed in the root hairs of *nhx5/nhx6* knockouts and the *clcd* knockout with inducible *clcf* knockdown (Bassil et al., 2011) (Scholl, 2017). The precise cause of the reduced cell elongation may be difficult to pinpoint due to the numerous potential causes including alterations in hormone signalling, cell wall synthesis or osmoregulation (Refrégier et al., 2004; Braidwood et al., 2014; Barbez et al., 2017; Liu et al., 2021). Interestingly, the elongation rate of *Atccc1* root hairs can be rescued when grown on media containing 150 mM mannitol (Chapter 3, Fig. 2). Increasing the external osmolality could rescue root hair elongation in *Atccc1* if the osmoregulation of root hairs is defective. This may be compounded by changes

in the cell wall composition. Changes to the extensibility of the cell wall result in changes in turgor and cell elongation (Liu and Hussey, 2014). It is likely that there is a relationship between cell wall rigidity and cell osmoregulation. These two factors work in tandem to maintain cell elongation as alterations to one result in alterations to the other (Bacete and Hamann, 2020). If the osmolality of root hairs in *Atccc1* is poorly regulated and is too high, root hairs may increase the rigidity of the cell walls to prevent bursting and this would result in decreased cell elongation. The receptor kinase FERONIA (FER) is thought to regulate cell wall rigidity, especially in response to salt stress (Feng et al., 2018). *fer* knockouts exhibit uncontrolled cell wall loosening in response to salt stress which results in the bursting of elongating epidermal root cells, highlighting the importance of regulating cell wall rigidity to prevent cell bursting. When grown on media with a higher osmolality, root hair elongation may be improved as the difference between the internal and external osmolality is lower, resulting in a reduced force on the cell wall. Consistent with this, epidermal root cells in *Atccc1* required a higher external osmolality to plasmolyse indicating a higher osmolality in the epidermal cells (Chapter 3, Fig. 3). When the total root osmolality was measured, however, it did not reveal an increased cell sap osmolality in *Atccc1* (Chapter 3, Fig. 3). This may suggest that only specific cells, such as actively expanding cells, have an altered osmolality.

Double knockouts of *fer* and *Atccc1* may be useful for investigating if *Atccc1* root hairs may grow slower due to an elevated cellular osmolality, resulting in increased rigidity of cell walls. *fer* knockouts lack an important cell wall regulatory mechanism and exhibit reduced cell wall rigidity and increased cell bursting. *fer* x *Atccc1* mutants may, therefore, display a severe degree of root hair bursting if *Atccc1* cells have a high osmolality and lack FER to induce an increased cell wall rigidity in response. To investigate if an elevated osmolality is occurring in a specific subset of cells, the turgor of root cells can be measured with a pressure probe.

5.5 The TGN/EE may be Important for Ion Transport Across the PM

TGN/EE trafficking has a role in the delivery and regulation of PM ion transporters. *Atccc1* plants exhibit alterations in root to shoot translocation of ions. Hydroponically grown *Atccc1* plants accumulate more Cl^-, K^+, and Na^+ in shoots in salt (50 mM NaCl) conditions (Henderson et al., 2015). Similarly, soil grown *Atccc1* plants accumulate more shoot, and less root, Cl^- when grown in 50 mM Cl^- salts (Colmenero-Flores et al., 2007). Due to the TGN/EE

localisation of AtCCC1, it can be excluded that *Atccc1* directly contributes to xylem unloading, or ion export out of cells. Trafficking of the transporters that are directly involved in ion export or ion retrieval from the xylem sap might therefore be affected. For example, the PM transporter SALT OVERLY SENSITIVE (SOS1, also known as NHX7) is a Na^+/H^+ antiporter that exports Na^+ and therefore reduces total accumulation of Na^+ in plants (Qiu et al., 2002). Retrieval of ions from xylem sap can be mediated through transporters such as HIGH AFFINITY K^+ TRANSPORTERS (HKTs). Retrieval reduces the quantity of ions in the xylem sap and therefore the quantity of ions translocated to the shoot (Assaha et al., 2017). In *Atccc1* and other trafficking mutants such as *det3* and *nhx5/nhx6*, reduced abundance of PM proteins is observed which might extend to ion transporters. Interestingly, *det3* and *nhx5/nhx6* plants have previously been characterised as salt sensitive (Krebs et al., 2010; Bassil et al., 2011). Regulation of shoot ion accumulation, particularly the Na^+/K^+ ratio, is important for mediating salt tolerance (Møller et al., 2009). Poor exclusion of Na^+ from shoots may be part of the cause of the observed salt sensitivity. However, salt sensitivity of *det3* and *nhx5/nhx6* was measured as reduced root growth. Elevated Na^+/K^+ ratios in leaves typically causes early leaf senescence and can be measured by decreased chlorophyll content (Awlia et al., 2016).

While *Atccc1* plants accumulate more K^+ and Na^+ in shoots, both elements are found in lower abundance in *Atccc1* seeds (McDowell et al., 2013). *Atccc1* seeds accumulate more Ca and S. Neither Ca nor S are substrates of AtCCC1, highlighting that the TGN/EE localised transporter impacts the ion content of ions other than its own substrates. The PM abundance of root PM ion transporters such as the boron transporter, BOR1, and the iron transporter, IRT1, are regulated by endomembrane trafficking (Barberon et al., 2011; Kasai et al., 2011). PM abundance of other ion and nutrient transporters are likely to be perturbed in plants with altered TGN/EE conditions. The SULPHATE TRANSPORTER (SULTR) family of proteins are primarily involved in the uptake and distribution of sulphate in Arabidopsis (Takahashi, 2019). Altered abundance of SULTR proteins in roots and vascular tissue could result in altered uptake and root to shoot transport of sulphate causing increased accumulation of S in shoot tissue.

Measuring root and shoot ion concentrations of *Atccc1*, *det3* and *nhx5/nhx6* plants could help to determine if these mutants share the same alterations in root to shoot ion translocation. Measuring chlorophyll content of *det3*, *Atccc1* and *nhx5/nhx6* plants could then help assess if

altered root to shoot translocation is impacting the salt sensitivity of the endomembrane trafficking mutants. Assaying the PM abundance and trafficking of GFP tagged PM ion transporters such as NHX7 and BOR1 in the three mutants will begin to determine if altered trafficking and reduced PM abundance of ion transporters occurs in mutants with altered TGN/EE luminal conditions. Such work may open up new avenues of manipulating salt tolerance in plants.

5.6 CCCs in Arabidopsis, Rice and Grapevine

There is evidence that the genomes of all angiosperms contain *CCC* genes, and that the proteins share a high degree of homology (Henderson et al., 2018). It will be important to determine if the cellular role of CCCs is conserved amongst land plants, particularly angiosperms. This will aid in bringing the outcomes of work from the model plant, Arabidopsis, into species of agronomical and economical significance. There is evidence that CCC1 function is conserved among angiosperms. The knockout phenotypes of *Atccc1* plants can be complemented by the grapevine (*Vitis vinifera*) CCC, VviCCC (Henderson et al., 2015). This indicates that the grapevine CCC can perform the same cellular role as AtCCC1 and is likely localised in the TGN/EE in Arabidopsis. Meanwhile, knockouts of the rice (*Oryza sativa)* homolog of AtCCC1, *Osccc1.1*, also have reduced shoot and root growth as well as an altered accumulation of ions including K, Cl, Na, Mn, Cu and Zn (Chen et al., 2016). Previous studies have suggested that OsCCC1.1 might be localised to the PM (Kong et al., 2011; Chen et al., 2016). It is possible that CCCs of monocots and dicots diverged in their functional role and therefore localisation. However, CCCs transport K^+, Cl^- and Na^+. The altered accumulation of Mn, Cu and Zn cannot be a direct effect of the loss of OsCCC1.1 as they are unlikely to be substrates of OsCCC1.1. Instead, OsCCC1.1 could play a similar role to AtCCC1 and regulate luminal conditions in the TGN/EE of rice. Clarification of the subcellular localisation of OsCCC1.1 is needed.

Determining if OsCCC1.1 can complement *Atccc1* plants would be the first step in determining if monocot and dicot CCC proteins have a conserved function or perform different roles at different membranes. Such work can be applied to other species as well to determine how conserved the role of CCC is amongst angiosperms.

5.7 Conclusions and Outlook

The severe defects in the growth and development of *Atccc1*, *det3* and *nhx5/nhx6* plants highlights the importance of the luminal conditions of the TGN/EE in plants. Defects in luminal conditions result in altered endomembrane trafficking, leading to the phenotypes observed in these mutants. Future work can now focus on elucidating the mechanisms by which the luminal conditions of the TGN/EE impact trafficking and to tease apart the roles of pH and ion accumulation in the TGN/EE. Understanding the underlying mechanisms of the TGN/EE are important due to the role of endomembrane trafficking in agronomically significant traits like pathogen resistance, yield, biomass production, nutrient uptake and salt tolerance.

5.8 References

Assaha, D.V.M., Ueda, A., Saneoka, H., Al-Yahyai, R., and Yaish, M.W. (2017). The role of Na^+ and K^+ transporters in salt stress adaptation in glycophytes. Frontiers in Physiology **8,** 509.

Awlia, M., Nigro, A., Fajkus, J., Schmoeckel, S.M., Negrão, S., Santelia, D., Trtílek, M., Tester, M., Julkowska, M.M., and Panzarová, K. (2016). High-throughput non-destructive phenotyping of traits that contribute to salinity tolerance in *Arabidopsis thaliana*. Frontiers in Plant Science **7,** 1414.

Bacete, L., and Hamann, T. (2020). The role of mechanoperception in plant cell wall integrity maintenance. Plants **9,** 574.

Barberon, M., Zelazny, E., Robert, S., Conéjéro, G., Curie, C., Friml, J., and Vert, G. (2011). Monoubiquitin-dependent endocytosis of the iron-regulated transporter 1 (IRT1) transporter controls iron uptake in plants. Proceedings of the National Academy of Sciences **108,** E450-458.

Barbez, E., Dünser, K., Gaidora, A., Lendl, T., and Busch, W. (2017). Auxin steers root cell expansion via apoplastic pH regulation in *Arabidopsis thaliana*. Proceedings of the National Academy of Sciences **114,** E4884-e4893.

Bassil, E., Ohto, M.A., Esumi, T., Tajima, H., Zhu, Z., Cagnac, O., Belmonte, M., Peleg, Z., Yamaguchi, T., and Blumwald, E. (2011). The Arabidopsis intracellular Na^+/H^+ antiporters NHX5 and NHX6 are endosome associated and necessary for plant growth and development. Plant Cell **23,** 224-239.

Bhaskara, G.B., Wen, T.N., Nguyen, T.T., and Verslues, P.E. (2017). Protein phosphatase 2Cs and microtubule-associated stress protein 1 control microtubule stability, plant growth, and drought response. Plant Cell **29,** 169-191.

Bischof, H., Rehberg, M., Stryeck, S., Artinger, K., Eroglu, E., Waldeck-Weiermair, M., Gottschalk, B., Rost, R., Deak, A.T., Niedrist, T., Vujic, N., Lindermuth, H., Prassl, R., Pelzmann, B., Groschner, K., Kratky, D., Eller, K., Rosenkranz, A.R., Madl, T., Plesnila, N., Graier, W.F., and Malli, R. (2017). Novel genetically encoded fluorescent probes enable real-time detection of potassium in vitro and in vivo. Nature Communications **8,** 1422.

Braidwood, L., Breuer, C., and Sugimoto, K. (2014). My body is a cage: mechanisms and modulation of plant cell growth. New Phytologist **201,** 388-402.

Chen, Z.C., Yamaji, N., Fujii-Kashino, M., and Ma, J.F. (2016). A Cation-Chloride Cotransporter gene is required for cell elongation and osmoregulation in rice. Plant Physiology **171,** 494-507.

Colmenero-Flores, J.M., Martínez, G., Gamba, G., Vázquez, N., Iglesias, D.J., Brumós, J., and Talón, M. (2007). Identification and functional characterization of cation-chloride cotransporters in plants. Plant Journal **50,** 278-292.

Demes, E., Besse, L., Cubero-Font, P., Satiat-Jeunemaitre, B., Thomine, S., and De Angeli, A. (2020). Dynamic measurement of cytosolic pH and $[NO_3^-]$ uncovers the role of the vacuolar transporter AtCLCa in cytosolic pH homeostasis. Proceedings of the National Academy of Sciences **117,** 15343-15353.

Domingos, P., Dias, P.N., Tavares, B., Portes, M.T., Wudick, M.M., Konrad, K.R., Gilliham, M., Bicho, A., and Feijó, J.A. (2019). Molecular and electrophysiological characterization of anion transport in *Arabidopsis thaliana* pollen reveals regulatory roles for pH, $Ca2^+$ and GABA. New Phytologist **223,** 1353-1371.

Dragwidge, J.M., Scholl, S., Schumacher, K., and Gendall, A.R. (2019). NHX-type $Na^+(K^+)/H^+$ antiporters are required for TGN/EE trafficking and endosomal ion homeostasis in *Arabidopsis thaliana*. Journal of Cell Science **132**.

Dragwidge, J.M., Ford, B.A., Ashnest, J.R., Das, P., and Gendall, A.R. (2018). Two endosomal NHX-type Na^+/H^+ antiporters are involved in auxin-mediated development in *Arabidopsis thaliana*. Plant Cell Physiology **59,** 1660-1669.

Feng, W., Kita, D., Peaucelle, A., Cartwright, H.N., Doan, V., Duan, Q., Liu, M.C., Maman, J., Steinhorst, L., Schmitz-Thom, I., Yvon, R., Kudla, J., Wu, H.M., Cheung, A.Y., and Dinneny, J.R. (2018). The FERONIA receptor kinase maintains cell-wall integrity during salt stress through Ca^{2+} signaling. Current Biology **28,** 666-675.e665.

Gu, Y., Zavaliev, R., and Dong, X. (2017). Membrane trafficking in plant immunity. Molecular Plant **10,** 1026-1034.

Guo, W., Zuo, Z., Cheng, X., Sun, J., Li, H., Li, L., and Qiu, J.L. (2014). The chloride channel family gene CLCd negatively regulates pathogen-associated molecular pattern (PAMP)-triggered immunity in Arabidopsis. Journal of Experimental Botany **65,** 1205-1215.

Han, B., Jiang, Y., Cui, G., Mi, J., Roelfsema, M.R.G., Mouille, G., Sechet, J., Al-Babili, S., Aranda, M., and Hirt, H. (2020). CATION-CHLORIDE CO-TRANSPORTER 1 (CCC1) Mediates Plant Resistance against Pseudomonas syringae. Plant Physiology **182,** 1052-1065.

He, Y.M., and Ma, B.G. (2016). Abundance and temperature dependency of protein-protein interaction revealed by interface structure analysis and stability evolution. Scientific reports **6,** 26737.

Henderson, S.W., Wege, S., and Gilliham, M. (2018). Plant cation-chloride cotransporters (CCC): evolutionary origins and functional insights. International Journal of Molecular Sciences **19**.

Henderson, S.W., Wege, S., Qiu, J., Blackmore, D.H., Walker, A.R., Tyerman, S.D., Walker, R.R., and Gilliham, M. (2015). Grapevine and Arabidopsis cation-chloride cotransporters localize to the Golgi and trans-Golgi network and indirectly influence long-distance ion transport and plant salt tolerance. Plant Physiology **169,** 2215-2229.

Hurtado-Lorenzo, A., Skinner, M., El Annan, J., Futai, M., Sun-Wada, G.H., Bourgoin, S., Casanova, J., Wildeman, A., Bechoua, S., Ausiello, D.A., Brown, D., and Marshansky, V. (2006). V-ATPase interacts with ARNO and Arf6 in early endosomes and regulates the protein degradative pathway. Nature Cell Biology **8,** 124-136.

Kasai, K., Takano, J., Miwa, K., Toyoda, A., and Fujiwara, T. (2011). High boron-induced ubiquitination regulates vacuolar sorting of the BOR1 borate transporter in *Arabidopsis thaliana*. Journal of Biological Chemistry **286,** 6175-6183.

Katsiarimpa, A., Kalinowska, K., Anzenberger, F., Weis, C., Ostertag, M., Tsutsumi, C., Schwechheimer, C., Brunner, F., Hückelhoven, R., and Isono, E. (2013). The deubiquitinating enzyme AMSH1 and the ESCRT-III subunit VPS2.1 are required for autophagic degradation in Arabidopsis. Plant Cell **25,** 2236-2252.

Kirsch, T., Paris, N., Butler, J.M., Beevers, L., and Rogers, J.C. (1994). Purification and initial characterization of a potential plant vacuolar targeting receptor. Proceedings of the National Academy of Sciences **91,** 3403-3407.

Kong, X.Q., Gao, X.H., Sun, W., An, J., Zhao, Y.X., and Zhang, H. (2011). Cloning and functional characterization of a cation-chloride cotransporter gene OsCCC1. Plant molecular biology **75,** 567-578.

Krebs, M., Beyhl, D., Görlich, E., Al-Rasheid, K.A., Marten, I., Stierhof, Y.D., Hedrich, R., and Schumacher, K. (2010). Arabidopsis V-ATPase activity at the tonoplast is required for efficient nutrient storage but not for sodium accumulation. Proceedings of the National Academy of Sciences **107,** 3251-3256.

Kulich, I., Cole, R., Drdová, E., Cvrcková, F., Soukup, A., Fowler, J., and Zárský, V. (2010). Arabidopsis exocyst subunits SEC8 and EXO70A1 and exocyst interactor ROH1 are involved in the localized deposition of seed coat pectin. New Phytologist **188,** 615-625.

Liu, J., and Hussey, P.J. (2014). Dissecting the regulation of pollen tube growth by modeling the interplay of hydrodynamics, cell wall and ion dynamics. Frontiers in Plant Science **5,** 392.

Liu, X., Cui, H., Zhang, B., Song, M., Chen, S., Xiao, C., Tang, Y., and Liesche, J. (2021). Reduced pectin content of cell walls prevents stress-induced root cell elongation in Arabidopsis. Journal of Experimental Botany **72,** 1073-1084.

Luo, Y., Scholl, S., Doering, A., Zhang, Y., Irani, N.G., Rubbo, S.D., Neumetzler, L., Krishnamoorthy, P., Van Houtte, I., Mylle, E., Bischoff, V., Vernhettes, S., Winne, J., Friml, J., Stierhof, Y.D., Schumacher, K., Persson, S., and Russinova, E. (2015). V-ATPase activity in the TGN/EE is required for exocytosis and recycling in Arabidopsis. Nature Plants **1,** 15094.

Lupanga, U., Röhrich, R., Askani, J., Hilmer, S., Kiefer, C., Krebs, M., Kanazawa, T., Ueda, T., and Schumacher, K. (2020). The Arabidopsis V-ATPase is localized to the TGN/EE via a seed plant-specific motif. Elife **9**.

Marmagne, A., Vinauger-Douard, M., Monachello, D., de Longevialle, A.F., Charon, C., Allot, M., Rappaport, F., Wollman, F.A., Barbier-Brygoo, H., and Ephritikhine, G. (2007). Two members of the Arabidopsis CLC (chloride channel) family, AtCLCe and AtCLCf, are associated with thylakoid and Golgi membranes, respectively. Journal of Experimental Botany **58,** 3385-3393.

Marshansky, V. (2007). The V-ATPase a2-subunit as a putative endosomal pH-sensor. Biochemical Society transactions **35,** 1092-1099.

McDowell, S.C., Akmakjian, G., Sladek, C., Mendoza-Cozatl, D., Morrissey, J.B., Saini, N., Mittler, R., Baxter, I., Salt, D.E., Ward, J.M., Schroeder, J.I., Guerinot, M.L., and Harper, J.F. (2013). Elemental concentrations in the seed of mutants and natural variants of *Arabidopsis thaliana* grown under varying soil conditions. PloS One **8,** e63014.

McFarlane, H.E., Watanabe, Y., Gendre, D., Carruthers, K., Levesque-Tremblay, G., Haughn, G.W., Bhalerao, R.P., and Samuels, L. (2013). Cell wall polysaccharides are mislocalized to the vacuole in *echidna* mutants. Plant Cell Physiology **54,** 1867-1880.

Møller, I.S., Gilliham, M., Jha, D., Mayo, G.M., Roy, S.J., Coates, J.C., Haseloff, J., and Tester, M. (2009). Shoot Na^+ exclusion and increased salinity tolerance engineered by cell type-specific alteration of Na^+ transport in Arabidopsis. Plant Cell **21,** 2163-2178.

Noguchi, T., Fujioka, S., Choe, S., Takatsuto, S., Yoshida, S., Yuan, H., Feldmann, K.A., and Tax, F.E. (1999). Brassinosteroid-insensitive dwarf mutants of Arabidopsis accumulate brassinosteroids. Plant Physiology **121,** 743-752.

Nolan, T.M., Vukašinović, N., Liu, D., Russinova, E., and Yin, Y. (2020). Brassinosteroids: multidimensional regulators of plant growth, development, and stress responses. Plant Cell **32,** 295-318.

Novarino, G., Weinert, S., Rickheit, G., and Jentsch, T.J. (2010). Endosomal chloride-proton exchange rather than chloride conductance is crucial for renal endocytosis. Science **328,** 1398-1401.

Papaneophytou, C.P., Grigoroudis, A.I., McInnes, C., and Kontopidis, G. (2014). Quantification of the effects of ionic strength, viscosity, and hydrophobicity on protein-ligand binding affinity. ACS Medicinal Chemistry Letters **5,** 931-936.

Qiu, Q.S., Guo, Y., Dietrich, M.A., Schumaker, K.S., and Zhu, J.K. (2002). Regulation of SOS1, a plasma membrane Na^+/H^+ exchanger in *Arabidopsis thaliana,* by SOS2 and SOS3. Proceedings of the National Academy of Sciences **99,** 8436-8441.

Rameau, C., Bertheloot, J., Leduc, N., Andrieu, B., Foucher, F., and Sakr, S. (2014). Multiple pathways regulate shoot branching. Frontiers in Plant Science **5,** 741.

Refrégier, G., Pelletier, S., Jaillard, D., and Höfte, H. (2004). Interaction between wall deposition and cell elongation in dark-grown hypocotyl cells in Arabidopsis. Plant Physiology **135,** 959-968.

Reguera, M., Bassil, E., Tajima, H., Wimmer, M., Chanoca, A., Otegui, M.S., Paris, N., and Blumwald, E. (2015). pH regulation by NHX-type antiporters is required for receptor-mediated protein trafficking to the vacuole in Arabidopsis. Plant Cell **27,** 1200-1217.

Reiland, S., Messerli, G., Baerenfaller, K., Gerrits, B., Endler, A., Grossmann, J., Gruissem, W., and Baginsky, S. (2009). Large-scale Arabidopsis phosphoproteome profiling reveals novel chloroplast kinase substrates and phosphorylation networks. Plant Physiology **150,** 889-903.

Rinaldi, M.A., Liu, J., Enders, T.A., Bartel, B., and Strader, L.C. (2012). A gain-of-function mutation in IAA16 confers reduced responses to auxin and abscisic acid and impedes plant growth and fertility. Plant Molecular Biology **79,** 359-373.

Robinson, D.G., and Neuhaus, J.M. (2016). Receptor-mediated sorting of soluble vacuolar proteins: myths, facts, and a new model. Journal of Experimental Botany **67,** 4435-4449.

Rogers, L.A., Dubos, C., Surman, C., Willment, J., Cullis, I.F., Mansfield, S.D., and Campbell, M.M. (2005). Comparison of lignin deposition in three ectopic lignification mutants. New Phytologist **168,** 123-140.

Roitinger, E., Hofer, M., Köcher, T., Pichler, P., Novatchkova, M., Yang, J., Schlögelhofer, P., and Mechtler, K. (2015). Quantitative phosphoproteomics of the ataxia telangiectasia-mutated (ATM) and ataxia telangiectasia-mutated and rad3-related (ATR) dependent DNA damage response in *Arabidopsis thaliana*. Molecular & Cellular Proteomics **14,** 556-571.

Scholl, S. (2017). pH in the *trans*-Golgi network/early endosome of *Arabidopsis thaliana*: Suppliers and consumers. (Doctor of Philosophy PhD thesis), Universität Heidelberg.

Sinclair, R., Rosquete, M.R., and Drakakaki, G. (2018). Post-Golgi trafficking and transport of cell wall components. Frontiers in Plant Science **9,** 1784.

Takahashi, H. (2019). Sulfate transport systems in plants: functional diversity and molecular mechanisms underlying regulatory coordination. Journal of Experimental Botany **70,** 4075-4087.

Usadel, B., Kuschinsky, A.M., Rosso, M.G., Eckermann, N., and Pauly, M. (2004). RHM2 is involved in mucilage pectin synthesis and is required for the development of the seed coat in Arabidopsis. Plant Physiology **134,** 286-295.

Wang, F.L., Tan, Y.L., Wallrad, L., Du, X.Q., Eickelkamp, A., Wang, Z.F., He, G.F., Rehms, F., Li, Z., Han, J.P., Schmitz-Thom, I., Wu, W.H., Kudla, J., and Wang, Y. (2021). A potassium-sensing niche in Arabidopsis roots orchestrates signaling and adaptation responses to maintain nutrient homeostasis. Developmental cell **56,** 781-794.e786.

Western, T.L., Burn, J., Tan, W.L., Skinner, D.J., Martin-McCaffrey, L., Moffatt, B.A., and Haughn, G.W. (2001). Isolation and characterization of mutants defective in seed coat mucilage secretory cell development in Arabidopsis. Plant Physiology **127,** 998-1011.